



Max-Planck-Institut für Metallforschung
Stuttgart

Temperature - Induced Direct Casting of SiC

Ruishuo Li

Dissertation
an der
Universität Stuttgart

Bericht Nr. 102
Juni 2001

Temperature - Induced Direct Casting of SiC

**von der Fakultät Chemie der Universität Stuttgart
zur Erlangung der Würde eines Doktors der
Naturwissenschaften (Dr. rer. nat.) genehmigte Abhandlung**

vorgelegt von

Ruishuo Li

aus Shanxi, China

Hauptberichter: Prof. Dr. rer. nat. F. Aldinger

Mitberichter: Prof. Dr. Ir. Eric J. Mittemeijer

Tag der mündlichen Prüfung : 01.06.2001

INSTITUT FÜR NICHTMETALLISCHE ANORGANISCHE MATERIALIEN

UNIVERSITÄT STUTTGART

MAX-PLANCK-INSTITUT FÜR METALLFORSCHUNG

ABTEILUNG ALDINGER

STUTTGART 2001

Danksagung

Die Forschungsarbeiten, die der vorliegenden Dissertation zugrunde liegen, wurde in der Zeit vom Mai 1997 bis April 1999 am Pulvermetallurgischen Laboratorium des Max-Planck-Instituts für Metallforschung und dem Institut für Nichtmetallische Anorganische Materialien der Universität Stuttgart, in Stuttgart durchgeführt.

Mein besonderer Dank gilt Prof. Dr. F. Aldinger für die Unterstützung während der ganzen Arbeit.

Herrn Dr. W. M. Sigmund gilt mein herzlicher Dank für die wissenschaftlicher Betreuung und Förderung der Arbeit, und für seine Bereitschaft zu intensiven und anregenden Diskussionen. Herrn Dr. G. Rixecker gilt mein Dank für die sorgfältigen Durchführung der Korrekturen.

Für die finanzielle Förderung danke ich dem KAAD und Herrn Dr. Heinrich Geiger.

Bei allen anderen Kollegen, vor allem auch den technischen Mitarbeitern am Max-Planck-Institut für Metallforschung bedanke ich mich ganz herzlich für die sehr gute und freundschaftliche Zusammenarbeit.

Ich danke insbesondere meiner Ehefrau Ying He, die mit mir die zeitweise nicht immer einfache Zeit durchgestanden und mir den Freiraum gelassen hat, diese Arbeit zu vollenden.

Herzlichen Dank.

Ruishuo Li

Index

	Abbreviations	5
1	Abstract	6
2	Introduction	11
	2.1 Current powder processing	11
	2.2 Silicon carbide	21
	2.2.1 Properties	21
	2.2.2 Production and sintering	22
	2.2.3 Applications	23
	2.3 Temperature - induced direct casting for SiC	25
3	Theoretical Background	28
	3.1 Colloidal stability	28
	3.2 Particle-particle interaction in suspension	28
	3.2.1 Van der Waals attraction	29
	3.2.2 Electric double layer (EDL) stabilization	30
	3.2.3 Polymeric stabilization	33
	3.2.3.1 Steric stabilization	34
	3.2.3.2 Depletion stabilization	35
	3.2.4 Combinations of stabilization methods	36

3.3	Methods for coagulation.....	37
3.3.1	Modification of the electrical double layer	37
3.3.2	Changing steric layers	38
4	Powder characterization.....	39
4.1	BET	39
4.2	Laser granulometry.....	39
4.3	XRD	42
4.4	Chemical analysis.....	42
4.5	FTIR	43
4.6	Sedimentation.....	46
4.7	Zeta potential.....	47
4.7.1	Optimal measuring condition	48
4.7.1.1	Solution concentration.....	48
4.7.1.2	Solution selection	48
4.7.1.3	Ball milling time.....	49
4.7.1.4	Measuring condition.....	49
4.7.2	Zeta potential results	50
5	SiC suspension preparation.....	54
5.1	Slurry formation with pH adjustment.....	54
5.1.1	Colloidal property calculation by STABIL program	54

5.1.2	Viscosity measurements of SiC suspensions	55
5.1.3	Empirical SiC viscosity model	57
5.2	Slurry formation with polymer as dispersant	57
5.2.1	Sedimentation measurement.....	59
5.2.2	Zeta potential measurement.....	60
5.2.3	Viscosity measurement.....	63
5.2.4	Temperature effects on SiC suspensions.....	65
5.2.5	Suggestions for temperature - induced direct casting	66
5.2.5.1	Zeta potential adjustment for SiC/PEI2.....	66
5.2.5.2	Slurry formation	67
6	AlN protection	69
6.1	AlN surface properties in SiC suspension.....	70
6.2	AlN protection through calcination and coating	72
6.2.1	Calcination	72
6.2.2	Coating	73
6.3	Conclusion.....	74
7	Temperature - induced direct casting of SiC.....	76
7.1	Temperature effects on SiC suspensions.....	76
7.1.1	pH change with temperature.....	76
7.1.2	Temperature effects on zeta potential	77

7.1.3	Temperature effects on viscosity.....	79
7.1.4	Hypothesis for temperature - induced direct casting.....	81
7.1.4.1	Reprecipitation of Y_2O_3 on to SiC surfaces	81
7.1.4.2	Near net shape forming by modification of Y_2O_3	83
7.1.4.2.1	Rheological behavior of a mixed 20 vol% SiC/ Y_2O_3 /AlN suspension....	85
7.1.4.2.2	Rheological behavior of a mixed 30 vol% SiC/ Y_2O_3 /AlN suspension....	87
7.2	Temperature effects on SiC suspensions with dispersant	89
7.2.1	High solid content SiC suspension and steric stability.....	89
7.2.2	pH change with temperature.....	91
7.2.3	SiC/PEI7 flocculation.....	92
7.2.4	Suspension with sintering additives	95
8	Outlook.....	99
9	Zusammenfassung.....	100
10	Figures	108
11	References	114

Abbreviations

BET	Brunauer-Emmett-Teller
BUMA	Butylmalonic acid
DEMA	Diethylmalonic acid
DRIFT	Diffuse reflectance infrared fourier transform spectroscopy
DMA	Dimethylacetanilide
EDL	Electric double layer
HASS	1-Hexanesulfonic acid Sodium salt Monohydrate
MELA	Melamine
OLAK	Oleic acid, potassium salt
PAA2	Poly(acrylic acid), average MW ca 2000
PEI2	Polyethylenimine, average MW ca 2000
PEOP	Poly(ethylene oxide)-Poly(methacrylic acid)
PMAA	Polymethacrylic acid
SHMP	Sodium hexametaphosphate P ₂ O ₅
SILO	3-(2-Aminoethylamino)-propyltrimethoxysilane
STEA	Stearic acid
TAC	Tri-ammonium citrate
TEOP	n-(Triethoxysilylpropyl)-O-polyethylene Oxide Uret
TEOS	Tetraethoxysilane
TSPP	Tetra-Sodium pyrophosphate anhydrous
XRD	X-ray diffraction

1 Abstract

Silicon carbide is an important engineering ceramic for structural and electrical applications because of its excellent mechanical properties at high temperature. The application of advanced ceramics in engineering structures largely depends on the possibility of reliable mass production of complex-shaped parts at an acceptable cost. The machining of fired ceramic preforms is very costly, and may cause substantial surface flaws.

In order to improve the forming technology, the colloidal processing is under development. Through temperature-oriented control of pH, ion strength and adsorption of organic additives (dispersants) the ceramic suspension can be coagulated in a controllable way. Basic studies revealed that coagulation can also be achieved just by heating up to 60-70°C. A further advantage of this processing is the small quantity of organic additives (< 1 wt%) needed. Till now this kind of ceramic processing has been intensively researched only with alumina. The goal of this work is to apply this processing to SiC (silicon carbide) aqueous system through a detailed study on particle interaction in SiC suspensions. As the first step the surface characterization of the SiC powder is implemented and then its dispersing in an aqueous system is analyzed. At last the colloidal behavior of SiC suspensions, which depends on dispersants, the pH and the temperature, is studied under consideration of the system containing sintering additives (AlN, Y₂O₃).

For the development of a stable aqueous suspensions, the surface properties of SiC, AlN and Y₂O₃ powders were studied in detail.

On the SiC surface, NH and Si-O-Si bands were determined by DRIFT-spectroscopy. The specific surface area of SiC is 11.4 m²/g estimated by BET method. Because as-received SiC powder can not be completely dispersed in water at pH 10 for the characterization of particle size distribution using laser granulometry, PEI was used as dispersant for ball milling. Under this condition the SiC powder size is $d(0.5) = 0.18 \mu\text{m}$. Zeta potential measurement was used to characterize the powder properties in water. The pH_{IEP} of as-received SiC powder is pH 3.41. Above pH 3.41 SiC powder is negative charged and the surface charge reaches a maximum value of -25mV above pH 8. Zeta potential measurements of SiC powder were also carried out using different dispersants, such as PEI, MELA, DMA, PEOP, BUMA, PMAA,

OLAK, DEMA, SILO and STEA. PEI shifts pH_{IEP} to the basic range, whereas STEA, SILO and DEMA shift it to the acidic range. Dispersants can be adsorbed on SiC surface through specific sites if electrostatic force is attractive. As a result, PEI, SILO, OLAK, DEMA and STEA are adsorbed on SiC powder and the pH_{IEP} is changed correspondingly.

AlN and Y_2O_3 are necessary for a successful liquid phase sintering of SiC. As they are an integral part of the suspensions, their surface properties are also studied in detail. OH bands are dominating on AlN and Y_2O_3 surfaces. AlN powder reacts in water. The reaction is prevented in SiC suspension because of reprecipitation of $Si(OH)_4$ on AlN surfaces at room temperature. However, at elevated temperature AlN hydrolyzes. Up to $80^\circ C$ this can be prevented by coating the surface with TEOS and calcinating afterwards in flowing air for one hour, whereby a protective layer of Si-Al-O-N is formed. The AlN coated that way has a particle size of $d(0.5) = 0.89 \mu m$ after being dispersed by ball milling. Y_2O_3 was measured after ball milling and showed a size of $d(0.5) = 0.89 \mu m$. The specific surface area of AlN and Y_2O_3 is 12.9 and $4.8 m^2/g$, respectively. Modified AlN is charged negatively in water above pH 2 and the absolute value of surface charge is larger than 25 mV. Y_2O_3 has $pH_{IEP} = 10.2$ and is positively charged below pH 10.2. Its surface charge is also too low to provide a sufficient EDL (electrical double layer). Therefore, TAC (tri-ammonium citrate) was used to modify Y_2O_3 . After such a modification, Y_2O_3 is charged negatively above pH 2.6 and the surface charge has absolute values larger than 25 mV.

Besides the surface properties the colloidal properties of SiC were also studied. Sedimentation experiments with SiC powder were carried out in a pH range from 2 to 14. The suspensions were prepared with a 7 vol% solid content and dispersed by ultrasound. Around pH 10-12, a density of 41% of the theoretical density was obtained. Using dispersants at neutral pH, only 10-18% of the theoretical density were obtained due to poor deagglomeration by ultrasonic treatment, through which less fresh powder surface is exposed to dispersant.

10 vol% and 20 vol% SiC suspensions were prepared at various pH using HNO_3 and NH_4OH solutions in order to find an appropriate pH for preparing SiC suspensions. The viscosities reached a minimum at $pH = 10$. The viscosity of SiC suspensions at pH 10 with different solid contents can be successfully described by an empirical model (equation 4.1) in the range of shear rate $1-100 s^{-1}$.

According to DLVO (Derjaguin, Landau, Verwey and Overbeek) theory, the ceramic powders can be dispersed through modification of EDL. Another possibility is changing steric layers in an aqueous system.

Coagulation diagrams of SiC suspensions at room and elevated temperature were calculated according to the DLVO theory using the STABIL computer program by J. Adair. With this diagram, the dispersion state of SiC suspension can be predicted theoretically as a function of pH and temperature.

The surface charge of SiC in aqueous suspensions is sufficient to provide an electrical stabilization by EDL. Such electrical stabilization were verified in 10 vol% and 20 vol% SiC suspensions at various pH adjusted by HNO₃ and NH₄OH solution (Figure 5.2). However, the viscosities reached a minimum at pH 10 because of the dissolution of SiO₂ placed at SiC surfaces, which causes a high salt concentration in suspension above pH 10 and therefore compresses the EDL. SiC suspensions at solid loadings of 30-40 vol% were prepared at pH 10 and displayed shear thinning behavior.

The viscosity of SiC suspensions, which are stabilized through electrostatic stabilization, depends on several parameters, such as pH (Figure 5.2), ionic strength (Figure 3.6), solid loading (Figure 5.3) and system temperature (Figure 7.5 and Figure 7.6). With increasing temperature, ionic strength increases (Figure 7.3) and lower pH values was observed (Figure 7.1) because of the dissolution of SiO₂ placed at SiC surfaces. Therefore, an increase in viscosity is observed in SiC aqueous systems. The sintering additives were added to the SiC suspensions and the colloidal behavior was studied using pH and viscosity measurements at various solid loading. The viscosity of SiC/AlN/Y₂O₃-suspensions is not high enough to be used in forming technique for solid contents below 30 vol%. Coagulation of SiC suspensions mixed with sintering additives occurs only above a solid loading of 30vol% due to intensive interparticle reaction. However, the viscosity of SiC/AlN/Y₂O₃ suspensions above 40vol% is too high for casting.

To obtain a steric stabilized SiC slurries various polymers as dispersant, such as PEOP, DEMA, STEA, BUMA, SILO, OLAK and PEI2 were used. Using PEOP, DEMA, STEA and BUMA, the viscosities of SiC suspensions were increased due to poor adsorption. The adsorption of dispersant on SiC surfaces is effected by electrostatic forces or by Lewis

acid/base reactions at specific surface sites. The SiC suspension was stabilized by SILO, OLAK and PEI2 which have a good adsorption caused by H-bonds, interactions between the hydrocarbon chain of the oleate and the carbon atoms in the crystallographic lattice of SiC, and by electrostatic force. The 20 vol% suspensions using PEI, SILO and OLAK as dispersant display Newtonian behavior (Figure 5.7). By using PEI (polyethylenimine) with a molecular weight of 70,000 the SiC suspension was sterically stabilized at solid loadings of up to 50 vol%. This system was more suitable for this work because of the viscosity increased in proportion to temperature.

The colloidal behavior of suspension with changing temperature was researched through pH and viscosity measurements. The pH of the suspensions decreases with increasing temperature, and consequently the ion strength increases. The conformation of the polymer adsorbed on the surface of SiC depends on temperature, ionic strength and pH value of the suspension. If temperature raises, the ionic strength increases and pH decreases. As a result, the “Brush-structure” of the adsorbed polymer can be changed to a “pan-cake”-like structure. The steric force provided by the “Brush-structure” is used to resist van der Waals attraction in this system. For the pan-cake structure van der Waals attractive force dominates the interparticle repulsion, which results in coagulation of the suspension. The SiC/AlN/Y₂O₃ suspension was made at different solid loading and was coagulated through increasing temperature. In such a process 1 wt% of polymer was used for a dispersed slurry and a high solid loading of 50 vol% was obtained. The experiments showed that the steric repulsion will not collapse through increasing temperature up to 60°C at lower solid contents (<40 vol%). Above 40 vol%, the viscosity of suspension is high above 30°C.

For temperature - induced direct casting two possible forming methods are suggested. In the first method, SiC and AlN suspensions each with a solid loading of 30-40 vol% are dispersed at pH 10 using NH₄OH and HNO₃ for pH adjusting, respectively. Suspensions of 30-40 vol% Y₂O₃ were dispersed using 0.05 wt% TAC. The three suspensions were mixed by ball milling at low velocity. The mixture was cast and put into an oven at 70°C. The green body was demolded after 2 hours. The amount of dispersant in the Y₂O₃ powder is as low as 0.05 wt% thus no defined burnout is needed. However, the solid loading is relatively low for obtaining high density green bodies;

In the second method, a SiC suspension was prepared by adding 1 wt% of PEI. Suspensions of sintering additives Y_2O_3 and AlN were prepared by adjusting the pH. After combining the suspensions, the mixture was cast in a mold and put into an oven at 70°C. The green body was demolded successfully after 2 hours. In this processing method, the conformation of the polymer is changed by raising temperature, allowing a successful dispersion of the inorganic powders at room temperature and solidification at elevated temperature, of suspension with a solid loading of up to 50 vol%. A further advantage of this processing method is the small quantity of organics (< 1 wt%).

2 Introduction

2.1 Current powder processing

In the production process of advanced ceramics the powder preparation and the forming of green parts are critical process stages [1]. Each defect introduced during these manufacturing steps remains in the product even after a successful sintering process. The existing methods of preparing ceramic green bodies of a complicated shape include dry shaping, wet shaping and plastic shaping (Figure 2.1). In any case near-net-shape-forming techniques, which include powder injection molding (PIM) and direct casting, are crucial for the reduction of the cost of compounds [2].

Of special importance for wet shaping processes is a homogeneous state of a dense slurry with a high solid loading. Conventional wet shaping processes, such as slip casting, pressure casting and centrifugal casting, are often bothered by common problems concerned with a solid-liquid separation process to form a green body. The liquid flow is either driven by an external pressure gradient (slip casting, pressure casting) or centrifugal forces (centrifugal casting). The liquid flow will affect the suspension microstructure and tend to orient non-spherical constituents such as whiskers. Stress gradients induced by these techniques may lead to non-uniform densities of the green body and cause mass-segregation due to differences in particle size and density. Near-net-shape-forming techniques may avoid the before-mentioned problems.

PIM processing has been developed since the late 1920's. It is based on mixing a selected powder with a suitable binder to produce homogeneous granular pellets, which are injected in a closed die [3]. The major problem of this process is burnout, which can take up to several days or even weeks and risks slumping and crack formation. More importantly, the removal of organic binders and solvents can produce severe pollution problems and in several cases also cause fire and health hazards.

Nowadays, more and more attention is paid to using direct casting, in which water is used as dispersing medium instead of organic solvents. As a result, environmental pollution caused by the removing of organic solvent can be avoided. Subsequently, the cost of ceramic

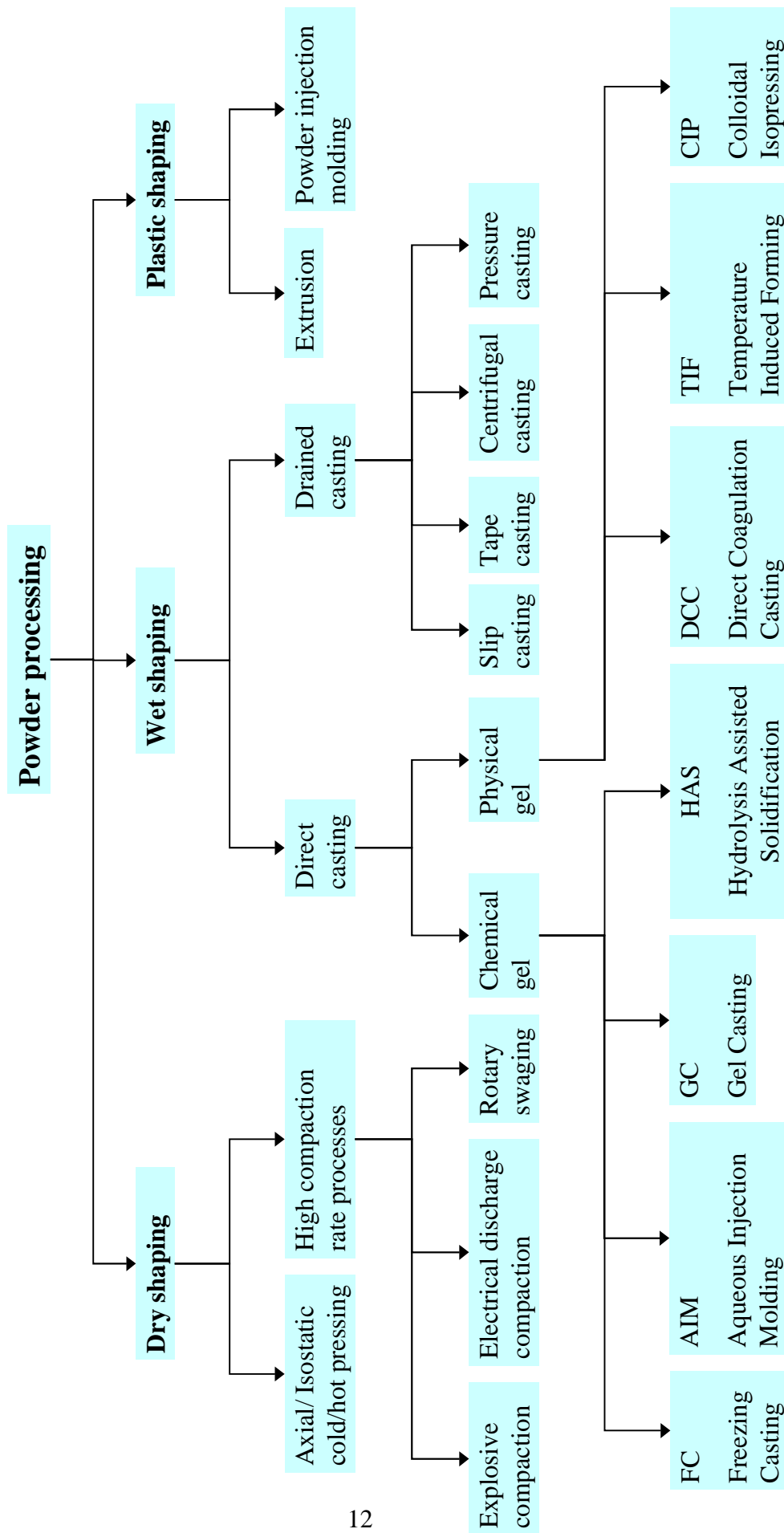


Figure 2.1: Current powder processing

processing dealt with organic solvent can be spared. For example, freeze casting (FC) uses water to disperse the ceramic powders and keeps the system below the freezing point of water to maintain the shape. Aqueous injection molding (AIM) uses cellulose derivatives to disperse and gel the aqueous system. Gel casting (GC) is based on the in situ polymerization of organic monomer binder. Hydrolysis of AIN in water is exploited in hydrolysis assisted solidification (HAS) to uphold the shape. In processes like direct coagulation casting (DCC), temperature induced forming (TIF) and colloidal isopressing (CIP), the interparticle force is changed by chemical reaction, polymer adsorption or an isostatic pressure. However, water is a polar solvent, it possesses a high dielectric constant and can not dissolve most commonly used additional processing aids and protect solid particles against oxidation or hydration. It is very difficult to obtain a well-dispersed ceramic suspension using water as a dispersing medium. Because of that, those direct casting methods also suffer from some disadvantages. This includes poor strength of the green body (AIM, FC and DCC), high viscosity (AIM, GC), expensive and sometimes toxic additives (AIM, GC and DCC), sensitive suspension preparation (AIM, HAS) and limited time and temperature stability (GC, DCC and HAS). A detail of variants of direct casting methods and their benefits and disadvantage will be discussed below.

Direct casting methods have been developed in the last decade. They utilize some of the inherent properties of dense suspensions to transform a fluid suspension into a stiff gel. The homogeneous state of the dense slurry is maintained during the green body formation step, the disturbance of the slurry by gelation and the density gradients are minimized and the introduction of larger heterogeneities can be avoided. Efforts have been made in developing a reliable cost effective forming technology. This resulted in a number of different processes, which differ in their gel preparation methods exploited for the solidification of an aqueous suspension in a die. The methods to be exploited for ceramic forming can be classified according to the physical and chemical principles that are used to form the gel as shown in Figure 2.1. Physical gels are defined by mainly van der Waals attractive bonds between the particles, i.e. the system gels due to an interconnected particle network. Whereas chemical gels are defined by an interconnected network of the gelled dispersing media.

As a chemical gel oriented method of direct casting, FC, for example, the “Quick-SetTM”, is based on a liquid-solid phase transformation by freezing of a water-based

suspension in a mold, which is kept below the freezing point of water [4, 5]. The extraction of the solvent is completed by its sublimation and therefore capillary forces during drying are avoided, thus minimizing cracking and shape distortion problems. Nevertheless, its industrial application is still limited because of some disadvantages such as heat transfers during solidification, poor green strength and complicated drying [2].

AIM was developed in several phases. It was first reported by Rivers in 1978 [6]. Methyl-cellulose polymers are mixed with a concentrated ceramic suspension. Cellulose derivatives are soluble in cold water. The dissolved molecules are hydrated but they have little interaction with each other. The hydrated molecules release the hydration water with increasing temperature. The viscosity of methyl-cellulose versus temperature is described in Figure 2.2.

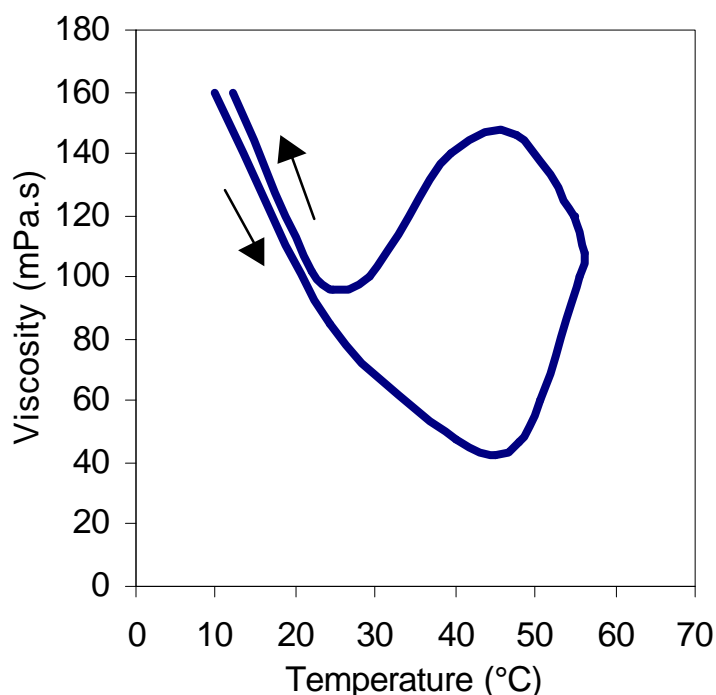


Figure 2.2: Change in viscosity and gelation of an aqueous solution of 2wt.% methylcellulose (Methocel A100, Dow Chemical Co., Midland, MI) on heating at 0.25°C/min [2]

The high viscosity caused by hydration decreases till a certain temperature is reached. At this temperature sufficient dehydration of the polymer occurs to cause a polymer-to-polymer association and the solution begins to gel, which is reflected in an abrupt increase in

viscosity. The thermal gelation process is reversible. The viscosity drops as temperature decreases with a special hysteresis. A forming process can be designed by adding ceramic powder in the range of minimum viscosity and a fast increase in viscosity with raising temperature. A strong elastic network is formed by the association of dehydrated polymer molecules in order to hold the ceramic powder together, and the hysteresis of viscosity decrease can be used to maintain the shape. However, this process has several serious disadvantages, for example, high viscosity of the suspension and low solids loading, which reflect in a narrow molding window and low green density. The poor green density makes handling and storage difficult.

Therefore, agar is employed by Fanelli et al. [7] to improve the process. Agar is a structural polysaccharide of the cell walls of a variety of red seaweed. With water (83 %), it forms an elastic hydrocolloid gel below 37 °C and a sol at the liquefaction temperature (70 °C). At pH > 5, agar is heat stable. Agar is insoluble in cold water and solubilizes on heating, and it gels on cooling. The formation of an extended network is based on the association of agarose molecules from the disordered random coil into double helices, which aggregate into junction zones containing many chains [8]. By using agar the low viscosity and high green body strength can be obtained. However, the agar is expensive and special equipment is needed for compounding.

As further development, GC is named for the ceramic forming. This concept was first used by Golibersuch in 1962 for consolidating of metallic particles in a slurry with polymerization and first used in ceramic application by Omatete in 1991 as a promising technique for complex shapes of structural ceramics[9, 10]. A concentrated slurry of ceramic powder in a solution of organic monomers and dispersant is poured into a mold and then polymerized in-situ to form a green body in the shape of the mold cavity. Some organic monomers are soluble in water and become polymerized gel with increasing temperature. The particles are dispersed by electrostatic or steric stabilization using a small molecular dispersant. The slurry with low viscosity and high solid loading is poured into the mold. With in situ and permanent polymerization of monomer, the ceramic powder can retain the desired shape. Gel Casting can produce near-net-shape ceramic articles with complex shape, but the additives are sometimes toxic. Additionally the stability of the slurry is time limited. Some other methods, such as with cross-linking agents [11] or exposure to UV irradiation [12] and with coordinative chemistry [13], are also used for gel casting.

HAS is based on chemical bonding of water in a concentrated aqueous suspension by thermally activated and/or accelerated hydrolysis of added aluminum nitride powder [14]. AlN is fairly stable in aqueous system at room temperature due to a thin inert protective coating of alumina [15][16]. The layer of alumina dissolves on heating and the exposed AlN reacts with water according to equation(1.1):



During the hydrolysis reaction, water is consumed and the solids content in the suspension is increased while ammonia formation can be used to shift the pH of the suspensions toward the isoelectric point, which is reflected in coagulation of solid particles. Both effects result in rather fast solidification of the slurry within the mould. Figure 2.3 shows schematically both effects.

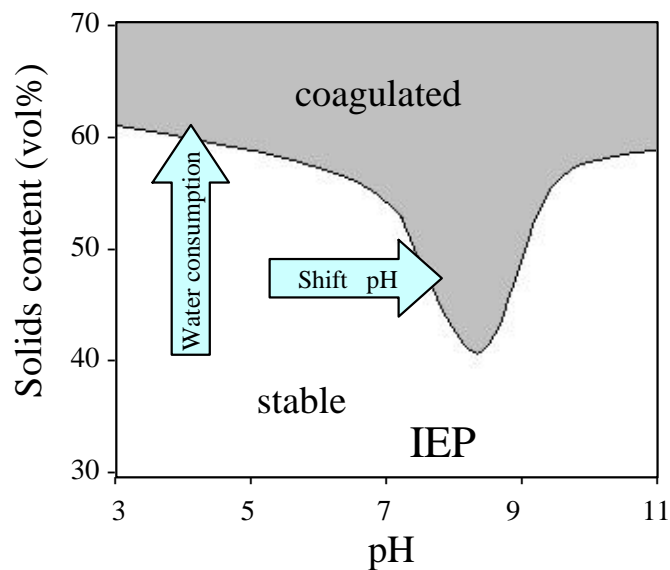


Figure 2.3: Colloidal stability diagram for HAS process of alumina suspensions [2].

Additionally, aluminum hydroxide is produced as a reaction product from AlN hydrolysis. High green density is obtained because of the gelation of aluminum hydroxide on heating. The disadvantages of HAS are the sensibility of feedstock preparation as well as limited time and temperature stability. Additional equipment to collect and neutralize ammonia is also needed.

Compared to chemical gels, ceramic direct casting using physical gels show promising potential in the material engineering application. The following discussion will be focused on the physical gels oriented methods used in direct casting for near-net shaped ceramics. The chemical gels are prepared with up to 3 weight percent organic additives. Through physical or chemical reaction, an interconnected network can be made to gel the system.

DCC, which was presented by Gauckler [17], is based on the idea to destabilize a high solids loaded suspension or a sol by a time-delayed internal reaction using a substrate and, in case needed, a catalyst. The well-dispersed, high solids loaded stabilized suspension containing the powder particles, a water soluble substrate, a catalyst and, optionally, polymer molecules is cast into a mold. It is destabilized by the decomposition products of the substrate in a time-delayed reaction. Thereby the decomposition products of the substrate either shift the pH of the suspension to the isoelectric point of the ceramic powder system or increase the ionic strength of the suspension. Figure 2.4 shows the stability diagram for an aqueous colloidal alumina dispersion and the arrows indicate the coagulation principles by pH shift or alternatively by a change of the ionic strength.

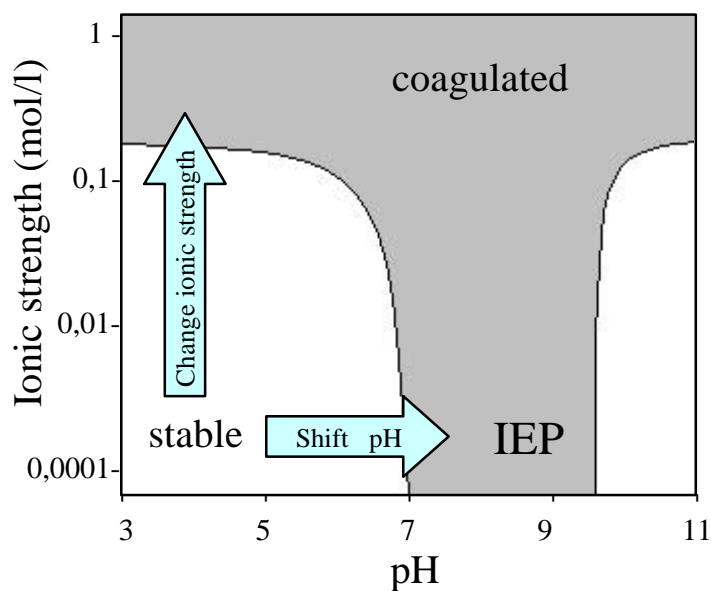
A reaction that shifts the pH or increases the ionic strength of the suspension may be catalyzed by an enzyme or, may be, a self-decomposing reaction. In case of enzyme catalyzed reactions, their kinetics can easily be controlled in terms of ambient temperatures. When using high solids loading, the destabilization causes the suspension to coagulate and to change its properties from a viscous liquid to homogenous, rigid, viscoelastic, ceramic green body [18]. Both destabilization reaction processes are performed using the following reaction (1.2):



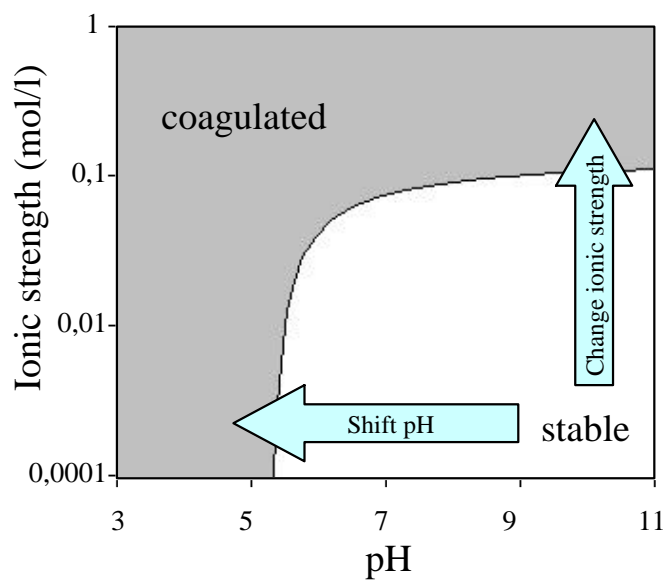
The urease works well at room temperature, but the reaction can be slowed down or nearly inhibited by cooling the slurry. This behavior is used for shaping by casting below 5°C and warming to room temperature in order to start coagulation [19].

During coagulation of high concentrated suspensions, no shrinkage occurs. Therefore, complex shaped products can be cast and consolidated. Typically less than 0.5 wt% of organic additives (dispersants and enzymes) are required. As a result, a separate burnout step can be

excluded. High solids loading leads to high green density. However, some disadvantages occur, such as, narrow pH window, limited time stability, and additional equipment is needed to collect and neutralize ammonia.



(a)



(b)

Figure 2.4: Stability limits for an aqueous alumina suspension (a) without a specific adsorbing deflocculant and (b) with 0.35 wt% citric acid as deflocculant [17].

TIF is a novel method for the preparation of complex shaped components in aqueous media [20]. The method is based on the temperature dependence of the solubility and the surface charge of Al_2O_3 particles in water. Dispersants with low-molecular-weight, e.g. Tri-ammonium citrate (TAC), induce a high surface charge for electrostatic stabilization at room temperature. Polymers, e.g. polyacrylic acid (PAA), are commonly added to induce bridging flocculation and increase the strength of the green body. When temperature is increased the alumina starts to dissolve in the solvent opening fresh surface sites for adsorption of polymers. The competitive adsorption of two dispersants causes bridging flocculation and therefore an increase in viscosity (Figure 2.6). The higher the molecular weight of the polymer, the higher the viscosity of the suspension [21]. Like Figure 2.5 shows, the gelation depends also on solids loading of alumina. Using the TIF process, a burnout can be avoided due to the very low organic content of below 0.5 wt% needed for stabilization and flocculation[22].

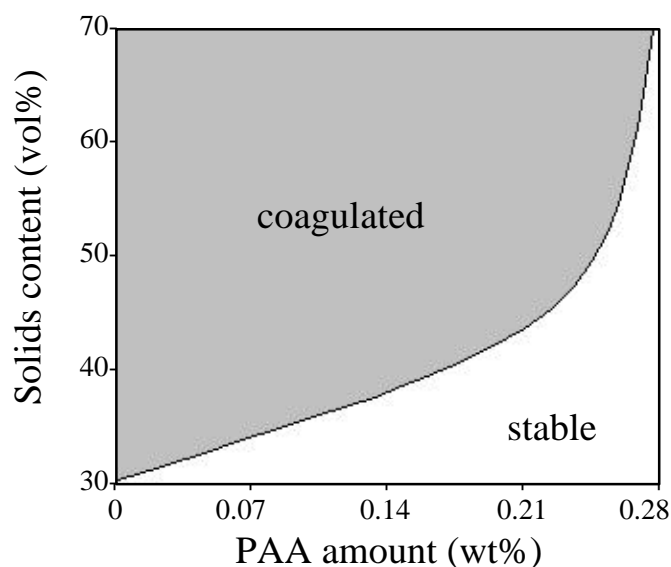


Figure 2.5: Gelation diagram of alumina suspension in water [1]

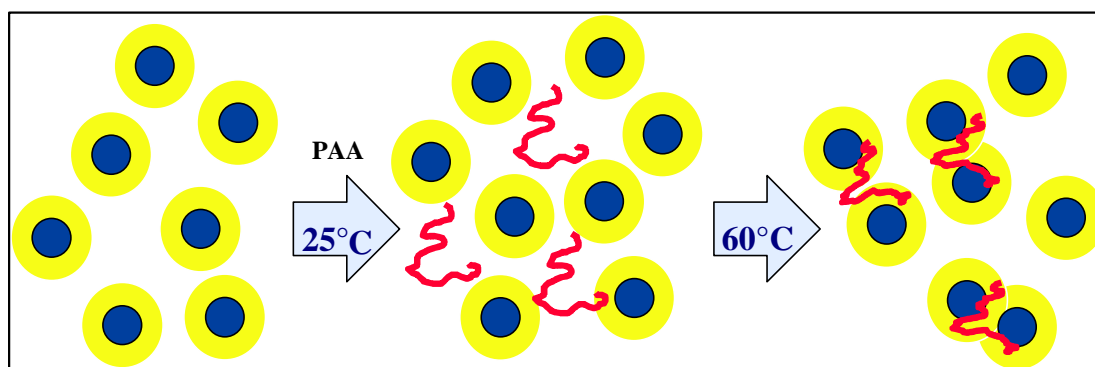


Figure 2.6: Mechanism for TIF process [21]

It was suggested by Zhang [23] that there is a region of the polymer concentration below full coverage where increases in adsorbed amount are seen with increasing temperature. A minimum amount of dispersant is used to stabilize an alumina slurry electrosterically and with increasing temperature more dispersant is needed for a full coverage on the surface. Because there is no additional polymer available during the process, the only way to fill the empty sites is by bridging and the slurry will be coagulated. The key of this process is to control the polymer concentration, which should not be larger than the minimum amount for full coverage at room temperature, no flocculation can be acquired when excess polymer is used, so maximum solid loading is limited [1].

Very recently, colloidal isopressing has been proposed for direct casting. It uses ceramic colloidal systems, which have a short-range interparticle potential [24]. A plastic-to-brittle transition is exhibited in the system when it is consolidated via pressure filtration. At low consolidation pressures, the saturated powder compacts will exhibit plastic behavior. A weakly attractive ceramic slurry is consolidated to produce a high volume fraction, plastic ceramic paste and extruded or vibrated to fill a plastic mold cavity. Via the mold an applied isostatic pressure will be transmitted to the particle network, pushing particles together, and thus changing the mechanical response of the consolidated body. The ceramic compacts become elastic and maintain the shape of the mold cavity.

2.2 Silicon carbide

Silicon carbide (SiC) has been an industrial product for over 100 years. It is regarded as an important engineering ceramic for structural and electrical applications because of its excellent mechanical and electrical properties at high temperature [25]. The development of advanced SiC ceramic materials is technologically important in a broad range of applications, which include medical biomaterials, high temperature semi-conductors, synchrotron optical elements and light weight/high strength structure materials. Structural SiC ceramics is widely studied and considered as one of the promising candidate materials for various applications such as compounds for combustion engines, gas turbines, industrial heat exchangers, high-temperature energy conversion systems and many other devices. Beside such engineering compounds it is produced in mass production for abrasive, refractory and metallurgical applications [26].

2.2.1 Properties

I. Crystal structure: SiC occurs in two basic modifications, β -SiC and α -SiC. Industrial SiC contains almost exclusively β -SiC (3C) and the α -poly-types such as 4H, 6H, and 15R [27] (C: cubic, H: hexagonal, R: rhombohedral).

β -SiC is metastable at room temperature and, in accordance with Ostwald's rule, is formed initially in SiC production. It changes into α -SiC at around 1900 °C. Above 2000 °C, β -SiC is the stable form, so that α -SiC transforms to β -SiC [28].

II. Color: Pure α -SiC is colorless, while the cubic β -modification is yellow. The only other elements that can be included in the SiC crystal lattice in amounts > 1 ppm are N, Al, and B. Nitrogen gives a green color to 3 C and 6 H, and a yellow color to 4 H and 15 R. The presence of the trivalent elements boron and aluminum gives all modifications and polytypes a blue-black color [29]

III. Hardness: The industrial importance of silicon carbide is mainly due to its extreme hardness of 9.5–9.75 Mohs. Only diamond, cubic boron nitride, and boron carbide are harder.

The Knoop microhardness depends on the crystal orientation, and lies in the range of $H_{K,0.1}$ 2100–2900 [30]. Silicon carbide is very brittle, and can therefore be crushed comparatively easily in spite of its great hardness.

IV. Thermal and calorimetric properties: SiC has an unusually high thermal conductivity: $150 \text{ kJ m}^{-1} \text{ h}^{-1} \text{ K}^{-1}$ at 20°C , and $54 \text{ kJ m}^{-1} \text{ h}^{-1} \text{ K}^{-1}$ at 1400°C [31]. α -SiC has a very low thermal expansion coefficient of $4.7 \times 10^{-6} \text{ K}^{-1}$ (20 – 1400°C), which is the reason why silicon carbide refractory products are so outstandingly resistant to thermal shock. The specific heat capacity of SiC is $0.67 \text{ J g}^{-1} \text{ K}^{-1}$ at room temperature, and $1.27 \text{ J g}^{-1} \text{ K}^{-1}$ at 1000°C . The standard enthalpy of formation $\Delta H_{298\text{K}}^0$ is $-71.6 \pm 6.3 \text{ kJ/mol}$, and the entropy $S_{298\text{K}}^0$ is $16.50 \pm 0.13 \text{ J mol}^{-1} \text{ K}^{-1}$ [32].

V. Optical properties: α -SiC is birefringent due to its crystal structure: $n_o = 2.649$ – 2.649 , and $n_E = 2.688$ – 2.693 (Na 589 nm, 20°C) [33]. For β -SiC, a refractive index of ca. 2.63 (Li 671 nm) has been reported [34].

VI. Electrical properties: Silicon carbide is a semiconductor. The resistivity lies between $0.1 \Omega \cdot \text{cm}$ and $10^{12} \Omega \cdot \text{cm}$ [35].

VII. Chemical properties: It is chemical resistant to organic solvents, alkalies, acids, salt solutions, and even aqua regia and fuming nitric acid.

VIII. Toxicology and occupational health: SiC is nontoxic, and is therefore a nonhazardous material as defined by GefStoffV [36].

2.2.2 Production and sintering

Silicon carbide is produced industrially from silicon dioxide and carbon, which react according to the overall equation (1.3):



The reaction is strongly endothermic with $\Delta H_{298K} = +618.5$ kJ/mol [32], corresponding to 4.28 kWh/kg α -SiC. Currently used powder processes include the Acheson Process [37], the ESK process [38] and CVD [39]. Different sintering processes are used, for example, SsiC (Solid-state sintering), LPSiC (liquid-phase sintering), RSiC (reaction sintering), HPSiC (hot pressed Sintering), HIPSiC (hot isopressed sintering) and SiSiC (reaction sintering/infiltration) [40]. The advantages of LPSiC are low sintering temperatures, fast densification and homogenization, high final densities and resulting microstructures often providing mechanical or physical material properties superior to solid state sintered materials [41]. Several additive systems were developed for LPSiC sintering, such as Al_2O_3 alone [42, 43], a mixture of rare-earth oxides in combination with Al_2O_3 and/or boron compounds [44] and Al_2O_3 - Y_2O_3 system [45]. However, SiC and oxides can react in an inert atmosphere, and result in formation of volatile components that cause serious vapor-phase transport and a substantial loss of mass. In industrial processes, sintering additives are needed for reproducibility and full density. Aluminum nitride combined with Yttrium oxide as sintering additives display better effects than other systems [46, 104].

In this work, 10vol% additives of 60mol% AlN and 40mol% Y_2O_3 are selected for liquid phase sintering of SiC, with which improved mechanical properties and failure behavior were obtained such as 3.2 g/cm³ density, 25 GPa hardness, 8 MPa \sqrt{m} fracture toughness, 725 MPa bending strength at 1200 °C and 1050 MPa at room temperature [104].

2.2.3 Applications

I. Abrasive: Silicon carbide is used directly as a loose-grain abrasive for cutting with wiresaws and for lapping. It is also used in bonded form. The latter use can be divided into two groups:

a) Bonded abrasives include grinding wheels, whetstones, hones, abrasive cutting-off wheels, and monofiles. The SiC grains can be bonded with plastics or ceramics.

b) Coated abrasives include abrasive paper and cloth in sheet or band form. They are produced by strewing the SiC grains onto a substrate coated with glue or bonding resin and then covering with a second layer of bonding agent [47];

II. Refractory: High resistance to oxidation, high thermal conductivity, and low coefficient of thermal expansion make silicon carbide ideal for use in refractory raw materials and finished products. For example: clay-bonded moldings and monolithics, heat exchangers, burner nozzles, etc.;

III. Metallurgy: The iron and steel industries consume large quantities of silicon carbide for deoxidizing high-alloy steels and for adding silicon and carbon to cast iron [48];

IV. Electrical technology: The semiconducting properties of silicon carbide have long been utilized in resistance heating elements, high-voltage cables and generators, floor coverings, etc. [49];

V. Electronics: Silicon carbide is a promising material for the construction of electronic equipment such as rectifying diodes for high temperatures and/or high energy densities, and rectifiers, light-dependent resistors, electrophotographic receptors and light-emitting diodes [50];

VI. Structural ceramics: Pumps used in the chemical industry for feeding and metering strongly corrosive and abrasive materials, radial loads, sliding bearings and shaft housings [51].

2.3 Temperature - induced direct casting for SiC

Complicated shaped parts of ceramics can be obtained without defects such as pores and cracks by direct casting due to homogenous structures in the green state. Nevertheless, those processes have some disadvantages. By using water as dispersing medium, the viscosity increases, when organic aids for gelling the suspension are dissolved and the solid loading has to be reduced to get a castable suspension.

The temperature is found to have a marked effect on the characteristics of a slurry, such as adsorption of dispersant, viscosity of slurry, electrophoretic mobility and density as well as the structure of the green body. The temperature effect on slurry is presented by K. Uematsu with an alumina-water-dispersant as a model [52]. In this model, the effect of temperature on the relationship between dispersant concentration and the viscosity of slurry was studied. With increasing dispersant concentration, the viscosity decreases in the region of low dispersant concentration and reaches a minimum at all temperatures (at 20°C and 40°C). Thereafter, the viscosity increases gradually with increasing dispersant concentration at all temperatures. The dispersant concentrations corresponding to the minimum viscosity increases with increasing temperature.

The effect of temperature on the adsorption of dispersant on the alumina surface was also investigated [52]. In the region of low concentration, all dispersants added to the slurry are adsorbed at the surface of alumina particles. With increasing concentration of dispersant, an increasing part of the dispersant added to the slurry remains in the solution. The critical concentration is where the incomplete adsorption starts. The influence of dispersant concentration on the density of green bodies, which are formed from slurries at various temperatures by centrifugation, is not significant. The effect of temperature on the volume of sediment was presented at 20 °C and 40 °C [52], the minimum volume being reached at both temperatures, but more dispersant is needed at 40 °C. And the electrophoretic mobility decreases with increasing temperature. All the effects are explained by the influence of temperature on adsorption of dispersant on the surface of alumina.

Recently, the reversible destabilization of a sterically stabilized suspension, which is caused by a change in temperature, was also used to form ceramic green bodies of

complicated shape [53]. In sterically stabilized systems the interparticle forces can be manipulated by changing the solution properties of the polymer. Temperature change may have a drastic influence on, for example, the polymer-layer-thickness and the amount of adsorbed polymer. When the solvency reaches a critical level, commonly characterized by the Flory–Huggins interaction parameter, χ , the sterically stabilized dispersion flocculates (incipient flocculation) [54]. χ depends on temperature. A concentrated, sterically stabilized ceramic suspension is reversibly flocculated by changing the temperature, therefore the χ for an amphiphilic polymer in pentanol is also changed. At temperature above 30°C, the suspension has a low viscosity and negligible elasticity because of an extended polymer layer. Below 20°C, the adsorbed polymer layer collapses because of decreased solvency, resulting in an increased viscosity and an elastic viscoelastic response.

A further important effect of temperature in a slurry is the change of the solubility of the solid, i.e. the ceramic powder. For most ceramic systems, an increase in temperature of the ceramic suspension leads to an increase in the concentration of soluble metal ions [55, 56, 57]. On heating, the network strength is gradually increased by dissolution and reprecipitation of soluble species to form necks between particles. It can be further increased by a reprecipitation of all soluble species at the toroidal region between the particles upon evaporation [21]. TIF is a forming method using competitive adsorption of two dispersants and the change of the solubility of the ceramic powder in the solvent of the suspension. Both are caused by temperature change. The suspension is flocculated with increasing temperature. It has been successfully applied to forming of green parts of Al_2O_3 [20].

It is the intention of this work to transfer the concept of temperature induced forming to SiC, in general and in special to powder mixture ready for liquid-phase sintering of SiC using AlN and Y_2O_3 as sintering additives. First of all, a stable SiC suspension must be prepared. In order to disperse ceramic powder effectively in water, ceramic powders (SiC, AlN and Y_2O_3) are characterized for a improved understanding of its surface and colloidal properties. Dispersants are introduced for higher solid loading. Then, AlN should be protected from hydrolysis because of its sensitivity in water. Third, suspensions of sintering additives can be prepared for adding to SiC suspension without significant increase of viscosity. Finally and most importantly, the ceramic suspension must have suitable colloidal properties. In other

words, the suspension should be stable at room temperature and coagulating at raising temperatures.

3 Theoretical Background

3.1 Colloidal stability

The dispersed phase in colloidal systems may be solid, liquid or gas. Such colloidal dispersions play a pivotal role in our everyday lives: from blood, that is vital to the human organism, through polymer lattices, which are generated for use in the manufacture of plastics and paints, to agricultural emulsions and suspensions, exploited in the efficient production of food. Particles are said to be colloidal in character if they possess at least one dimension in the size range 1 to 1000 nm [58]. In the case of ceramic colloidal processing the ceramic powder is considered as dispersed phase and the liquid is termed the dispersion phase or dispersion medium. In near-net-shape forming, the principles underlying the stability of suspensions must be well understood for preparing high solid loading, stable suspensions, defect free ceramic green bodies and successfully sintered parts in sequence.

A suspension in which the dispersed phase remains essentially as discrete, single particles on a long time scale (e.g. months or even years) is defined as a stable suspension. Such a suspension may be stable based on thermodynamic or for kinetic reasons. In the latter case, typified by electrostatic stabilization, the system is said to be thermodynamically metastable. The dispersed particles of a suspension can usually be induced to form doublets and higher multiplets by appropriately changing the system status. This aggregation is referred to either coagulation or flocculation.

3.2 Particle-particle interaction in suspension

Van der Waals attraction between particles is responsible for holding agglomerates together [59]. In order to impart colloidal stability, it is necessary to create repulsion forces between particles. This repulsion must be at least as strong as, and comparable in range to, the attractive interaction. Generally, there are two approaches, named electrostatic stabilization and polymeric stabilization, by which colloidal stability can be imparted.

3.2.1 Van der Waals attraction

The van der Waals attraction between gas molecules originate from three possible sources (ignoring the high multipole interaction):

- Permanent dipole-permanent dipole forces (Keesom);
- Permanent dipole-induced dipole interaction (Debye);
- Transitory dipole-transitory dipole forces (London).

Only the classical London dispersion forces contribute to the long-range attraction between colloidal particles. The van der Waals attraction between two atoms or two molecules instead is relatively short ranging, extending only over a few tenths of a nanometer. With colloidal particles, each atom or molecule of one particle attracts atoms of the other particles. Typically, a colloidal particle is composed of 10^6 - 10^{10} atoms. The net effect of adding all of the myriad of possible atomic interactions is used to generate a long range attraction between the particles. The van der Waals attraction depends essentially on the geometry of two interacting bodies.

Hamaker [60] calculated the dispersion forces between colloidal particles based upon London's treatment. The attraction (V_A) between two spheres, each of radius r and separated by a distance d (Figure 3.1 [83]), is related to Hamaker constant A and a geometrical term L :

$$V_A = -\frac{A}{6} \left[\frac{2r^2}{L^2 - 4r^2} + \frac{2r^2}{L^2} + \ln \left(\frac{L^2 - 4r^2}{L^2} \right) \right] \quad (3.1) [58]$$

with $L=d+2r$.

If the distance between two particles d is small compared to the particle radius r , viz. $d \ll r$, then the first term in the expression 3.1 is dominant, and it is simplified to:

$$V_A = -\frac{Ar}{12d} \quad (d \ll r) \quad (3.2)$$

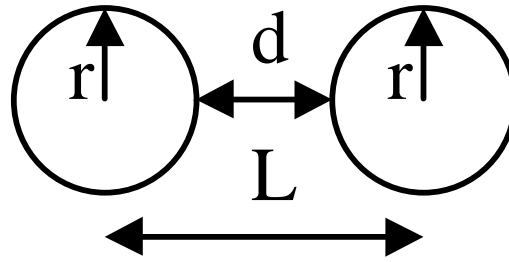


Figure 3.1: Two spheres model

The Hamaker constant is a materials constant that depends on the properties of the two materials and the intervening media.

3.2.2 Electric double layer (EDL) stabilization

One way to impart the repulsion over distances comparable to that of attraction is to use Coulombic repulsion which is of a long range character and can overcome the van der Waals attraction. But in liquid dispersion media, however, the principle of electroneutrality demands that the net charge in the dispersion medium is equal, but opposite in sign, to that of the particles. This leads to a more rapid fall-off in the potential with the separation distance, the counterions in the dispersion medium, however, generate the electrical double layers that surround the colloidal particles (Figure 3.2).

When a particle is immersed in a polar solvent such as water, the interface will acquire a charge, by either adsorbing or desorbing ions according to the chemical equilibrium with the surrounding solution. Ions of opposite charge, the counterions, are attracted and bound to the surface of the particle, which is called Stern layer. Others remain in solution for entropic reasons, forming a diffuse layer of charge adjacent to the particle. The stern layer plus the diffuse layer constitute the electrical double layer. The thickness of the double layer (Debye length) depends on the concentration of ions in solution. More ions available give a thinner double layer. The repulsive potential is related to the Debye length and can be expressed as:

$$V_R = 2pe\epsilon_0 a \Psi_0^2 \ln[1 + e^{-kd}], \quad (3.3)$$

where Ψ_0 is the surface potential, ϵ the dielectric constant of medium, ϵ_0 the permittivity of vacuum, a the particle diameter, d the separation distance and k the Debye parameter, which is the inverse of the Debye length and described as follows:

$$\mathbf{k} = \left(\frac{1000e^2 N_A}{\epsilon kT} \sum_i z_i^2 M_i \right)^{1/2}, \quad (3.4)$$

where z is the charge of ions, M the concentration of counter ions in solution, k the Boltzmann constant and N_A the Avogadro constant.

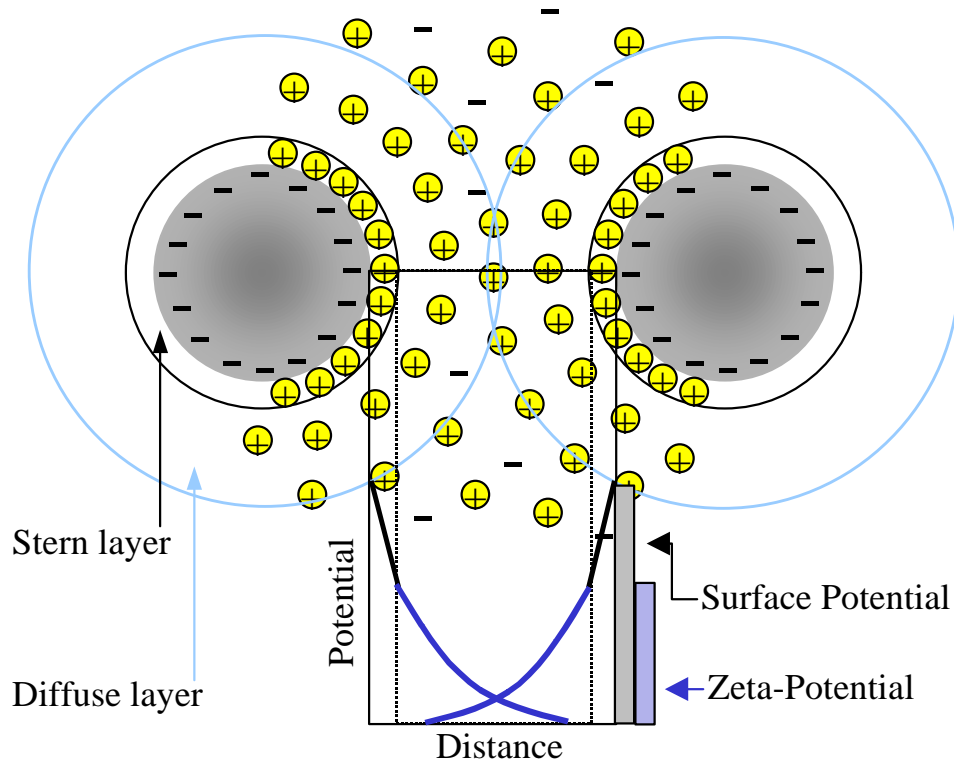


Figure 3.2: Schematic representation of electrical double layer

It is impossible to determine Ψ_0 experimentally since moving particles entrain films of liquid, but the zeta potential ζ is measured in the shear surface of the diffuse double layer of the particles; this is not identical to the interfacial potential, but both quantities are virtually identical in weakly polar phases.

In the well-known DLVO (Derjaguin, Landau, Verwey and Overbeek) theory the van der Waals attractive potential and the repulsive electrical double layer potential are added algebraic together to produce a combined interparticle potential, which is shown schematically in Figure 3.3.

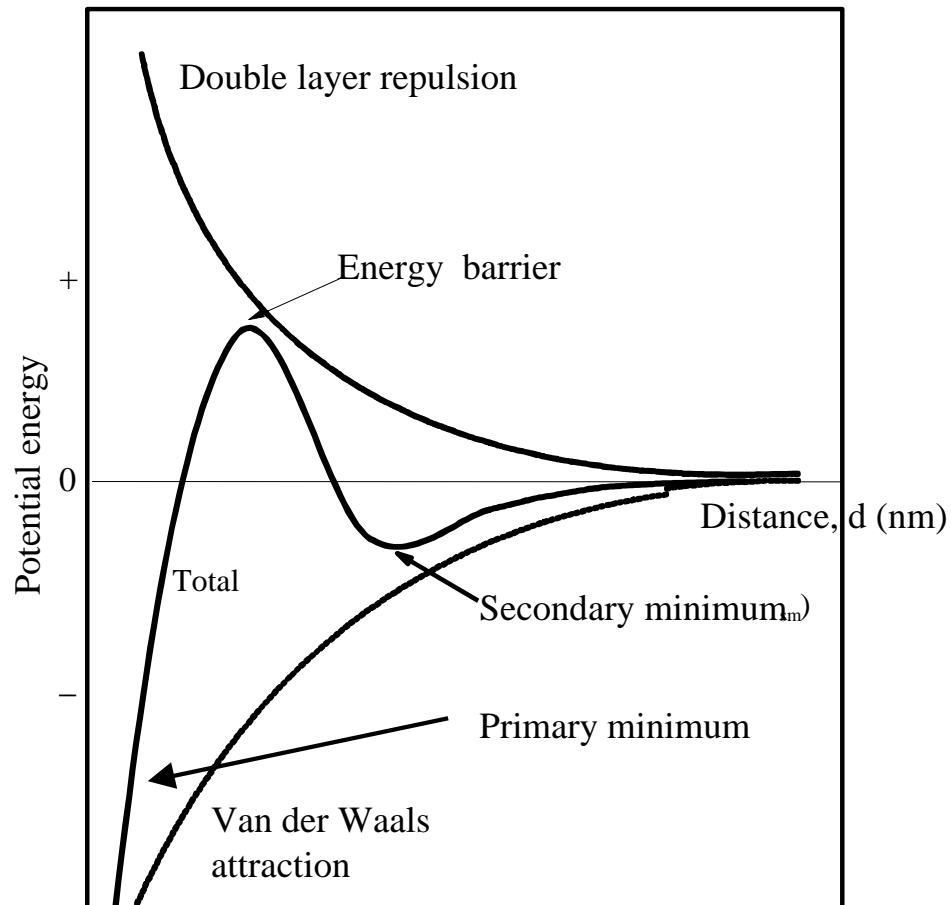
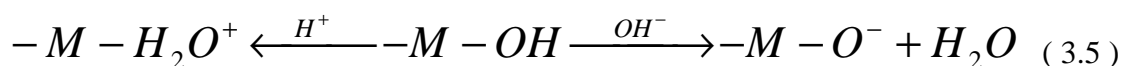


Figure 3.3: DLVO theory

EDL potential shows a positive (repulsive) exponential function, whose range depends on ionic strength (equation 3.3 and 3.4). Van der Waals is a negative (attractive) power-law function, which is insensitive to ionic strength (equation 3.2). Typically the sum of both reveal one maximum and two minima. The height of the maximum, if sufficiently large, will ensure an energy barrier resulting from the repulsive force resisting the approach of two particles. Only a few particles that have sufficient kinetic energy can “jump over” this barrier. Thus the system displays a long-term stability. Both minima are a consequence of the van der Waals attraction. If the depth of the primary minimum is sufficiently large, it can give rise to coagulation, always provided that the maximum can be surmounted at a kinetically significant

rate. In the secondary minimum, the particles are separated by a relatively large distance after coagulation, it leads to dispersed suspensions.

The range of the double layer repulsion can be modified by changing the ionic strength of the solution (equation 3.4). This mechanism provides also the possibility to vary the strength of the repulsion. For example, with many oxide surfaces in water, the charge is determined by proton association/dissociation with surface hydroxyl groups [61][62].



Charged oxide surfaces can be produced in water when the M-OH surface sites react with either H_3O^+ or OH^- ions. By controlling the pH, the net surface charge can be either positive (acidic conditions), neutral, or negative (basic conditions) (equation 3.5). The pH that produces a neutral surface is called iso-electric point (IEP). At IEP the thickness of double layer is zero, the van der Waals attraction dominates the interparticle reaction, thus flocculation occurs.

A surfactant can be coated on the surface to change the dielectric properties, and therefore the van der Waals attraction. But normally, it is not easy to control the van der Waals attraction. Surfactant adsorption are used to affect the forces in other ways. For example, the surface charge can be changed through ionic surfactant and repulsion force is modified, and van der Waals attraction can be influenced significantly, if the adsorbed surfactant layer is thick enough, which refers to steric stabilization or polymeric stabilization.

3.2.3 Polymeric stabilization

The spatial extension of polymer molecules of even modest molecular weights is usually comparable to, or greater than, the range of the London attraction between colloidal particles and of course greater than the range of van der Waals force. Hence polymer molecules are of the right dimensions to be used to impart colloid stability, provided that they do not interact and can generate repulsion. There is a minimum thickness of a polymer layer at the particles surface for stabilization. The minimum depends on the particle size and the magnitude of the Hamaker constant. One major advantage of macromolecules is that their dimensions are relatively insensitive to electrolyte concentration, unlike electrical double

layers. In addition, polymeric stabilization can be more powerful than electrostatic stabilization, providing stability for a longer time and at high solids loading. When flocculation or phase separation does occur, it is normally reversible, i.e. a suitable change in the solvent conditions will redisperse the particles spontaneously.

There are at present two different mechanisms whereby polymer chains can impart colloid stability: steric stabilization and depletion stabilization.

3.2.3.1 Steric stabilization

Steric stabilization of colloidal particles is produced by macromolecules that are attached (e.g. by grafting or by physical adsorption) to the surfaces of the particles. If enough polymer adsorbs, the thickness of the coating is sufficient to keep particles separated by steric repulsion between the polymer layers, and at those separations the van der Waals forces are too weak to cause the particles to adhere. This is presented schematically in Figure 3.4a. For small particles, Brownian motion is then sufficient to keep them suspended indefinitely.

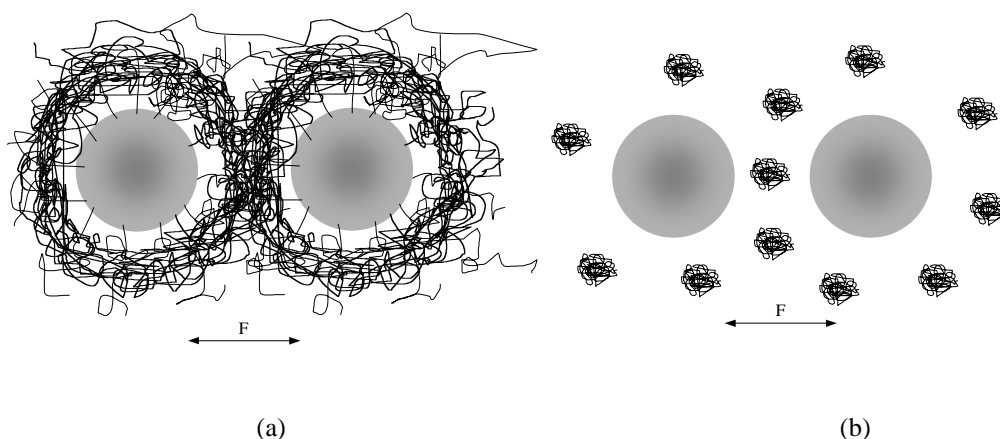


Figure 3.4: Schematic representation of (a) steric and (b) depletion stabilization

The steric repulsion can be regarded as a loss in configuration entropy that occurs when polymer chains of two particles interpenetrate. This produces an increase in the free energy of the system. The positive ΔG for polymer chain interpenetration which leads to steric stabilization is given in terms of the corresponding enthalpy and entropy changes by $\Delta G = \Delta H - T\Delta S$, and therefore, stabilization could be the result of a positive ΔH and/or a negative ΔS (83nap) [63][64]. A positive ΔH would reflect the release of bound solvent from

the polymer chains as they interpenetrate and a negative ΔS would reflect loss of configurational freedom as the polymer chains interpenetrate. If ΔH is positive and/or ΔS negative, the dispersion will be sterically stabilized at all accessible temperatures. However, if ΔH and ΔS are both positive, the dispersion should flocculate on heating above the theta-temperature (enthalpic stabilization), whereas if ΔH and ΔS are both negative, the dispersion should flocculate on cooling below the theta-temperature (entropic stabilization).

The interactions between particles for steric stabilization have not been quantified. To describe the magnitude and range of the interaction between polymer layers, the solution properties of the polymer and the conformations of the polymer at the solid-liquid interface need to be considered [65]. Repulsive steric forces for polymers in a good solvent can be characterized using de Gennes scaling theory [66, 67]. In this theory, the adsorbed polymer conformation is assumed to be either a low-surface-coverage “mushroom”, in which the volume of the individual polymer is unconstrained by neighbors, or a high-surface-coverage “brush,” where the proximity of neighboring polymer chains constrains the chain volume and causes extension of the polymer into the solvent. The repulsion U_s can be described as a function of temperature and geometry of the particles [68], in case of “Mushroom-structure” as:

$$U_s(D) \approx \frac{kT}{S^2 * f_1(D_1 L_1 \mathbf{d})} \quad (3.6)$$

and in case of “Brush-structure” as

$$U_s(D) \approx \frac{kT}{S^3 * f_2(D_1 L_1 \mathbf{d})} \quad (3.7)$$

where S is molecular distance, L_1 and δ are thickness of polymer in good and bad solvent for the polymer. D is the distance between two particles and k is Boltzmann constant.

3.2.3.2 Depletion stabilization

Depletion stabilization differs from steric stabilization in that the stability is imparted not by attached polymers but by macromolecules that are free in solution (Figure 3.4b). An

approach of the particles is accompanied by demixing of the polymer molecules and the solvent in the interparticle region. This process needs a force to extrude polymer out of the interparticle region. It corresponds to a repulsion between the particles that can lead to stabilization of the suspension

3.2.4 Combinations of stabilization methods

It is possible to combine electrostatic and steric stabilization, what has been termed electrosteric stabilization. The electrostatic component is supposed to originate from a net charge on the particle surface (Figure 3.5a) and/or charges associated with the polymer attached to the surface (i.e. through an attached polyelectrolyte) (Figure 3.5b). Electrosteric stabilization is common in biological systems.

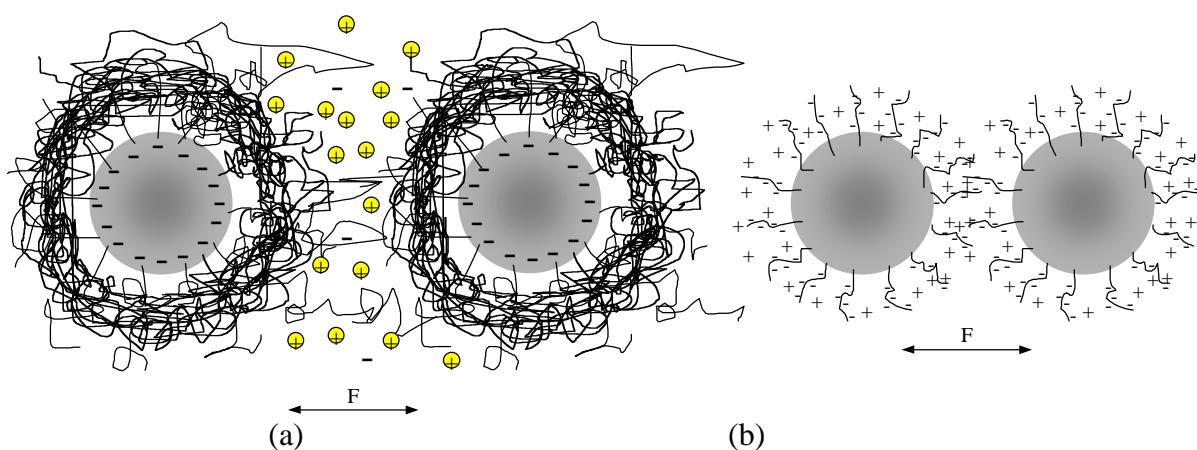


Figure 3.5: Schematic representation of electrosteric stabilization: (a) charged particles in combination with nonionic polymers and (b) polyelectrolytes attached to uncharged particles.

In addition to electrosteric stabilization, it is possible to have combinations of depletion stabilization with both steric and/or electrostatic stabilization. The combination of depletion and steric stabilization is quite common at high concentrations of free polymer in the dispersion medium.

3.3 Methods for coagulation

According to the general principles of colloidal stability, different methods are used to coagulate a dispersion, so that successful ceramic processing can be achieved.

3.3.1 Modification of the electrical double layer

In electrostatic stabilized systems, the repulsive force is dominated by the electrical double layer. The stability of the suspension can be controlled by the modification of the electrical double layer. According to expression (3.3) and (3.4), the electrical repulsive force is exponentially affected by the surface ion concentration and charge of ion in suspension. The total force in such a system is combined from van der Waals force and electrical repulsive force.

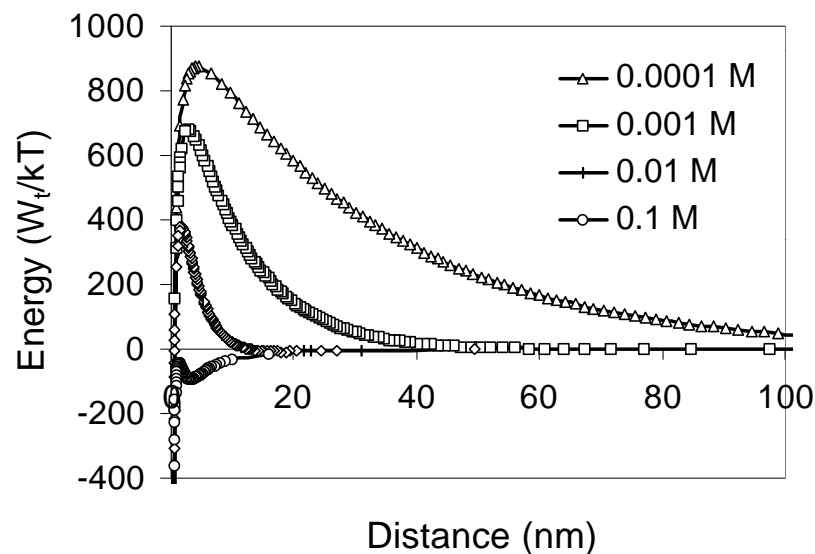


Figure 3.6 Effect of ion concentration on interparticle potential in colloidal suspension (calculated using STABIL [69])

Figure 3.6 shows the total interparticle potential between two colloidal particles at different KNO_3 concentration. In 0.0001M solution, a very high energy Barrier must be overcome for approaching of two colloidal particles. As a consequence, the suspension is very stable. In 0.1 M KNO_3 solution, the energy barrier is rather small and the colloidal particles

coagulate easily. It is reasonable to change the ion concentration to coagulate or disperse colloidal particles.

3.3.2 Changing steric layers

In steric stabilized systems, van der Waals attraction is prevented by an adsorbed polymer layer. Typically, the adsorbed polymer can be desorbed to eliminate steric stabilization or partly desorbed to form bridging flocculation [58]. The magnitude and range of the interaction between polymer layers can be related to the solution properties and the conformation of the polymer at the solid-liquid interface. At a critical solvency level, the sterically stabilized dispersion flocculates. The solvency can be changed through temperature change and by the addition of non-solvent [70, 71]. In principle, all sterically stabilized system can be flocculated through decreasing solvency, but many system flocculate far from room temperature [53].

4 Powder characterization

In colloidal processing powder characterization is crucial to fully analyze the rheological behavior and to understand the surface chemistry. The powder characteristics as particle size, surface area, surface function groups, bulk element and zeta potential are disclosed by Laser granulometry, BET, FTIR, XRD, ICP-OES and zeta potential.

4.1 BET

BET (Brunauer-Emmett-Teller) analysis is employed to determine the surface area, pore size and pore size distribution by nitrogen adsorption. With a Micromeritics Gemini (Micromeritics, Neuss, Germany), the specific surface area of the powder is derived from the nitrogen adsorption isotherms measured at the temperature of liquid nitrogen.

Before the measurement the powder is heated to 200°C for 30 minutes under nitrogen in order to remove the physisorbed water. The results are shown in table 4.1.

4.2 Laser granulometry

The particle size of the powder is determined using a laser particle size analyzer (Mastersizer 2000 Particle Analyzer; Malvern Instrument Ltd., United Kingdom).

In order to avoid agglomeration, deagglomeration methods were used, which include ultrasonic treatment (Branson Sonifier 450) and planetary ball milling with dispersant and pH adjustment. (table 4.1)

Silicon carbide A10 (SiC) (10 vol%) was ball milled at pH 10 and with Polyethylenimine (PEI) as dispersant for 2 hours, respectively. The suspensions were used to determine the particle size with and without ultrasonic treatment. The results are shown in Figure 4.1.

SiC powder dispersed by pH adjustment at pH 10 without ultrasonic treatment has a broad size distribution of 1.58 μm at $d(0.5)$ (curve SiC-KOH-0-U). SiC powders dispersed

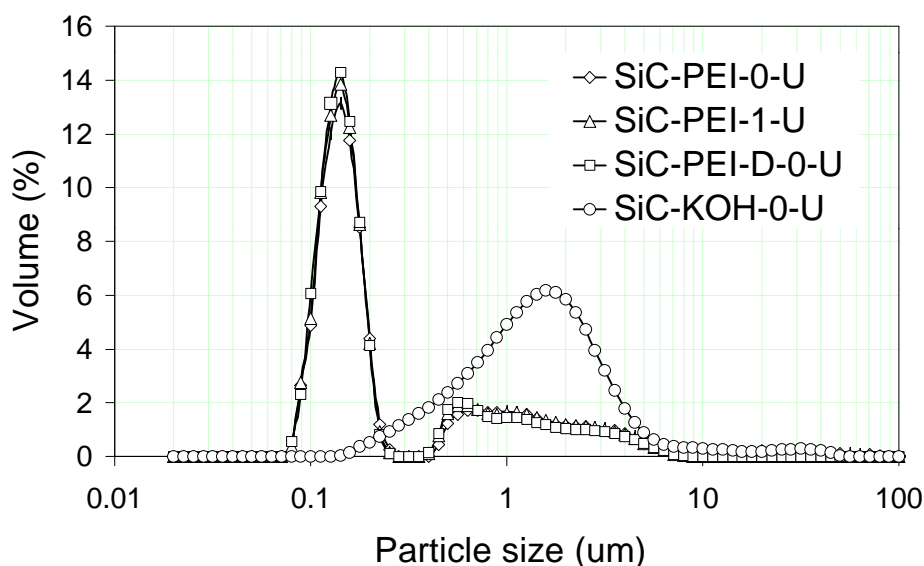


Figure 4.1: Particle size distribution of SiC: 1) SiC-KOH-0-U is SiC powder dispersed with two hours ball milling at pH 10 and without ultrasonic treatment; 2) SiC-PEI-0-U is SiC powder dispersed with dispersant and without ultrasonic treatment; 3) SiC-PEI-1-U with dispersant and one minute ultrasonic treatment and 4) SiC-PEI-D-0-U with degas after ball milling and without ultrasonic treatment

through dispersant, no matter with or without ultrasonic and degas treatment after ball milling, have a size distribution 0.15 μm at $d(0.5)$ (curves SiC-PEI-0-U, SiC-PEI-1-U and SiC-PEI-D-0-U). That means, by using Mastersizer 2000 Particle Analyzer SiC powder size can not be deagglomerated by pH adjustment. However, by using polymer as dispersant, no further deagglomeration method is needed for the measurement.

The dispersion of yttrium oxide (Y_2O_3) powder was attempted using planetary ball milling, pH adjustment and using a dispersant. The results are shown in Figure 4.2.

Using ball milling for half an hour the particle size distribution can be analyzed without ultrasonic treatment (curve 0-U in Figure 4.2). Y_2O_3 powder could be also dispersed using pH adjustment by HNO_3 (pH at 3) (HNO_3 -0-U). The same is with tri-ammonium citrate as dispersant (TAC-0-U and TAC-1-U). TAC-0-U curve shows Y_2O_3 particle size distribution dispersed by dispersant TAC and without ultrasonic treatment and TAC-1-U with one minute

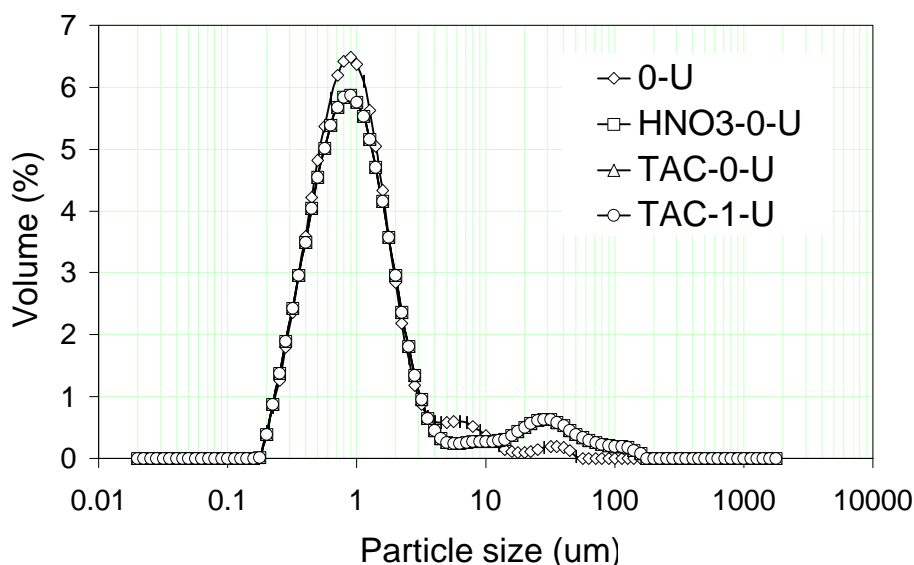


Figure 4.2: Particle size distribution of Y_2O_3 1) Y_2O_3 powder dispersed in water by physical stirring (0-U); 2) dispersed at pH 3 using 0.1M HNO_3 (HNO3-0-U); 3) dispersed by TAC (TAC-0-U); and 4) dispersed by TAC and one minute ultrasonic treatment (TAC-1-U)

ultrasonic treatment before measurement. The curves show similar results, with a $d(0.5)$ value of $0.89 \mu m$. This hints that size distribution of Y_2O_3 powder can be determined by Mastersizer 2000 Particle Analyzer without further dispersing treatment.

AlN powder reacts very strongly with water. Therefore, it was protected by a coating layer of Si-Al-O-N. The detail is described in chapter 6. After coating AlN powder is stable in water and can be used for measurement by Mastersizer 2000 Particle Analyzer. Figure 4.3 shows the results with and without ultrasonic treatment.

AlN was dispersed by planetary ball milling for half an hour and stirred in water to determine the particle size distribution (curve AlN-0-U in Figure 4.3). The $d(0.5)$ value is $0.89 \mu m$. After AlN was dispersed by half minute ultrasonic treatment additionally, the particle size shifts to $1.58 \mu m$ at $d(0.5)$. It is supposed that AlN reacts with water through ultrasonic and produces $Al(OH)_3$, which precipitates at the AlN surface and enlarges particle size.

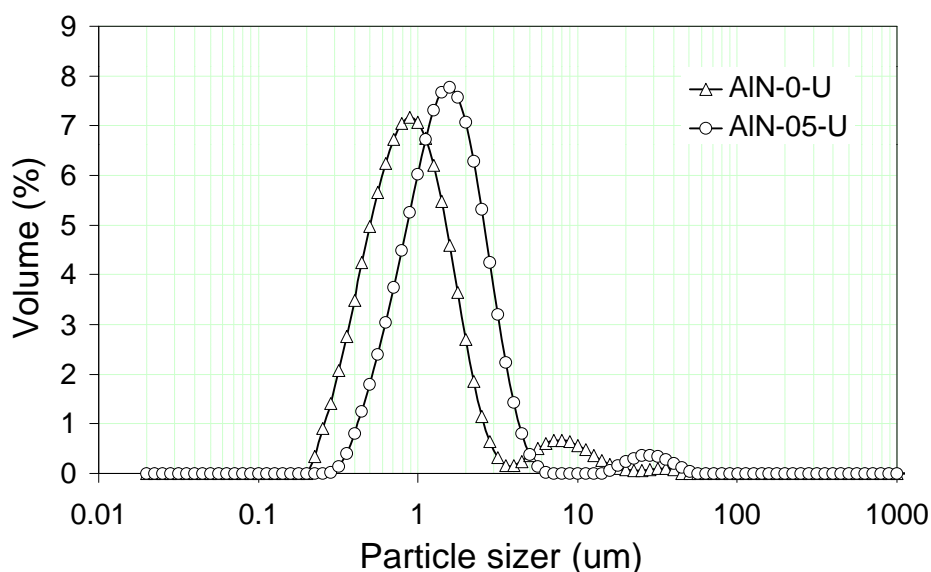


Figure 4.3: Particle distribution of AlN 1) AlN powder is dispersed by physical stirring (curve AIN-0-U); and 2) by half a minute ultrasonic treatment additionally (curve AIN-05-U)

4.3 XRD

Crystallinity of powders was checked by powder X-ray diffraction. The crystallographic phases of the powders are listed in (table 4.1). Data were determined by XRD, using Cuká radiation D 5000 diffractometer (Siemens, Germany).

4.4 Chemical analysis

The bulk elemental composition was chemically analyzed using ICP-OES in Argon (Inductively Coupled Plasma – Optical Emission Spectroscopy; Jobin Yvon, Grasbrunn, Germany). The carbon was reacted with O_2 to CO_2 which was determined by an infrared detector (Elementar Vario EL). The oxygen content was examined by TC-436DR (LECO Corporation; St. Joseph, MI, USA). Using this method the samples were first burned before measurements in order to remove the physisorbed O_2 and the rest of free O was reacted with C to CO_2 which was also determined by the infrared detector. (table 4.1)

Table 4.1: Physical and chemical properties of powders

Properties/powder		SiC A10	Y ₂ O ₃	AlN
BET special surface area (m ² /g)	Company result	15.4	14.7	4.7
	Experimental result	11.4	12.9	4.8
Particle size (d _{0.5} , μm)	Company result	0.60	0.27	1.0
	Experimental result	0.15	0.89	0.89
Crystallographic phases (H: Hexagonal, C: Cubic)		α-SiC (H)	Y ₂ O ₃ (C)	AlN (H)
Content (wt%)	C	Company result	30.17	0.07
	O	Company result	0.86	1.6
		Experimental result	0.81	1.96
	Fe	Company result	0.02	0.0035
	Al	Company result	0.04	Balance
		Experimental result		Balance
	Ca	Company result	0.008	
	N	Company result		33.1
Experimental result		0.06	32.08	

* all powders are from H.C.Starck Germany.

4.5 FTIR

Diffuse reflectance infrared fourier transform spectroscopy (DRIFTs) was used to analyze the surface of dry powders. The results are shown in Figure 4.4, Figure 4.6 and Figure 4.7.

As Figure 4.4 shows, with as-received SiC powder peaks at 1590, 1600 and 1000 cm⁻¹ indicate N-H bonds in Si₂-NH and Si-O-Si bonds, respectively [72, 73, 74]. The surface of SiC is covered by a thin layer of SiO_x (x=1-2) [75, 76]. NH groups result from powder preparation. The SiO_x layer defines the surface charge of the powder. If the SiC powder is immersed in water, in the beginning the pH value of the slurry is 3 (Figure 4.5) because SiO_x

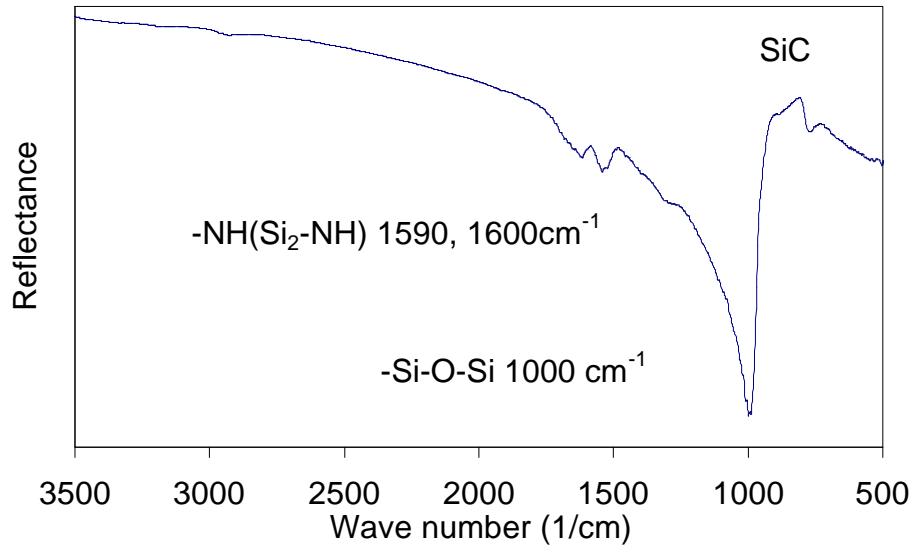
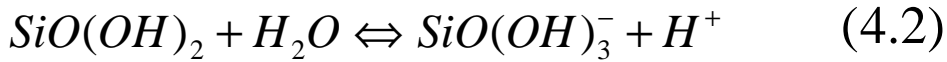
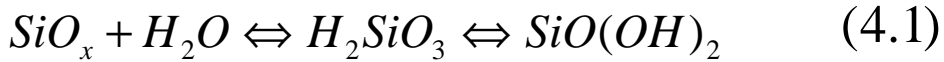


Figure 4.4: DRIFT spectrum of as received SiC powder

dissolves in water:



Through ball milling the fresh surface of SiC is exposed as well as Si₂-NH bonds, which display basic properties in water (equation 4.3) [77]:



Figure 4.5 shows the experimental results of 5 and 10 volume percent SiC slurries. In the beginning of ball milling pH=3.2, which is similar to the pH of the isoelectric point (Figure 4.11). After ball milling for 12 hours, the pH rises to pH=8. If the surface contains only amino groups the pH will be pH=9 [78].

The DRIFT spectra of Y₂O₃ and surface modified AlN (Figure 4.6 and Figure 4.7) contain OH groups and H-bond from adsorbed H₂O at the surface, which are shown through

peaks in the range of $2600\text{-}3800\text{ cm}^{-1}$ [79, 80]. According to equation (3.5), powder surfaces display different properties under different conditions.

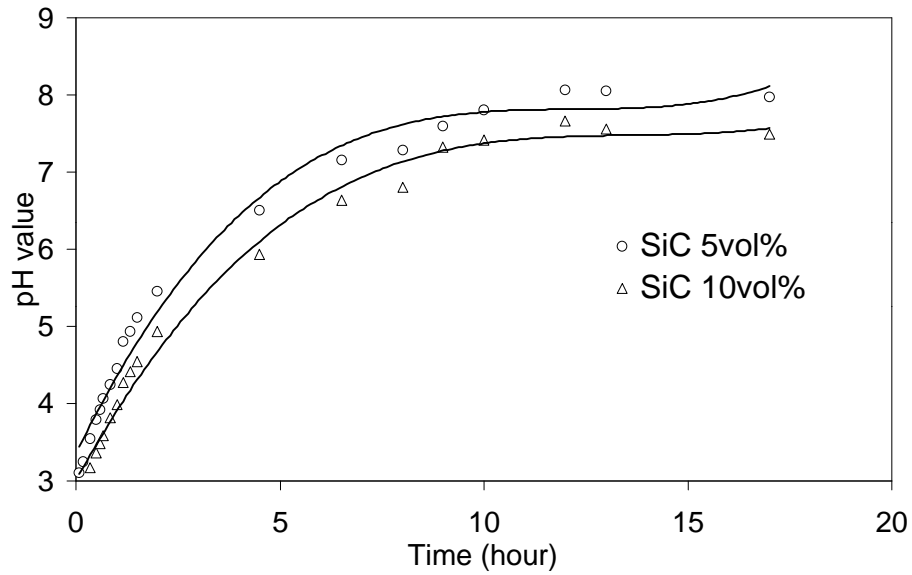


Figure 4.5: pH change of suspension with milling time

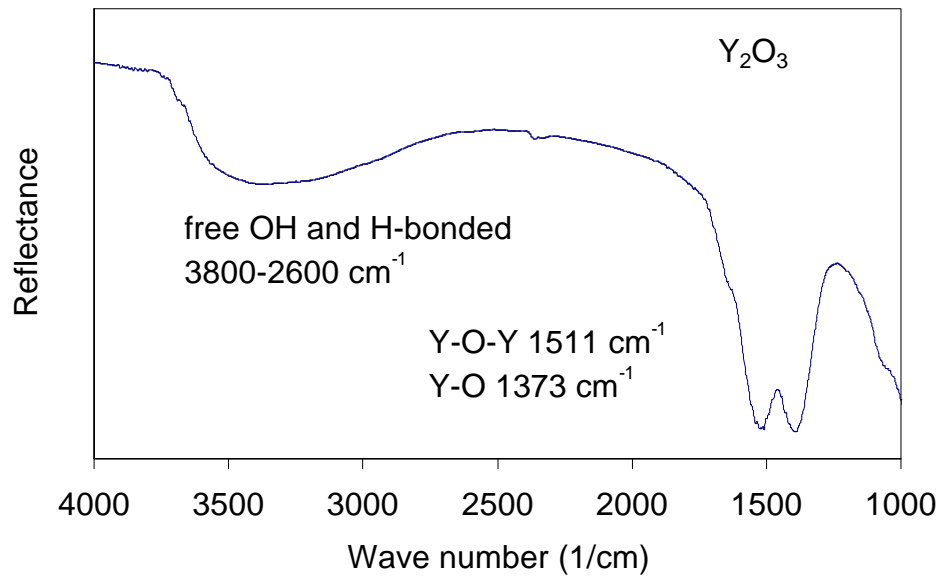


Figure 4.6: DRIFT spectrum of as received Y_2O_3 powder

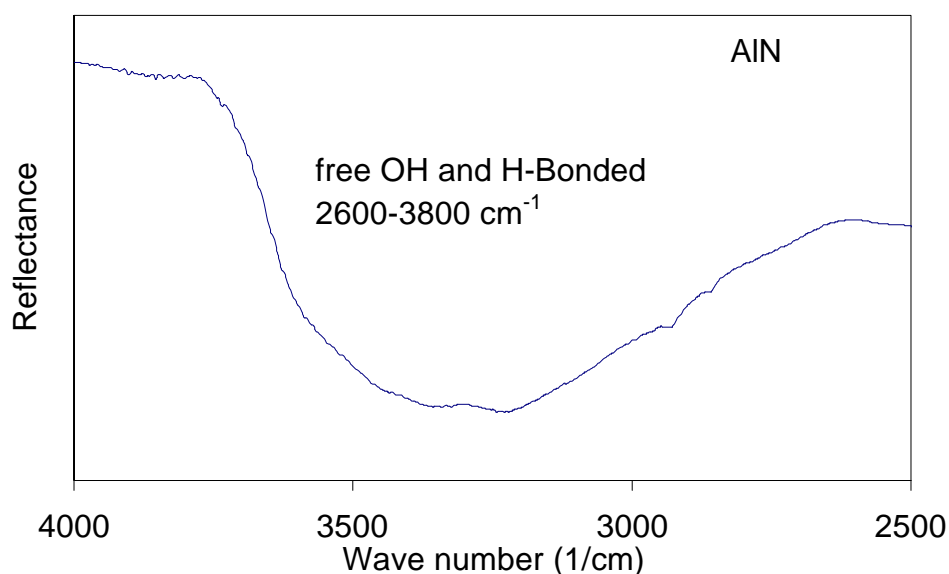


Figure 4.7: DRIFT spectrum of modified Si-Al-O-N AlN powder

4.6 Sedimentation

For sedimentation studies of SiC, 5 g SiC powder were dispersed in 20 ml distilled and deionized water at different pH using calibrated glass cylinders. The suspensions were dispersed by shaking and ultrasonic treatment for 15 min and put undisturbed and isolated for a time period of several days up to several months. Dispersed particles have a smaller sediment volume, which means higher packing density, whereas agglomerated particles pack loosely (Figure 4.8). The sediment density of the powder was calculated according to the theoretical density of SiC (3.22 g/cm^3) and is given in table 4.2.

Table 4.2: Sediment density of SiC suspension at different pH value

PH		3.4	5	9	10	11	12	14
Sediment density of theoretical density(%)	12 days	11.8	12.1	-	40.9	37.0	33.8	34.5
	30 days	11.9	12.3	33.8	40.9	40.9	37.0	37.0
	175days	11.9	12.3	37.0	40.9	40.9	40.9	38.8

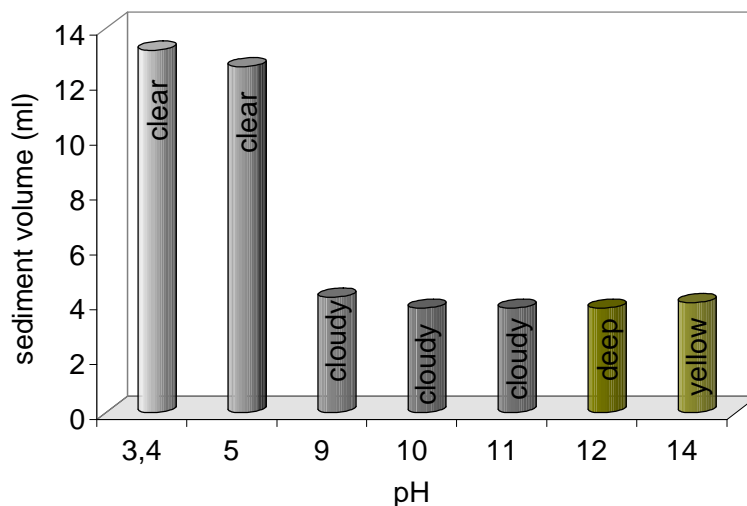


Figure 4.8: Sediment volume of SiC suspension versus pH after 175 days

From the results, it can be suggested that SiC powder disperses above pH 10 by electric double layer repulsion. At pH 14, SiC powder is partly dissolved and the suspension shows a color change from clear to yellow.

4.7 Zeta potential

According to the DLVO theory, the stability of a colloidal suspension is determined by the balance between the repulsive and attractive forces. The stability of SiC slurry is caused by the particle charge (electric double layer) and the repulsion force depends on the degree of double layer overlap [81]. The attractive force is provided by the van der Waals interaction, which depends on d^{-n} where $2d$ is the separation between the particles and $n=3-4$. The total potential energy of interaction, V_R (equation 3.3), can readily be changed by modifying the magnitude of the repulsion, either by increasing the ionic strength of the solution (adding indifferent electrolyte) or changing the surface potential of the particles [87, 82]. Thus, surface charge plays a critical role in aqueous systems.

As Figure 3.2 shows, surface charge (Y_0) can be indicated by electrical double layer. The actual measurement of Y_0 is not practical. A more useful and often very similar value is the zeta potential, which is defined as the potential at the shear plane around the particle and normally located very close to the Stern plane [83]. Therefore, zeta potential measurements are used to determine the potential the powder. In this work, the zeta potential is determined

using a Zeta-Plus zeta potential analyzer (Brookhaven Instruments Corporation, Holtsville, New York, US). This equipment uses the Doppler shift in the laser light scattering from the particles to obtain a mobility spectrum.

4.7.1 Optimal measuring condition

The zeta potential depends on the measuring condition. In order to find an accurate and realistic value in the suspension, the following tests were carried out.

4.7.1.1 Solution concentration

To analyze the influences of the salt concentration onto the zeta potential, measurements have been done with suspensions without and with salt concentration of 0.1, 0.01, 0.001 and 0.0001 M. Zeta potential values measured with salt concentrations higher than 0.01M are stable and reproducible. With a salt concentration lower than 0.001M, zeta potentials with high absolute values are obtained, but not reproducible. With a salt concentration higher than 0.1M, the zeta potential is relatively low. Since such high salt concentrations is less related to the real situation in ceramic powder processing, a solution with 0.01M salt concentration was selected for further investigations.

4.7.1.2 Solution selection

Zeta potential reports the surface charge of powders in suspension. Using different salts as electrolyte, varying results can be obtained. Figure 4.9 is a comparison of zeta potential measurement with different salts. The results indicate that higher zeta potential values can be obtained using KCl as solution compared to KNO₃. It is suggested that the diameter of Cl⁻ is similar with the ions (O⁻) on the powder surface and that Cl⁻ can be exchanged with surface ions to get higher zeta potential value. The diameter of NO₃⁻ is bigger than other surface ions, as for example, O⁻ in Si-OH, and has little influence on the measurement. In the following experiment a KNO₃ solution with a concentration of 0.01M was selected.

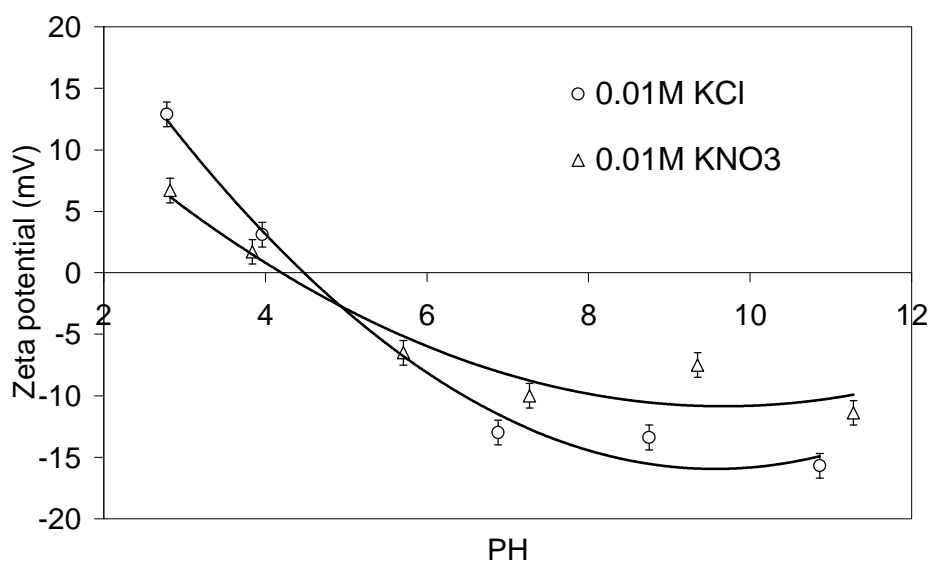


Figure 4.9: Salt effect on zeta potential measurement of SiC powder (SiC suspension with 0.01M KNO_3 and KCl salt concentration)

4.7.1.3 Ball milling time

In order to determine the zeta potential value under similar conditions as the slurry preparation in ceramic processing, ball milling is used as a dispersing method. Figure 4.10 shows the influence of ball milling time on zeta potential result. Using 7 hours ball milling SiC dissolves easily at higher pH. This increases ion concentration in solution and decreases surface charge at SiC surface. Because of that, the absolute value of zeta potential decreases at higher pH. Typically, the suspension is ball milled for 2-4 hours to obtain stable surface properties.

4.7.1.4 Measuring condition

10 vol% SiC suspension with distilled and deionized water content with a background electrolyte concentration for KNO_3 of 10^{-2} M is prepared. This suspension is ball milled with medium speed for 2 hours. Then one drop of the suspension is put into one liter 10^{-2} M KNO_3 solution. After the suspension is redispersed for 15 minutes in an ultrasonic bath it is used to measure the zeta potential. 0.1 M KOH and HNO_3 are used to adjust the pH value of suspension.

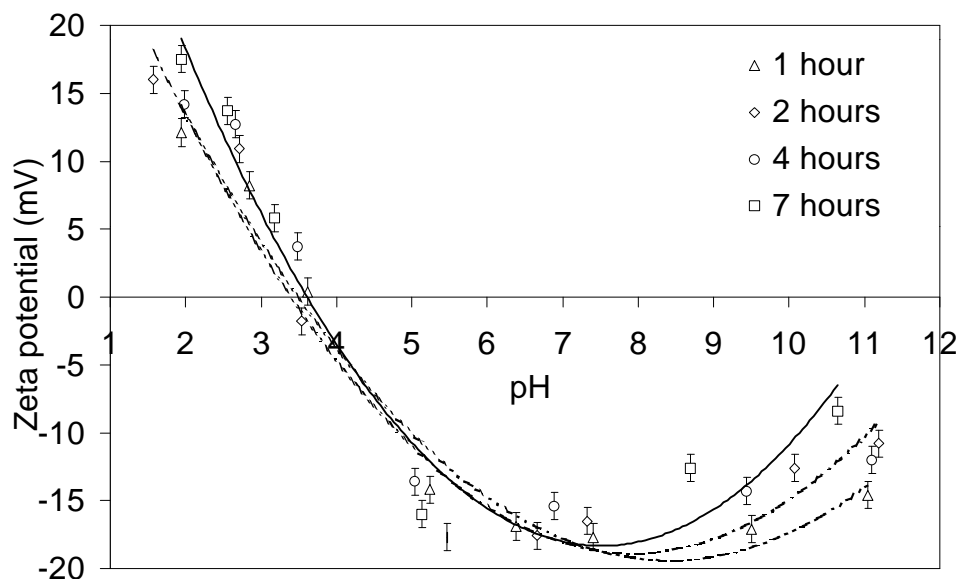


Figure 4.10: SiC powder zeta potential at different time of ball milling (SiC suspension with 0.01M KNO_3 salt concentration)

4.7.2 Zeta potential results

The zeta potential of SiC, Y_2O_3 , SiC with 10 vol% Y_2O_3 and modified AlN are measured. The optimized condition as described above were used. According to that a 10 vol% suspension is prepared through ball milling. one drop of suspension is added to one liter 0.01M KNO_3 solution and before measurement, the solution pH is adjusted by 0.01M HNO_3 and KOH.

As Figure 4.11 shows, the powder gets charged in water because of the reaction of surface hydroxyls with the aqueous media. For SiC the pH_{IEP} is about 3.4, this means that if the pH value is less than 3.4, the surface of SiC is positively charged and if the pH is above 3.4, the surface is negative. At pH 2 the potential is 12mV, which is the maximal measured value when the surface is charged positively. At $\text{pH} > 8$ the potential is -24mV when the surface is negatively charged. The higher the surface potential, the more stable the slurry can be made. As a result, the SiC slurry should be adjusted to $\text{pH} > 8$ in order to get a stable slurry. According to literature reports, the isoelectric point of SiC attains a value close to that of silica (pH2-3.7) due to a SiO_2 thin film on the SiC surface. The zeta potential of α -SiC and β -SiC were reported to be pH 3.2 and pH 2.6, respectively [99]. It was also measured by

Whitman [84] and Persson [85], the values were around pH 2.5 to pH 3.5 for α -SiC and pH 3.4 for β -SiC.

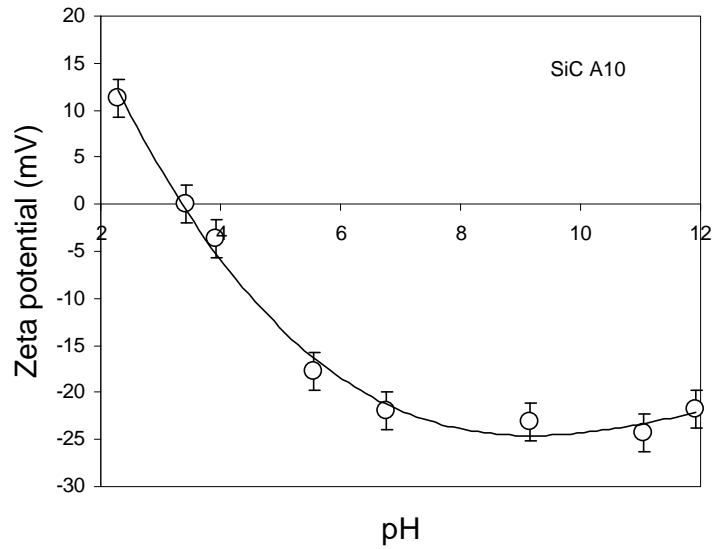


Figure 4.11: Zeta potential of SiC suspension (0.01M KNO₃ solution)

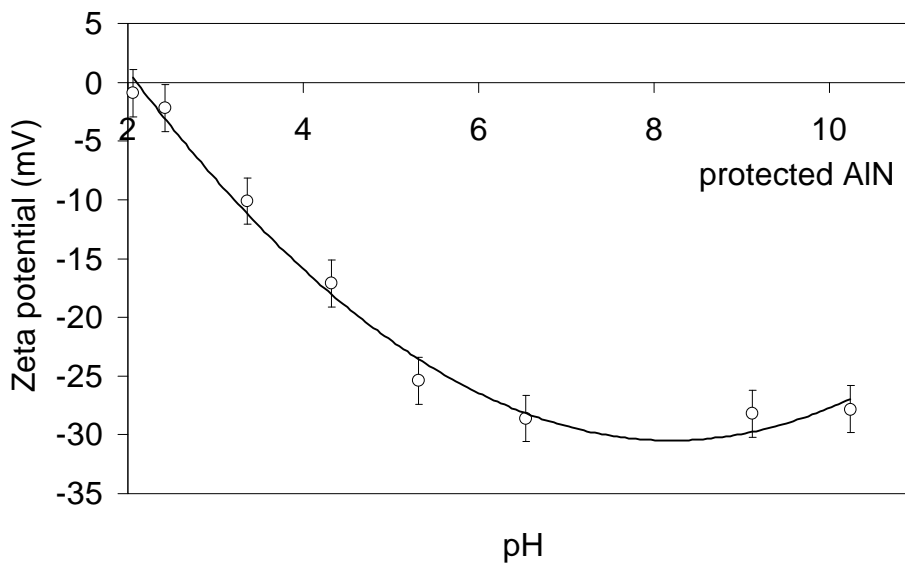


Figure 4.12: Zeta potential of modified AlN powder(0.01M KNO₃ solution)

AlN powder reacts with water and its zeta potential can not be measured directly in water. Therefore, the zeta potential of AlN is determined after it has been protected through an oxide layer of Si-Al-O-N, which is formed through the reaction of silicate with the AlN surface and bonded to the AlN surface (details will be reported in chapter 6). Upwards from pH 2 the protected AlN surface is negatively charged (Figure 4.12). The absolute zeta potential reaches a maximum of 30 mV at pH 7. It can be supposed that protected AlN suspensions should be stable at pH>7.

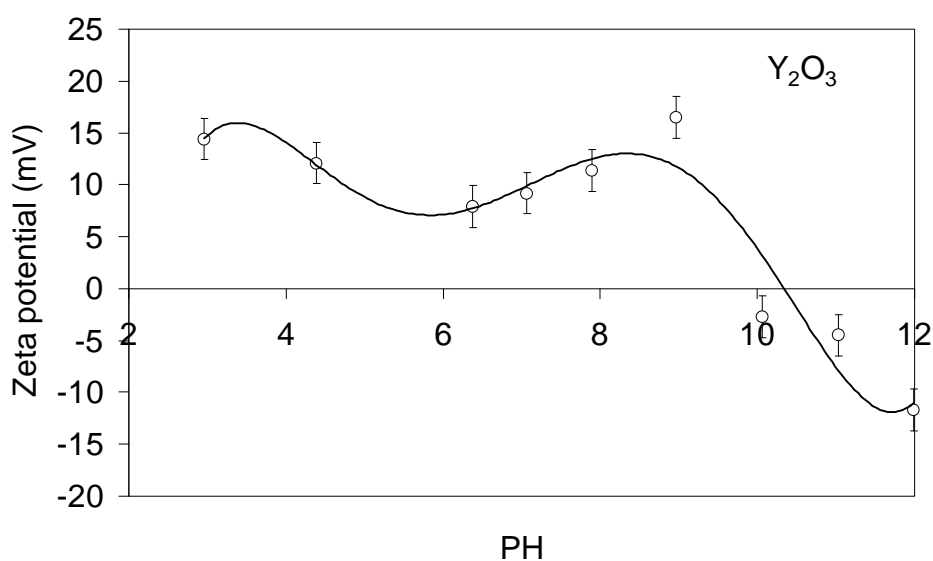


Figure 4.13: Zeta potential of Y_2O_3 powder (0.01M KNO_3 solution)

For Y_2O_3 the pH_{IEP} is 10.3 (Figure 4.13), in the considered processing windows the Y_2O_3 powder is charged positively if no specific adsorbing molecules are introduced. The reason for the minimum in the curve can be explained by the solubility behavior of Y_2O_3 powder in water.

Figure 4.14 shows the Y_2O_3 solubility at room temperature, which is calculated using OPAL. OPAL is a computer program for the calculation of the solubility of oxide in aqueous solutions, which is developed by R. V. Linhart and J. H. Adair at University of Florida [86].

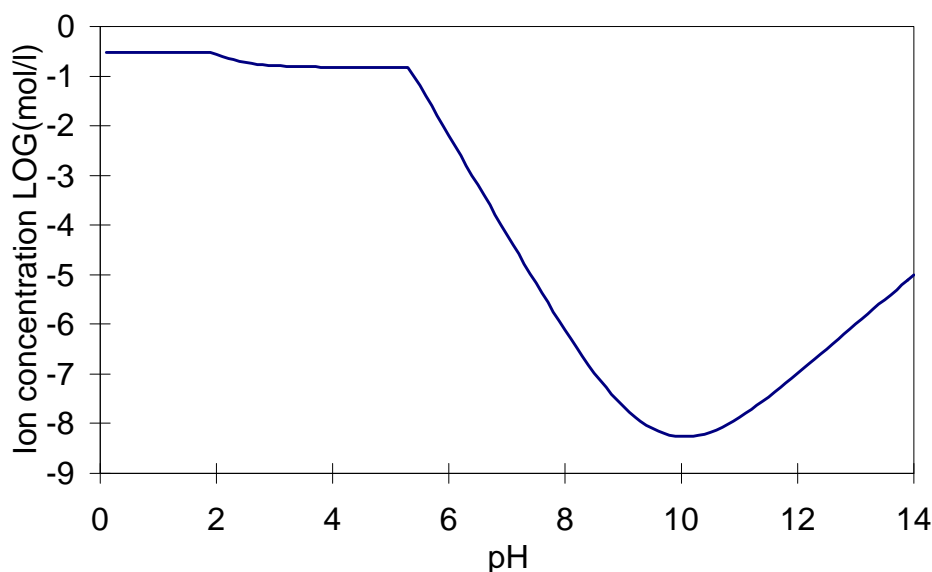
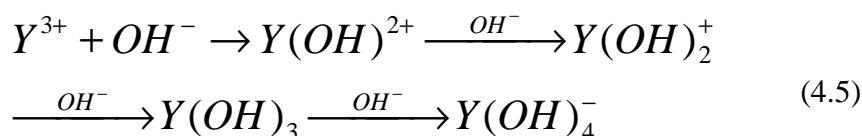
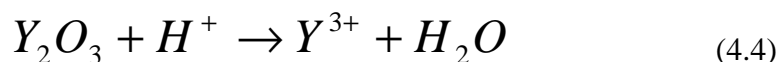


Figure 4.14: Calculated solubility of Y_2O_3 in water

The reaction of Y_2O_3 powder in water can be expressed as follows:



At low pH the Y_2O_3 powder surface is positive because it is terminated by Y^{3+} . With increasing pH Y^{3+} is substituted by $Y(OH)^{2+}$ and $Y(OH)_2^+$, thus the Y_2O_3 surface charge decreases. However, at $pH > 6$ the solubility of Y_2O_3 powder decreases significantly and the surface is covered by more positive ions, which leads to an increasing of surface charge. Up to pH 9, $Y(OH)_4^-$ becomes the majority at the Y_2O_3 surface. Therefore, the Y_2O_3 surface charge decreases and becomes negatively charged at $pH > 10.3$.

In any case, the absolute zeta potential value is not high enough for a stable suspension (smaller than 25 mV [87]).

5 SiC suspension preparation

From the results of previous chapters, SiC suspensions are prepared using pH adjustment for a electrostatic stabilization and using dispersant for a steric stabilization.

5.1 Slurry formation with pH adjustment

SiC powder is hydrophobic due to the adsorption of milling media in powder preparation processing, for example isopropanol [78]. It becomes hydrophilic in water by agitating. Using ball milling, SiC powder can be dispersed in water at a certain pH range.

5.1.1 Colloidal property calculation by STABIL program

STABIL is a computer program for calculation of interparticle potentials between two particles, which was developed by R. V. Linhart and J. H. Adair at the Pennsylvania State University [69]. The program takes the DLVO theory one step further by calculating interaction energy curves for systems with two different types of particles, as well as systems where a polymer layer is present at the particle surface. It has been written in a way that it accepts the necessary input variables, which include Hamaker constants from the material, ion concentration, zeta potential and pH value, and performs these calculations to generate curves for certain types of particle-solvent systems (equation 3.3 and 3.4). In Figure 5.1, the Hamaker constants were calculated by L. Bergström [72]. The SiC zeta potential was determined using a Zeta-Plus zeta potential analyzer (Figure 4.11). A summation of H^+ , OH^- , $HSiO_3^-$ [88] (Figure 7.3) and balance charge ion is inputted as the ion concentration in suspension.

The result is shown in Figure 5.1. The coagulation probability is defined according to DLVO theory. It equals to 1, if the energy barrier (Figure 3.3) is zero meaning a complete coagulation, and it equals to 0, if the energy barrier is infinite high meaning a perfect dispersion. Typically, a suspension is regarded as coagulated when the energy barrier is below 25 kT. At this condition the particles can jump over the barrier and form agglomerates. Corresponding to 25 kT, the coagulation probability is 0.5. In other words, in the pH range

4.5-10 SiC powder is dispersed in water according to theoretical calculation. Above pH10 and below pH4.5 SiC powder tends to agglomerate.

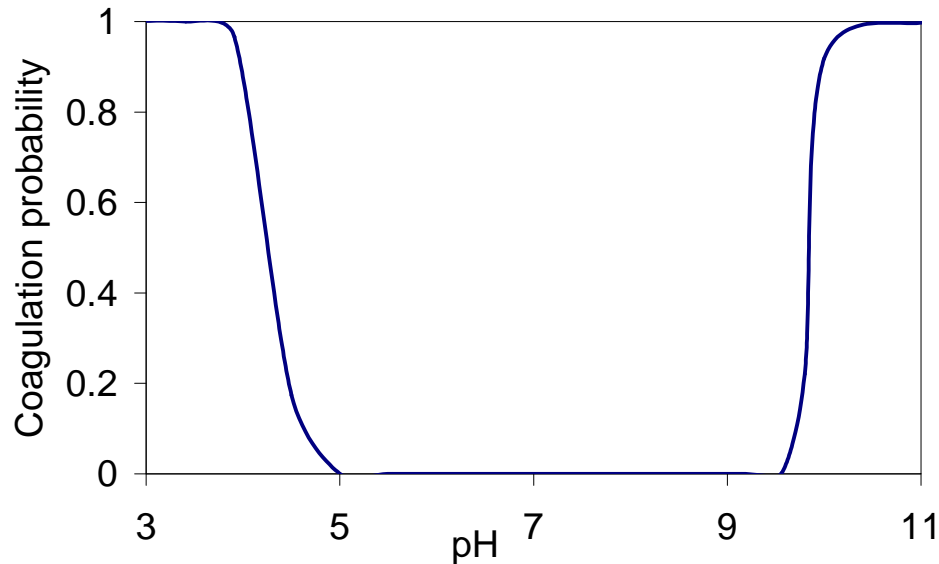


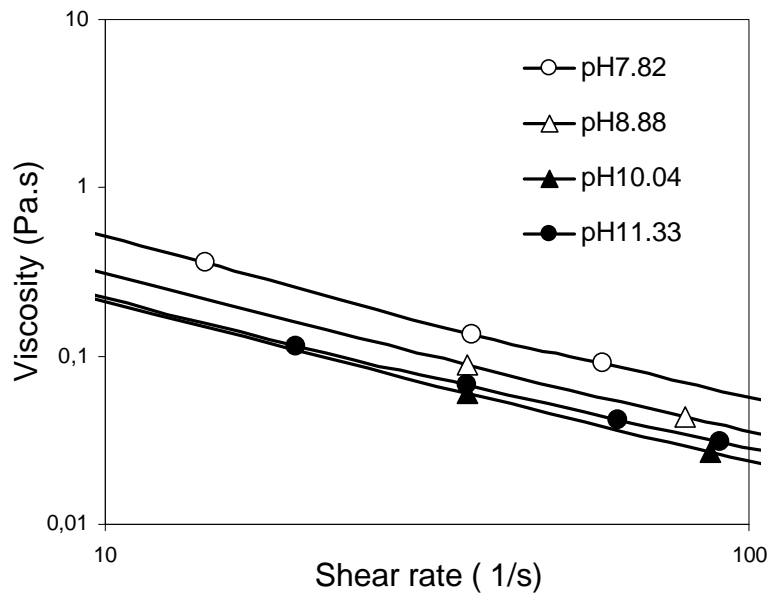
Figure 5.1: Coagulation probability of a SiC suspension

5.1.2 Viscosity measurements of SiC suspensions

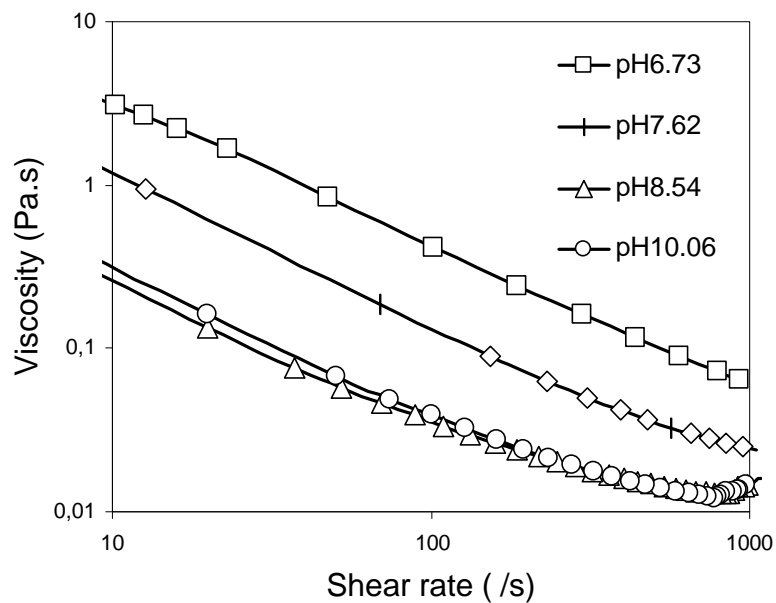
SiC powder is first added into distilled and deionized water adjusted to pH=10 by NH_4OH , followed by homogenizing using a ball mill (planetary ball mill with SiC balls) for two hours in a polyamide container. The viscosity of the slurry is determined by a rotational viscometer (SR500, Rheometric Scientific, USA). A conic cylinder geometry is used for measurement. The measurements were carried out using a steady shear method in the shear rate $0.1\text{-}1000\text{ s}^{-1}$ at constant temperature of 25°C . Before testing, the instrument is calibrated by setting the zero point and geometry. The testing condition is set according to the fluidity of the slurry. 13 ml slurry is needed for each measurement.

The results are shown in Figure 5.2a) and b). At a given shear rate the viscosity decreases with increasing pH value. It reaches a minimum value with a pH value between pH9 and pH10.

At both solid loading (10 vol% and 20 vol%), the viscosity decreases with increasing pH value. However, whereas at 10 vol% solid loading the viscosity decreases only slightly



a) 10vol% SiC suspension (at 25°C in 0.01M KNO₃ solution)



b) 20vol% SiC suspension (at 25°C in 0.01M KNO₃ solution)

Figure 5.2: Relationship of viscosity and pH value of SiC suspension

and stays almost content above pH 10, it decreases more significantly at 20 vol% solid loading due to a stronger interaction between particles of higher solid loadings. Above pH 9, the viscosity reaches a minimum. This correspondences with the zeta potential curve of SiC in

Figure 4.11, which reaches a maximum above pH 8-9. In the following preparation of SiC suspension, pH is adjusted to pH 10 for a minimum viscosity.

5.1.3 Empirical SiC viscosity model

An experimental model for predicting the viscosity of SiC suspension stabilized using electrical double layer is presented in this work. Viscosity depends on solid loading and is a power function of solid loading. The model is calculated according to some experimental data of viscosity and can be expressed with the following equation (5.1):

$$V=aR^{-0.89} \tag{5.1}$$

$$a=0,35(1-\varnothing)^{-10,04}$$

where V is viscosity in Pa.s, a is a parameter related to solid loading and powder colloidal properties, R is shear rate in reciprocal of second (1/s) and \varnothing is solid loading in volume percent.

SiC suspensions at different solid loading were prepared using ball milling for 2 hours at pH 10 and their viscosities were measured at same pH value. The experimental points are reported together with calculated fit curves in Figure 5.3.

The figure shows the measuring points fit into the calculated curve at shear rates ranging from 1 to 100 s⁻¹ at pH 10 and at room temperature. The viscosity of SiC suspensions at room temperature can be represented by the model. Viscosities for $\varnothing \leq 30$ vol% are below 1 Pa.s at a shear rate of 20 s⁻¹, which is acceptable for casting technique. Slurries with $\varnothing > 50$ vol% have a viscosity above 20 Pa.s at a shear rate of 20s⁻¹, which does not allow to cast the slurries in a mold.

5.2 Slurry formation with polymer as dispersant

The presence of hydrophilic silanol groups and hydrophobic carbon sites at the surface of SiC and the possibility of hydrophobic interactions between hydrocarbon chains and the nonpolar centers of SiC make the reactivity of SiC surface rather inhomogeneous [89].

Various functional groups can be adsorbed on the SiC surface, such as $-\text{COOH}$ and $-\text{NH}_2$. The mechanism of adsorption is not clear yet. It has been suggested that the conditions for strong adsorption are dominated by the interfacial Lewis acid-base interaction between the

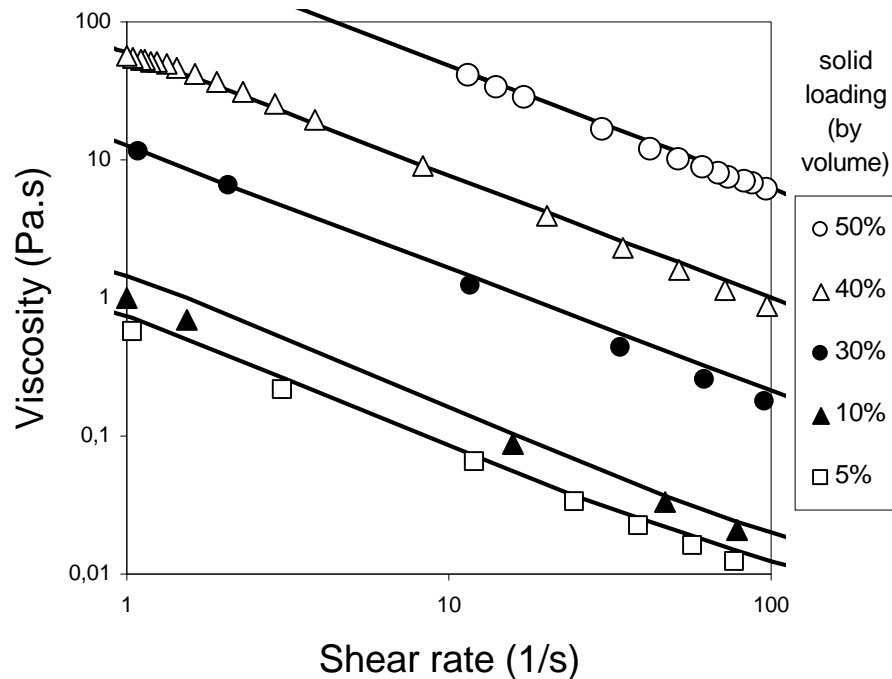


Figure 5.3: Theoretical fit curves and measured points of SiC slurry viscosity

polymer and the surface sites of the powder [90]. Some researchers believe that Lewis acid-base sites are the specific adsorption sites [83,91, 96]. Furthermore, electrostatic force has been used to explain polymer adsorption on SiC surface in aqueous system [96-102]. Some dispersants are described in the literature, for example, aluminum alkoxide [92], PVA (polyvinyl alcohol) [93], PEG (polyethylene glycol) [94, 94, 95], sodium oleate [96], PAA (polyacrylic acid) [97, 100], PVP (polyvinylpyrrolidone) [98], phosphoric ester [98], PEI (polyethylenimine) [99], styrene-maleic acid copolymer [100], Darvan C [93, 101] and Lignosulphonate [102]. In this work, dispersants with $-\text{COOH}$, $-\text{NH}_2$ groups are selected and tested through sedimentation, zeta potential and viscosity measurement. Other dispersants, which could be adsorbed at SiC surface, for example TEOP and SHMP, are also tested.

5.2.1 Sedimentation measurement

For sedimentation tests suspensions of 5 g SiC powder in 20 ml distilled and deionized water with 1wt% of different dispersant (table 5.1) and a pH in the range of pH4 to 7 were made through shaking and ultrasonic treatment for 15 minutes. According to the results (table 5.1) sediment densities are very low. That means that, shaking and ultrasonic dispersing were not strong enough to destroy agglomerates. After ball milling for 2 hours dispersants can be adsorbed at SiC surface and change the zeta potential and viscosities of SiC suspension. The results from zeta potential and measurement of viscosities of SiC suspensions are reported in next 5.2.2 and 5.2.3.

Table 5.1 Sediment density of SiC with different dispersants after 20 days
(5g SiC by 1 wt% dispersant in 20ml distilled and deionized water)

Dispersant	PAA2	HASS	SHMP	TSP	TEOP
Sediment Density / theoretical density (%)	14.2	13.7	14.2	14.2	10.6
Dispersant	STEA	OLAK	DMA	DEMA	BUMA
Sediment Density / theoretical density (%)	13.9	10.0	18.3	16.3	14.2

The structure of the dispersants are shown in Figure 5.4 and Figure 5.5. Of special importance is PAA2 because of the successful bridge flocculation. Its conformation changes with varying pH value. At low pH, its functional acidic groups are not fully dissociated, thus the PAA2 is set in a coiled conformation [97]. With increasing pH, dissociation increases, leading to repulsive negative forces and uncoiling of the PAA2 chain. However, at high pH, the surface of SiC is negatively charged, thus not allowing strong attraction to the negatively charged PAA2. As a result, PAA2 can not be strongly adsorbed on to SiC surface thus obtaining a high sediment density. So do also HASS, SHMP, TSP, OLAK, DEMA, STEA and BUMA. Furthermore, since the dispersing methods can not destroy agglomerates effectively, even the dispersants which are positively charged in suspensions and should be

adsorbed at the negative surface of SiC, as for example DMA and TEOP, can not increase the sedimental density.

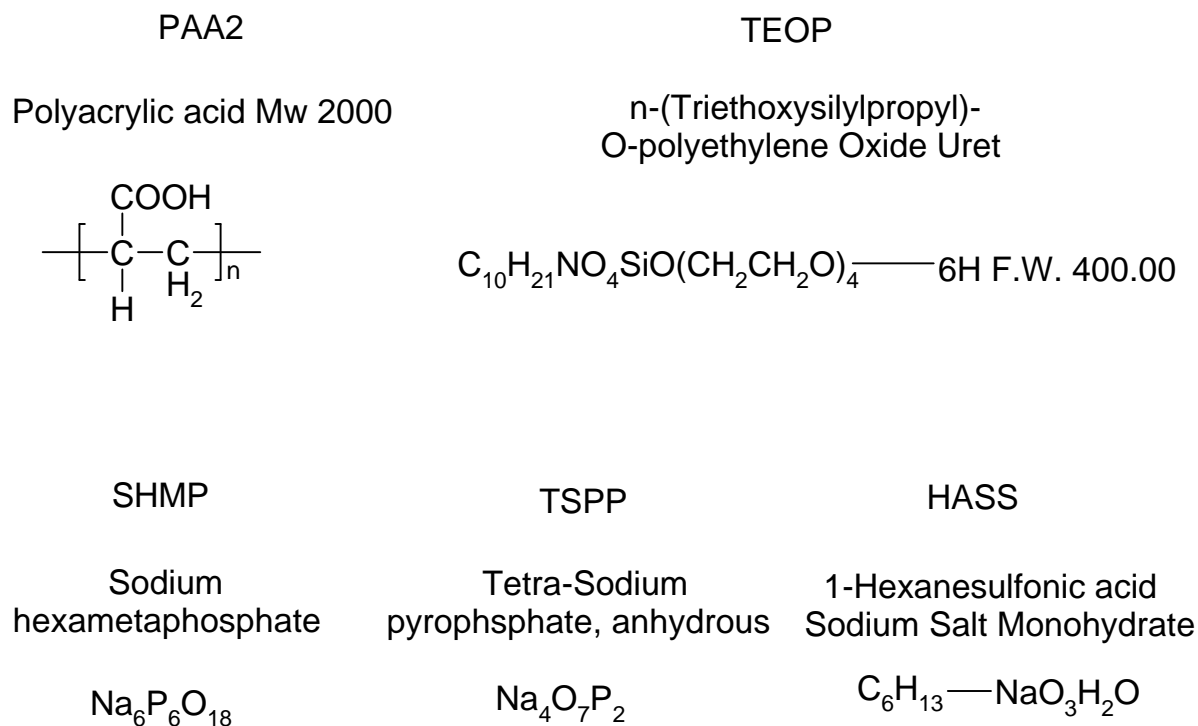
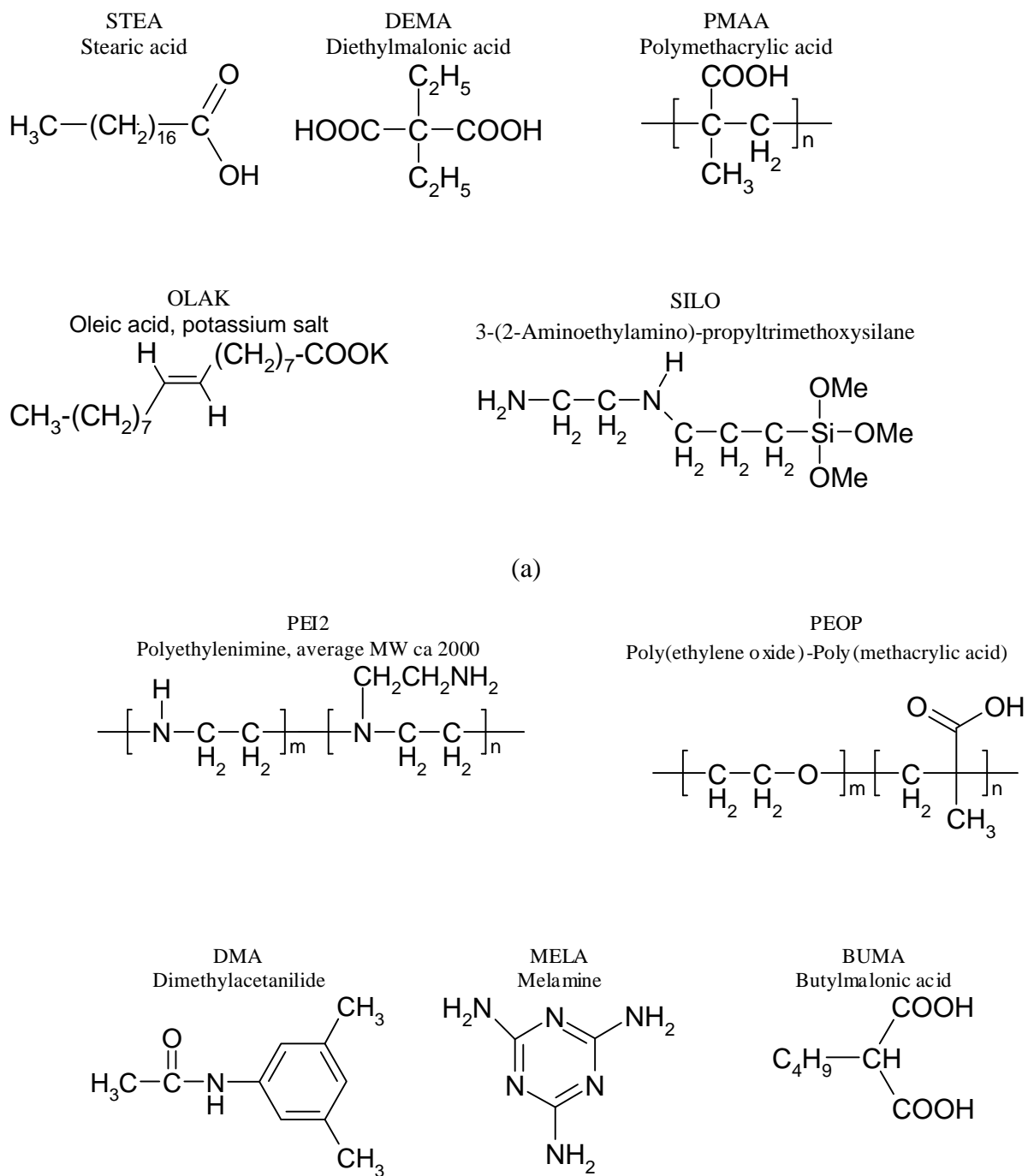


Figure 5.4: Dispersants for sedimentation experiments

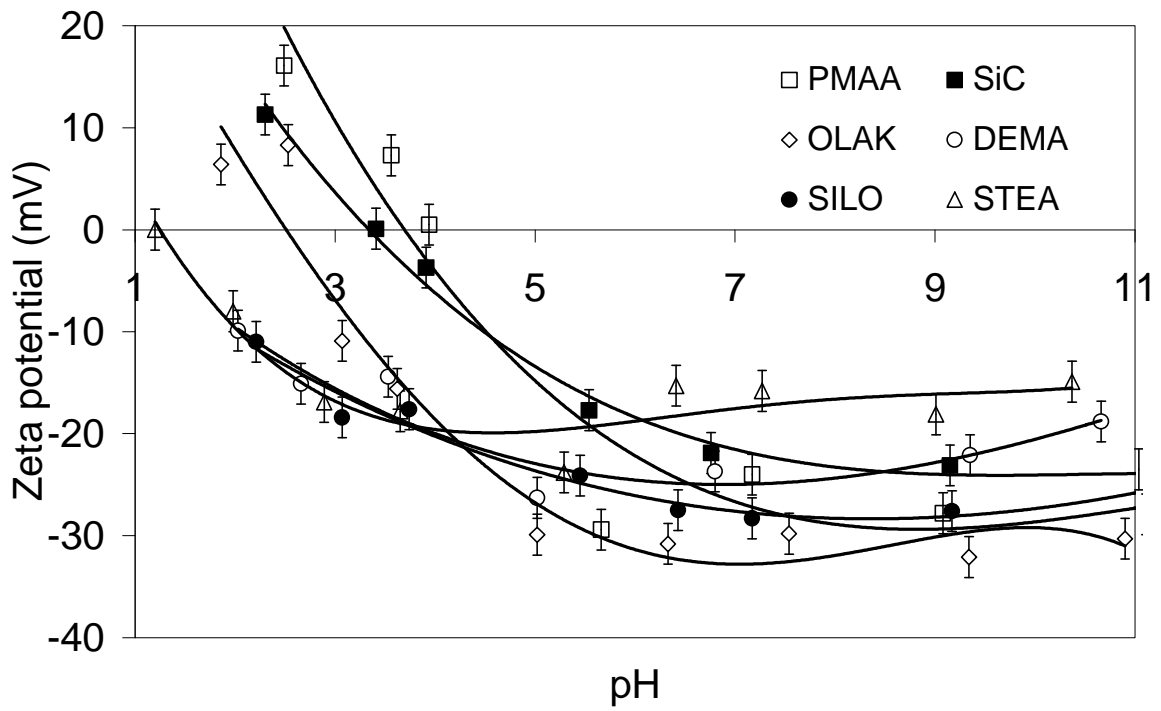
5.2.2 Zeta potential measurement

The total potential energy of interaction of two particles can be altered by changing the magnitude of the repulsion, either by increasing the ionic strength of the solution or by decreasing the surface potential of the particles (equation 3.3 and 3.4). In the high pH range SiC powder has a high zeta potential for electrostatic stabilization (Figure 4.11). However, it is not appropriate for molding to work in the high pH range. Since the viscosity of suspensions with solid content more than 40 volume percent (vol%) is very high even of high pH (Figure 5.3), organic dispersants are employed to increase the surface charge in order to get low viscosities. The zeta potential of SiC suspensions with dispersants shown in Figure 5.5 (a) are plotted in Figure 5.6 (a) and those of Figure 5.5 (b) are presented in Figure 5.6 (b).

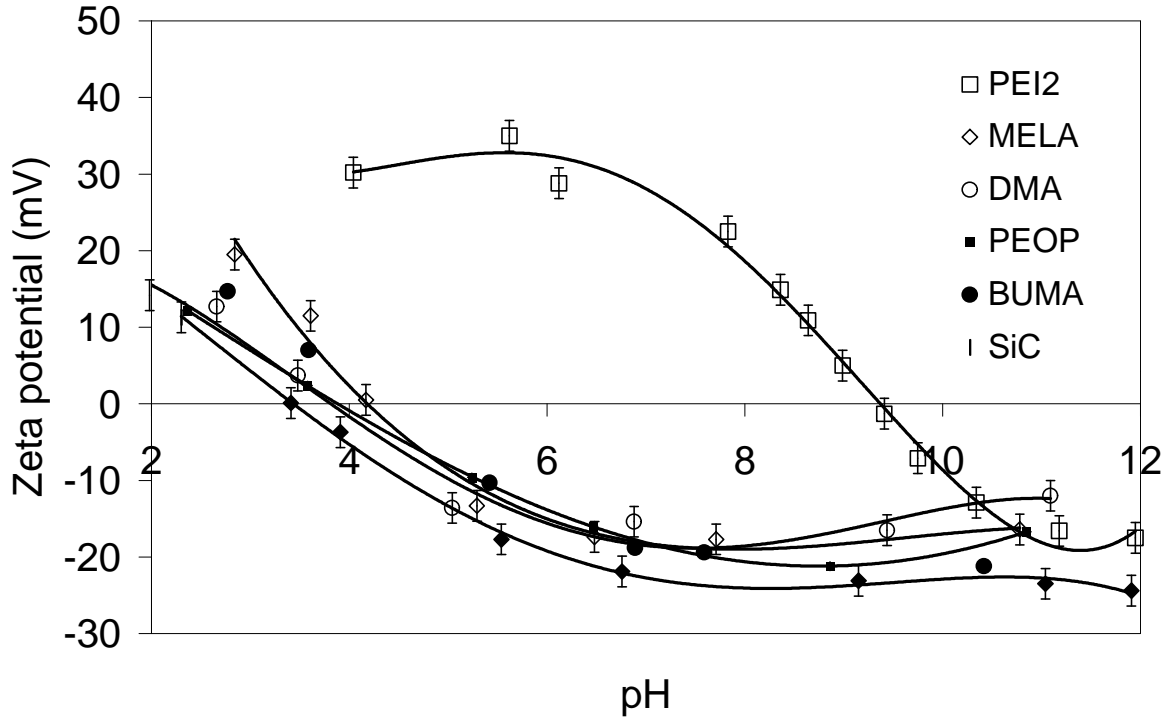


(b)

Figure 5.5: Structures of dispersant



(a)



(b)

Figure 5.6: Zeta potential of SiC powder with various dispersants (1wt%)

As can be seen in Figure 5.6(a) the zeta potential values of SiC powder are increased in certain pH ranges through dispersants. The dispersants are adsorbed on the SiC surface through H-bonds and the additional charge of dispersant increases the zeta potential of the powder. As a result the repulsive force among colloidal powders should be increased against van der Waals attractive force improving dispersion. A value of zeta potential higher than 25 mV can be obtained only with PEI2 in the acidic range. The isoelectric point is also changed significantly by this dispersant. These results indicate that the surface of the SiC is altered significantly by adsorbing PEI2 molecules. The molecular formula of PEI2 is $(\text{CH}_2\text{CH}_2\text{NH})_n$ when it is dissolved in neutral or acidic water, the lone electron pairs on its nitrogen atoms attract the protons in water. The acceptance of a proton makes PEI2 to become an ionic compound adsorbed with many H^+ ions, and hence increases the pH of the solution. Thus, in basic conditions ionic PEI molecules likely adsorb on the negatively charged surface of SiC. The reaction results in the exchange of the surface potential of SiC, which alters a negative potential to a positive potential surface.

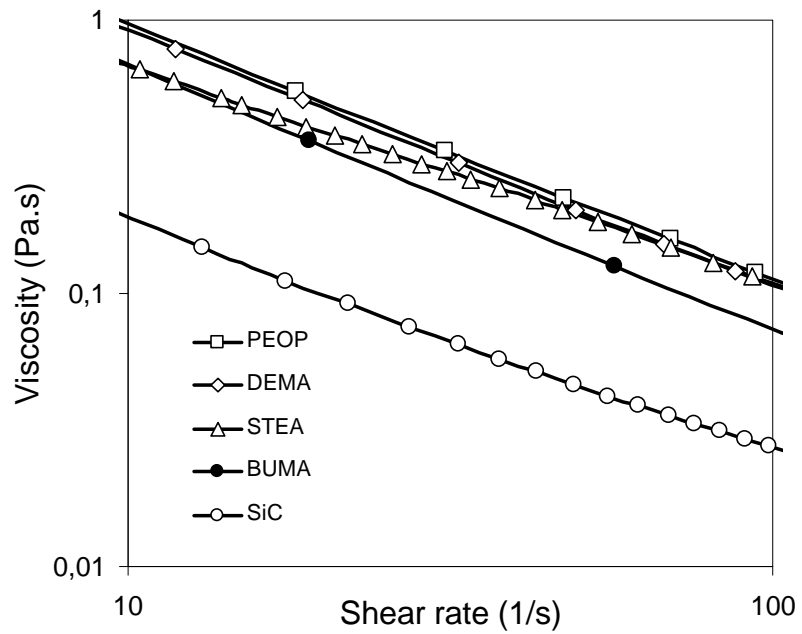
5.2.3 Viscosity measurement

The viscosities of SiC slurries dispersed by different dispersants and additionally ball milled for 2 hours are shown in Figure 5.7.

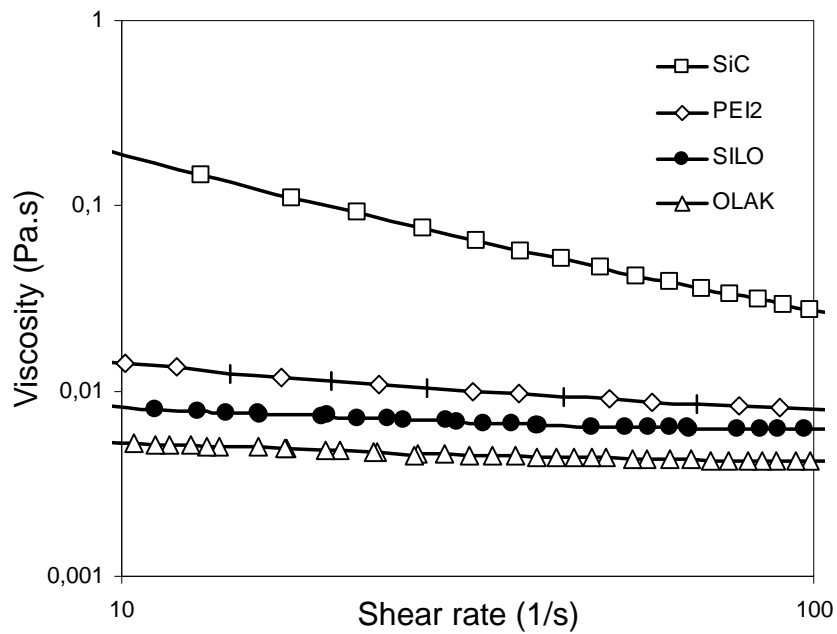
The rheological behavior of SiC slurries are strongly influenced by the presence of dispersants. Generally, the effects can be divided into two types: increasing and decreasing viscosity. Low viscosities are exhibited when SILO, OLAK and PEI2 were added (Figure 5.7b).

SILO is adsorbed on the SiC surface through the formation of hydrogen bonds between water and O from Si-O-Si, inherently present or formed through hydrolysis of siloxane. The reaction of the silanol groups of the intermediate phase with the OH groups of the inorganic substrate strongly alters the polarity and wettability of the latter. By that the dispersion of SiC powder in water is improved and the viscosity of the slurry is decreased.

OLAK can not be adsorbed through electrostatic forces because in the alkaline region it is negatively charged. The zeta potential of silicon carbide is definitively negative. However, it can not be precluded that oleate might be adsorbed on SiC in the pH range, where it has a negative surface charge in the presence of the activating effect of polyvalent metal cations [96]. Moreover, the growth of the negative charge in the presence of oleate characterizes the



(a) pH value of SiC suspensions with PEOP, DEMA, STEA and BUMA adjusted to pH 6, without dispersant adjusted to pH10



(b) pH value of SiC suspensions with PEI2, SILO and OLAK adjusted to pH 9, without dispersant adjusted to pH10

Figure 5.7: Viscosity of SiC suspension with dispersants ($\phi=20\text{vol}\%$)

kind of adsorption (Figure 5.6a), in which the polar $-\text{COO}^-$ group carrying the charge, remains chemically unbonded. Thus, it might be assumed that the adsorption of the OLAK was the result of interactions between the hydrocarbon chains of the oleate and the carbon atoms in the crystallographic lattice of SiC, as well as colloidal carbon which have not reacted during the synthesis of SiC [96]. Such a mechanism of adsorption, in which the carboxyl groups continue to be active and chemically unbonded, results in an increase of the negative charge at the surface, and hence also to a growth of the electrokinetic potential (Figure 5.6a) and a decrease of the viscosity of the SiC slurry as well.

The secondary amine group of PEI2 adsorbed on the SiC surface through electrostatic force due to negative charges on the SiC surface, such as dissociated OH groups [96]. The adsorbed polymer changes the sign of the surface charge to positive, the absolute value of the zeta potential becoming larger. This provides a stronger repulsive force (Figure 5.6b).

Hence SILO, OLAK and PEI2 can stabilize particles in slurries and deflocculated the submicrometer SiC particles.

However, the other dispersants, such as BUMA, STEA, DEMA and copolymer PEOP, increase the viscosity due to the poor adsorption at the SiC surface, therefore coagulation of SiC powders occurs (Figure 5.7a). The formation of H-bonds between dispersant and SiC surface is hindered because of the formation of negative $-\text{COO}^-$ and a repulsive force against negative SiC surface consequently. Sindel [103] has determined the hydrolysis of PEOP and PAA which is shown in Figure 5.8. Above pH 3.5 $-\text{COO}^-$ is dissociated in solution. The pH_{IEP} of SiC powder is at pH 3.4. As a result, in the range of pH value above pH 3.5, the carboxyl displays negative properties like SiC powder and can not be absorbed at the SiC surface.

5.2.4 Temperature effects on SiC suspensions

The viscosity is determined of constant shear stress as a function of temperature (Figure 5.9). The suspensions were adjusted at different pH values at which the viscosity reaches a minimum at room temperature. As Figure 5.9 shows, SiC slurries with PEOP, BUMA and SILO as dispersant display insignificant increase in viscosity. Whereas with PEI7 the viscosity increases with increasing temperature. PEI7 with an average molecular weight of 70,000 was used to replace PEI2 having an average molecular weight of 2000 in order to lower the viscosity of SiC slurry.

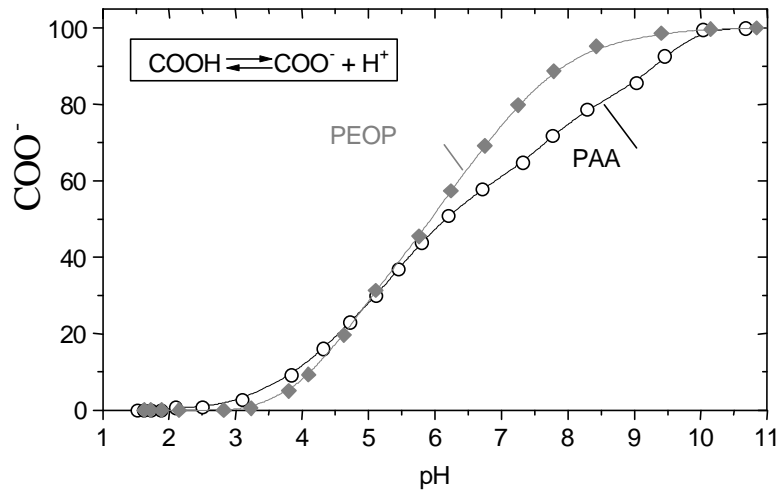


Figure 5.8: Hydrolysis of carboxyl [103]

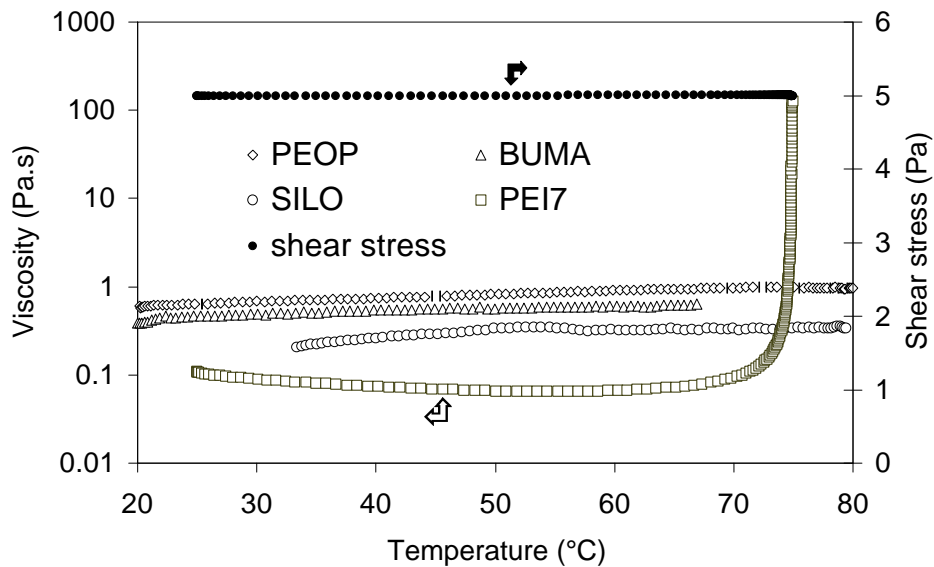


Figure 5.9: Temperature effect on viscosity of SiC suspensions ($\phi=20\text{vol}\%$, 1 wt% dispersant) at pH 6 using PEOP and BUMA and at pH 9 using SILO and PEI7

5.2.5 Suggestions for temperature - induced direct casting

5.2.5.1 Zeta potential adjustment for SiC/PEI2

Additives are necessary for liquid phase sintering of SiC. In this work, an amount of 10 vol% were used consisting of 60 mol% Y_2O_3 and 40mol% AlN. As Figure 4.11 shows, the SiC surface is negatively charged in aqueous system, whereas the surface charge of Y_2O_3 powder is positive up to pH 9.8. In order to avoid reaction among different surfaces, the

surface charge of SiC powder is modified using PEI2. As can be seen from Figure 5.10 the pH_{IEP} can be shifted adding different amounts of PEI2. At 1 wt% PEI2 the pH_{IEP} of SiC is close to that of Y_2O_3 (pH 9.8). AlN powder has a similar surface property as SiC after being modified using TEOP (chapter 6).

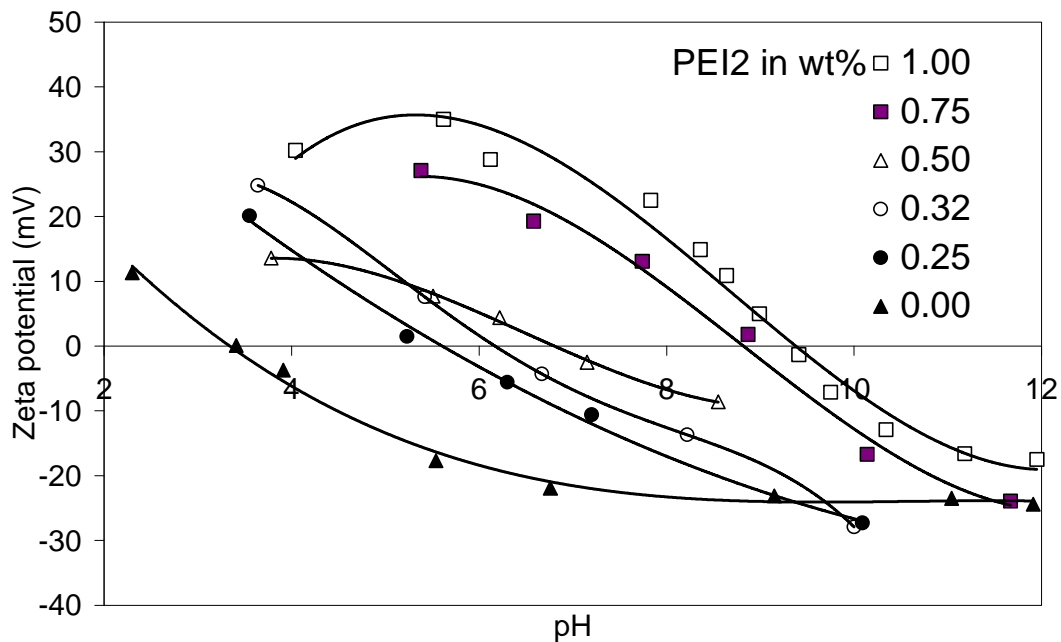


Figure 5.10: pH_{IEP} shift by adsorption of PEI2

5.2.5.2 Slurry formation

According to the zeta potential curve of Y_2O_3 stable slurries can be made at $\text{pH} < 9$. The pH change in the range of pH 5-10 has insignificant effect on the stability of a SiC suspension using PEI7 as dispersant. The surface property of AlN can also be changed through PEI7, which is in excess of full adsorption at SiC surface and stays free in the suspension. A stable suspension of SiC with sintering additives of Y_2O_3 and AlN is obtained at pH 8. The viscosities of slurries of SiC and of a mixture of $\text{Y}_2\text{O}_3/\text{AlN}/\text{SiC}$ are compared in Figure 5.11. They are quite similar.

After mixing these slurries, the viscosity does not change much because of their similar surface behaviors. A direct temperature casting is carried out using SiC powder. The detail of the process will be discussed in chapter 7.

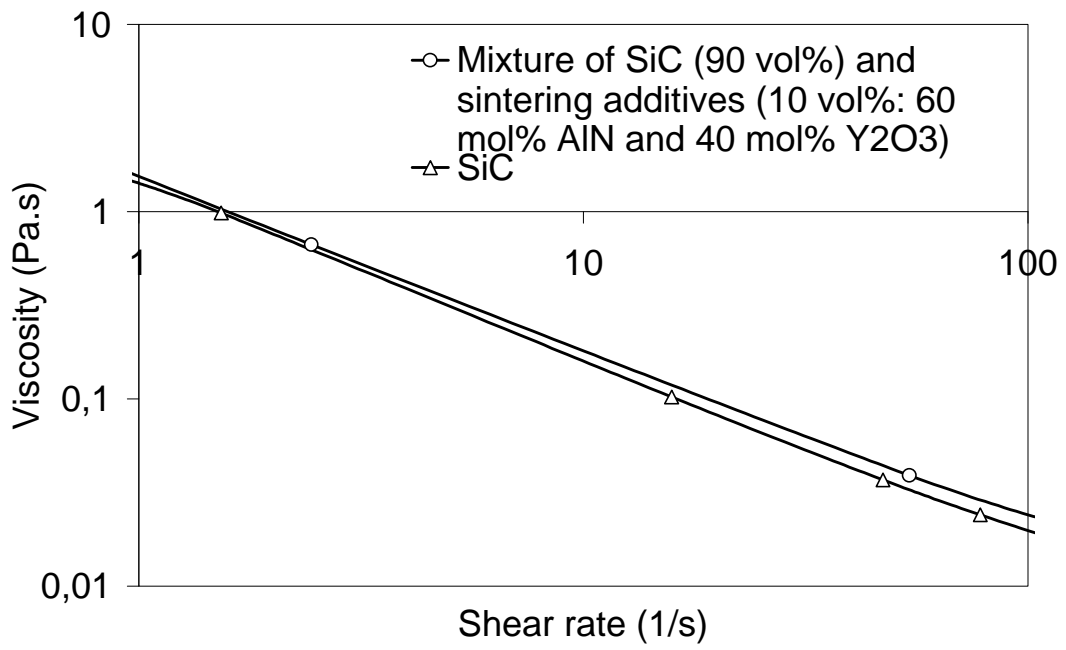
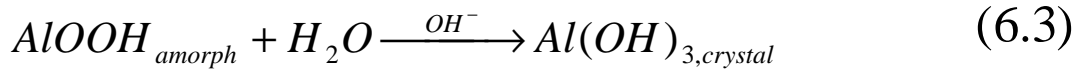
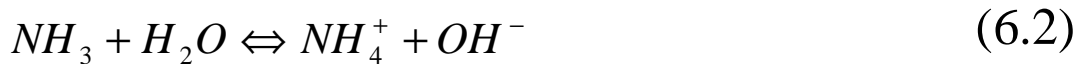
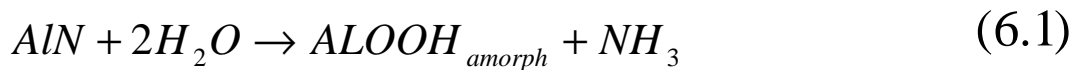


Figure 5.11: Influence of sintering additives on the viscosity of SiC suspensions with a solid loading of 10 vol% at pH 8

6 AlN protection

In this work, 10vol% additives of 60mol% AlN and 40mol% Y₂O₃ are selected for liquid phase sintering of SiC [104]. The application of AlN in water-based slurries encounters problems because of its strong hydrolysis reaction. Therefore, conventionally nonaqueous media have been used in wet powder processing. However, aqueous alternatives were extensively investigated in order to reduce the high production costs and to avoid the safety and environmental problems associated with nonaqueous powder processing [109].

The reaction kinetics between AlN and water were thoroughly studied by Bowen et al. [105]. Possible stoichiometric reactions are presented as follows:



Typically, AlN can be protected by coating with carboxylic acids (usually stearic acid) [106, 107]. Water is repelled by the long chain hydrophobic group attached to AlN, thus allowing slip casting, tape casting or spray drying of aqueous slurries. Hydrophobic powder exhibits foaming because of a high surface tension, therefore, an antifoaming agent is required.

Hydrolysis of AlN depends on the oxygen content of the starting powder, the pH value and the temperature of the slurry. The higher the oxygen content, the longer the time it needed for water to penetrate through the surface layer of AlN powder. The hydrolysis rate will be decreased at low pH and low temperature.

Inorganic and organic phosphoric acids were also tested for the coating of AlN powder [107,108]. Coating with these acids was done in aqueous solution and subsequent heating at about 150 to 800°C. Powder modified that way is reported to be stable in slurries even at high pH and at elevated temperatures. T. Kosmac has reported on the reactivity of diluted AlN

suspension at different temperatures using HCl, HNO₃, H₂SO₄ and H₃PO₄. He concluded that H₂SO₄ and H₃PO₄ can protect AlN in water at room temperature and silicic acid can protect AlN even at higher temperatures up to 90°C [109]. A Si-Al-O-N layer was coated on to AlN surface by Howard [110]. According to his method AlN powder is first coated with a layer of silicate and then heated in the temperature range between 350°C and 1000°C. The treated powder is reported to be stable in a humidity chamber for 100 hours at 85°C.

6.1 AlN surface properties in SiC suspension

Because SiC powder typically is covered with a thin SiO₂ layer, which could dissociate in water and form silicic acid, which can prevent hydrolysis of AlN (s. above), AlN/SiC slurries were prepared to determine the protecting effect. The mixed powder is put in distilled and deionized water and ball milled for two hours. Subsequently the slurry was dried

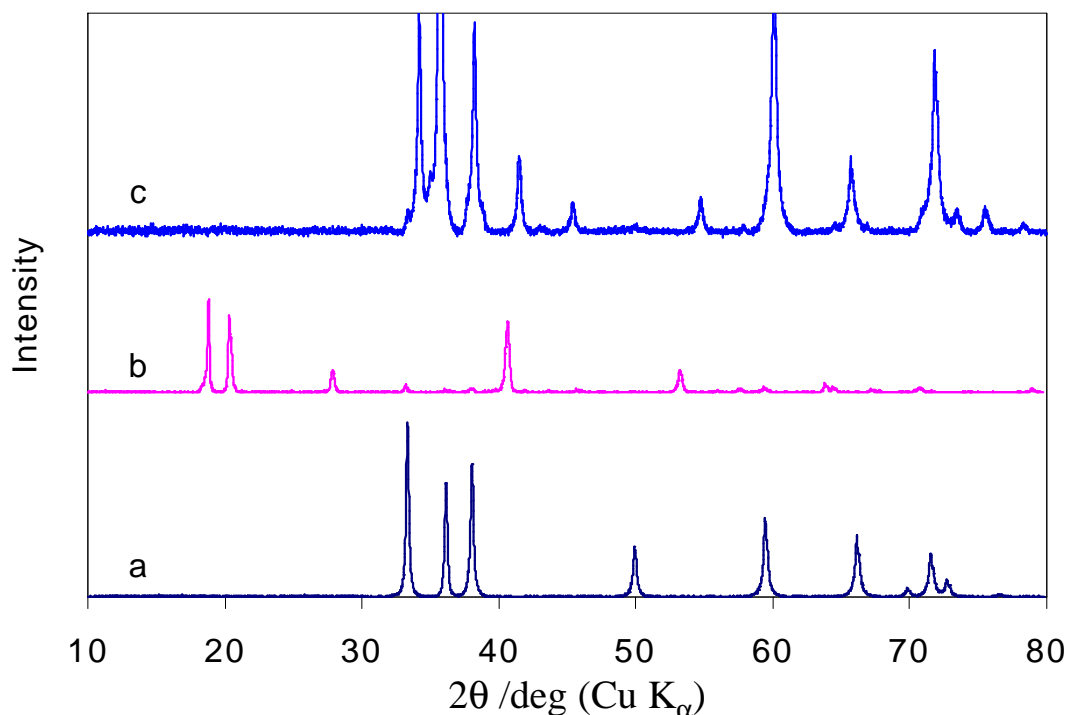
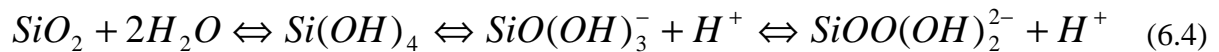


Figure 6.1: X-ray diffraction of a) as-received AlN powder, b) AlN powder after 2 hours ball milling in water, and c) aqueous AlN powder + SiC suspension after two hours of ball milling (0.89 mol AlN in 27.14 mol SiC)

and investigated by X-ray diffraction (XRD). For comparison an AlN slurry was also prepared at the same conditions. The diffraction patterns of both slurries as well as as-received AlN powder are shown in Figure 6.1.

Curve a) shows the XRD spectrum of as-received AlN powder. Curve b) is the XRD spectrum of the same AlN powder after 2 hours ball milling in water. With this treatment the AlN powder is almost completely hydrolyzed to Al(OH)₃ according to equation 6.1-6.3. Curve c) is the XRD spectrum of SiC/AlN powder dried after 2 hours ball milling. There is no evidence of Al(OH)₃ (Figure 6.1c). That means, the hydrolysis of AlN in water can be avoided in AlN/SiC suspensions. Considering surface and solution chemistry, the reason can be supposed as reprecipitation of SiO₂ on the AlN surface:



As equation (6.4) shows, SiO₂ dissolves in water and exists as soluble Si(OH)₄, SiO(OH)₃⁻ and SiOO(OH)₂²⁻. As a result of reprecipitation SiO₂ forms on to the AlN surface, which prevents AlN from hydrolysis.

Krnel and Kosmac [111] have presented a chemical adsorption model of AlN powder in silicic acid for explaining the protection of AlN from hydrolysis (Figure 6.2).

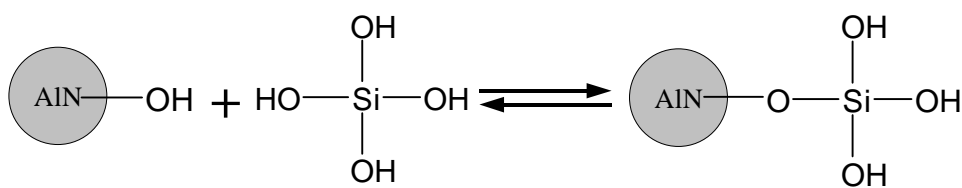


Figure 6.2: Reprecipitation scheme for silicic acid onto AlN powder [111]

However, this surface protection is not applicable in this work because the hydrolysis of AlN in SiC suspension is promoted by heating and forms NH₃.

6.2 AlN protection through calcination and coating

6.2.1 Calcination

AlN powder is calcined at 350°C for two hours to develop an oxide surface layer. Al₂O₃ appears (Figure 6.3b) after calcination. Al₂O₃ layer is expected to protect AlN against hydrolysis. However, after being stirred in water for 24 hours, Al(OH)₃ is produced (Figure 6.4b), which means that AlN can not be protected by calcination effectively.

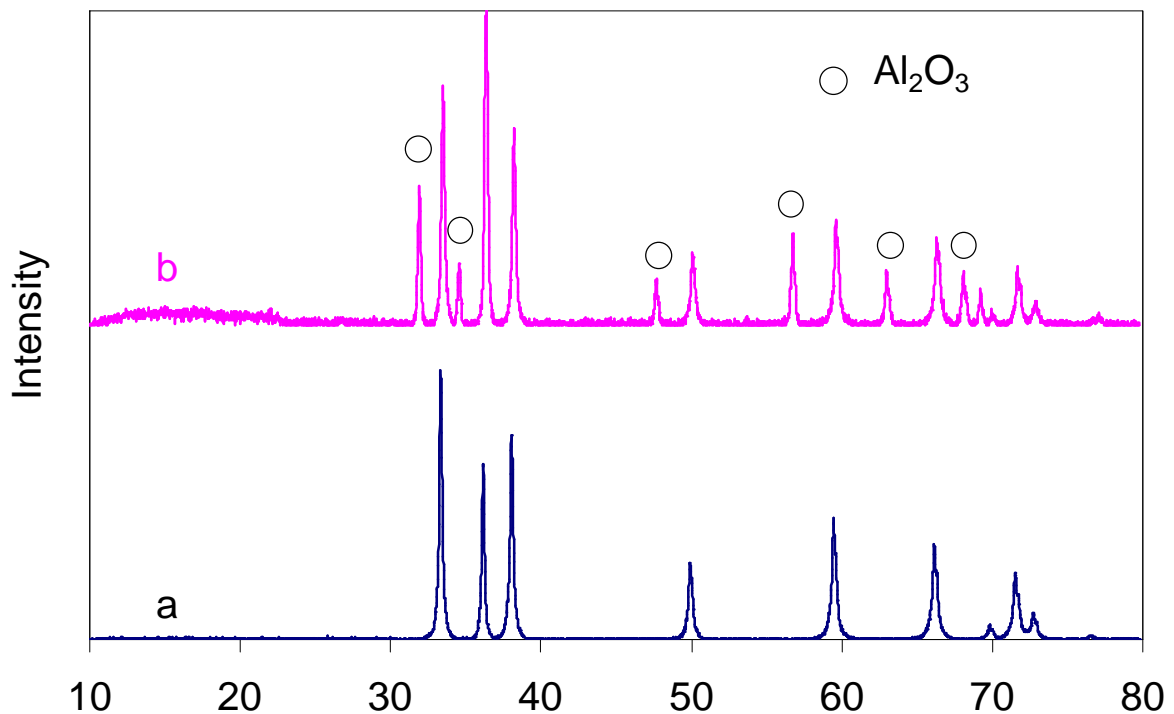


Figure 6.3: X-ray diffraction of AlN powder a), and AlN powder after heating at 350 °C in flowing O₂ for two hours b)

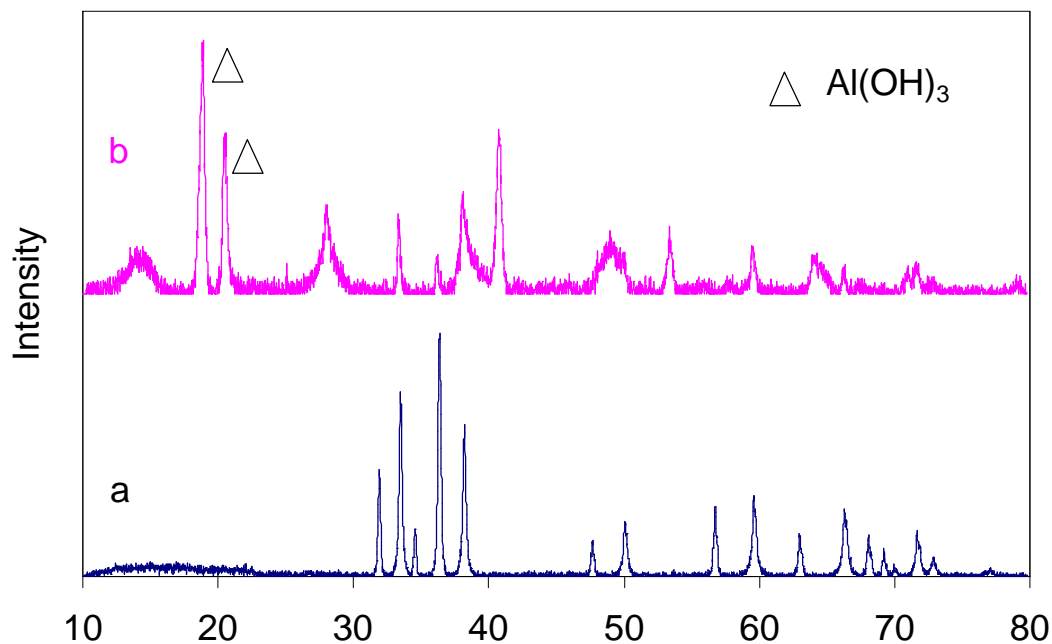


Figure 6.4: X-ray diffraction of AlN powder after heating a), and after heating in water for 24 hours b)

6.2.2 Coating

AlN is first coated by a layer of tetraethoxysilane (TEOS, $\text{Si}(\text{OCH}_2\text{CH}_3)_4$) and then calcined at 600°C in flowing air for one hour. Howard [110] has reported, the surface is covered by an amorphous layer of Si-O-Al-N by this treatment. The layer has a thickness of about 20-100 Å, thus creating a dense surface layer on the AlN powder and protecting AlN from water. It was also reported that, due to the reaction-bonding, the layer of Si-Al-O-N strongly adheres to the surface of AlN. The silicon and oxygen are found to be incorporated into the Si-Al-O-N layer in a ratio of about a 1:1.65 [110].

Modified AlN powder and as-received AlN powder are dispersed in water with ultrasonic treatment for 15 minutes and heated to 80°C . After this treatment the pH change is recorded as a function of temperature (Figure 6.5). As the results show as-received AlN powder is already hydrolyzed by ultrasonic and the pH value of AlN slurry reaches 9.15. By heating NH_3 is released. Therefore, the pH drops weakly from 9.15 to 8.80. After AlN is coated by a layer of Si-O-Al-N, the pH value increases a little at about 60°C , but no

significant pH change reveals the hydrolysis with increasing temperature. pH value is kept constant at a value of 6.50 after a weak increase of 1.0.

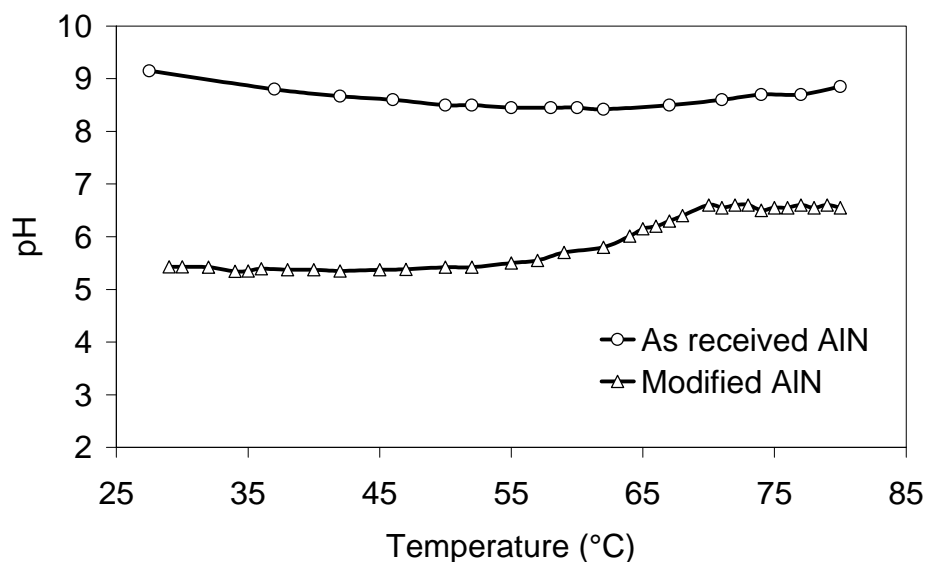


Figure 6.5: pH change of different AlN suspensions on heating

6.3 Conclusion

AlN powder can be protected against hydrolysis at elevated temperature in aqueous suspension by coating with TEOS and subsequent calcination. After the treatment there is no evidence for hydrolysis of the protected AlN in an aqueous slurry even not after heating. The protection process is schematically described in Figure 6.6.

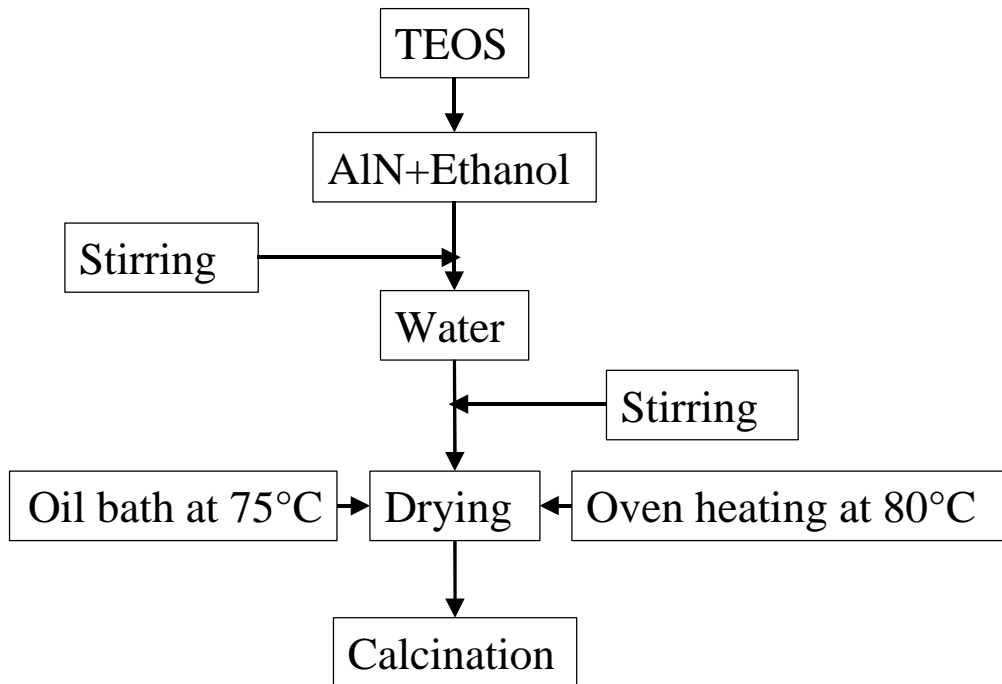


Figure 6.6: Schematic representation of AlN protection processing

7 Temperature - induced direct casting of SiC

Temperature effects on SiC suspension are studied, which include pH value, zeta potential and viscosity changes with temperature. Two methods of temperature - induced direct casting are suggested.

7.1 Temperature effects on SiC suspensions

SiC suspensions are first prepared using pH adjustment, in which there is no dispersant introduced. It is stabilized by an electrical double layer.

7.1.1 pH change with temperature

The pH value of a slurry is a critical parameter for its stability. The pH change of distilled and deionized water and SiC suspensions as a function of temperature, which are prepared through stirring, ultrasonic treatment and through additional two hours ball milling, are presented in Figure 7.1.

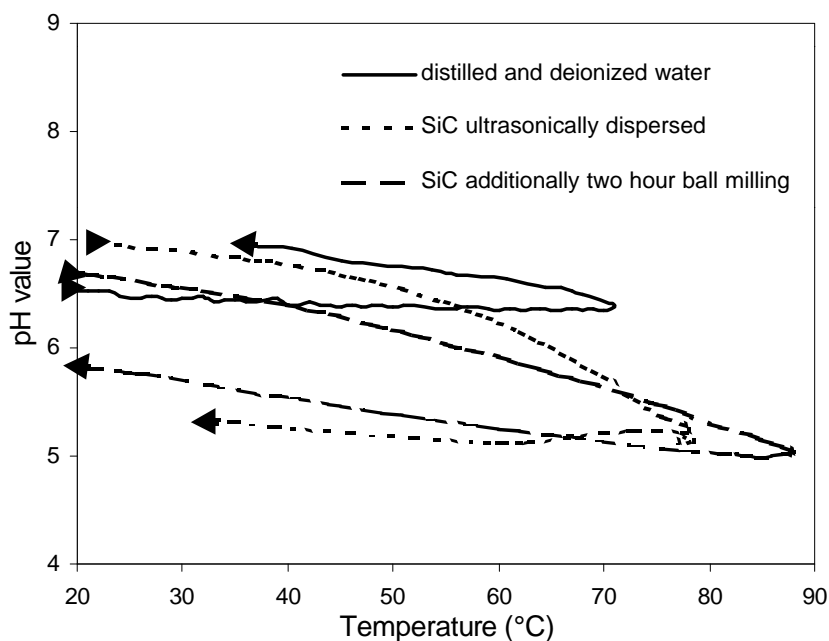
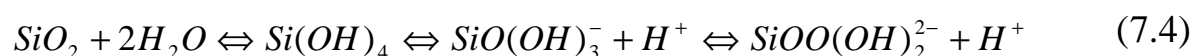
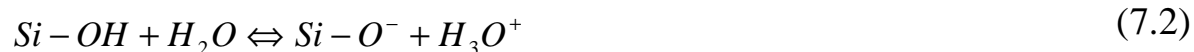


Figure 7.1: pH change of SiC suspensions with temperature ($\phi=10$ vol% SiC, in 0.01 M KNO_3 solution)

For comparison the pH change of water was also determined. As the curves show, the pH value of both SiC suspensions decreases with increasing temperature while the pH value of water stays constant. By cooling, the pH value of the ball milled SiC suspension increases whereas the pH of the SiC suspension without ball milling does not change. Possibly the following reactions happen in the suspension:



Equation (7.3) is a surface reaction and equation (7.2) is the dissolving of surface groups. Solution reactions (7.1) and (7.4) influence the pH value stronger than the surface reactions (7.2). The dissociation constant of water does not change significantly with increasing temperature (equation 7.1). By ball milling the SiO₂ is hydrolyzed according to equation (7.3) and (7.4), which makes the solution acidic. Reaction (7.4) depends on the temperature, therefore, the pH value decreases with increasing temperature. In the case of no ball milling, the pH value also decreases by heating. But less fresh surface is obtained as compared to ball milling. In this case the increase of H⁺ in solution comes mainly from dissolution of SiO₂. Hence the pH value does not increase clearly by cooling (dotted line in Figure 7.1).

7.1.2 Temperature effects on zeta potential

For the measurement of the change of the zeta potential with temperature suspensions were heated in an oil bath. After the pH value was adjusted at a certain temperature, the zeta potential is measured immediately. However, the temperature is not exactly due to the lack of heat preservation. Therefore, the curves shown in Figure 7.2 can only be used for a qualitatively understanding that the zeta potential decreases as temperature increases. This behavior can be explained by the dissolution of SiO₂ from the surface layer of the SiC powder. Figure 7.3 shows the calculated solubility of SiO₂ at various temperatures according to the Debye-Hückel model [112]. The solubility of SiO₂ increases with increasing temperature. The reaction (7.4) could happen as SiO₂ dissolves in water. The ionic strength in

the solution increases through dissolving SiO_2 , consequently, the thickness of electrical double layer and the zeta potential decreases.

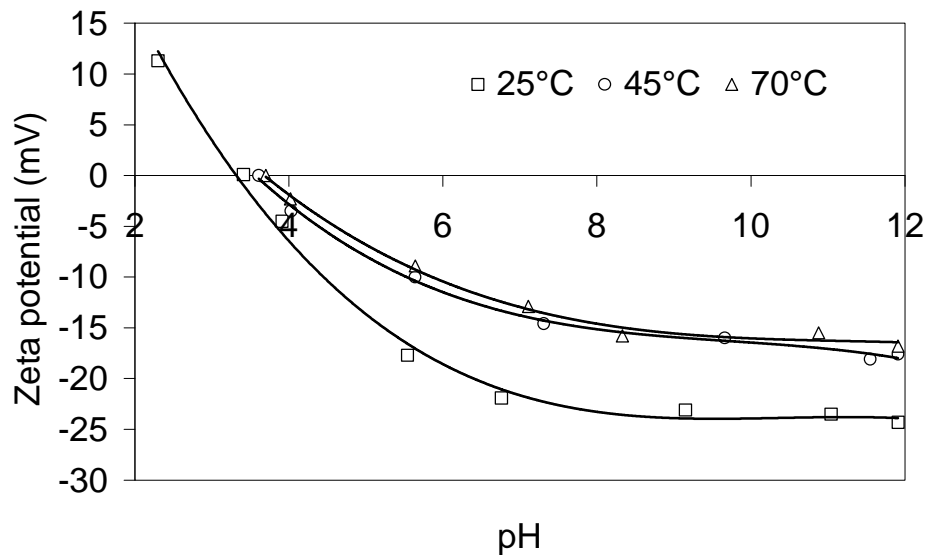


Figure 7.2: Zeta potential change with temperature (0.01M KNO_3)

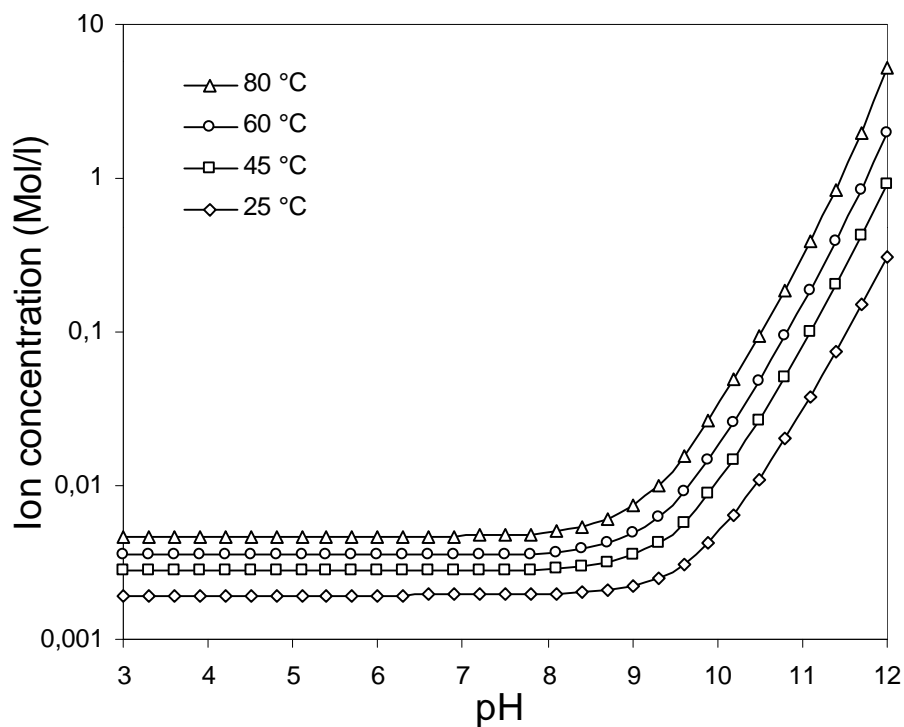


Figure 7.3: Calculated solubility of SiO_2 in water at different temperature (using Debye-Hückel model)

This can also be explained by the surface charge of SiO₂ (Figure 7.4). The surface charge depends on the pH value. In areas of lower pH SiO₂ gets less surface charged, therefore a lower value of zeta potential develops. The pH value of SiC suspension decreases with raising temperature (Figure 7.1), hence the absolute value of the zeta potential decreases at elevated temperature due to the dissolution of the thin SiO₂ layer on the SiC surface, because the dissolution increases ion concentration in the suspension.

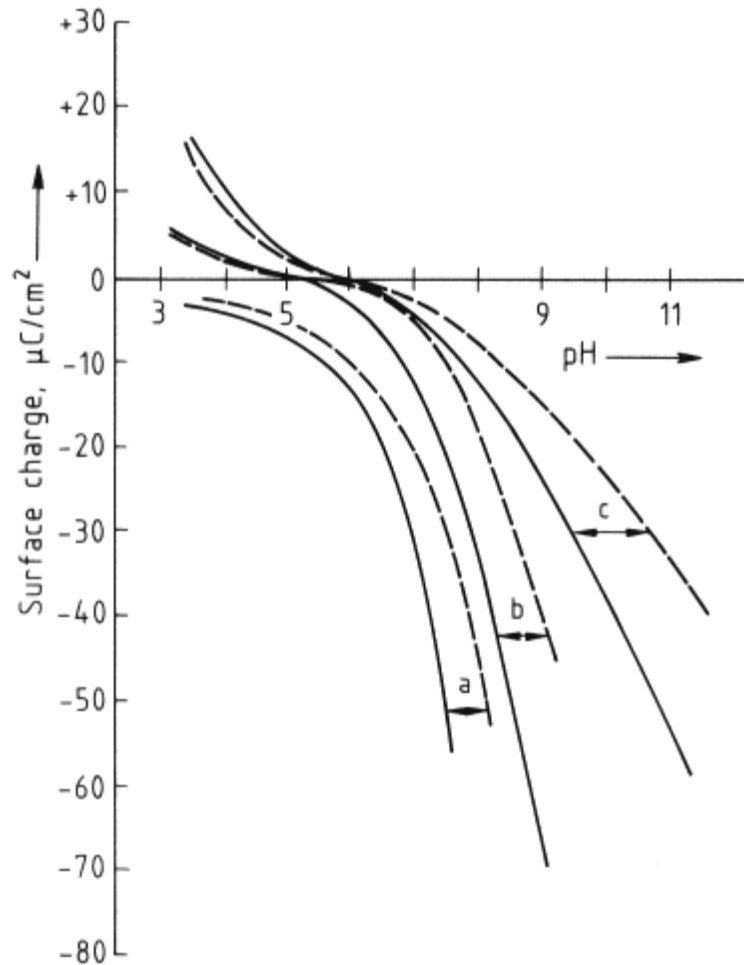


Figure 7.4: Variation of surface charge of oxides with pH in 0.1 mol/L (---) and 1 mol/L KCl (—) solutions at 20 °C a) Precipitated silica ; b) TiO₂ ; c) Hematite [113]

7.1.3 Temperature effects on viscosity

According to DLVO theory (equation 3.3 and 3.4), temperature influences interparticle repulsion through Debye parameter k . Using the STABIL program and the

required further parameters, such as solubility, a coagulation diagram of SiC suspension was calculated (Figure 7.5).

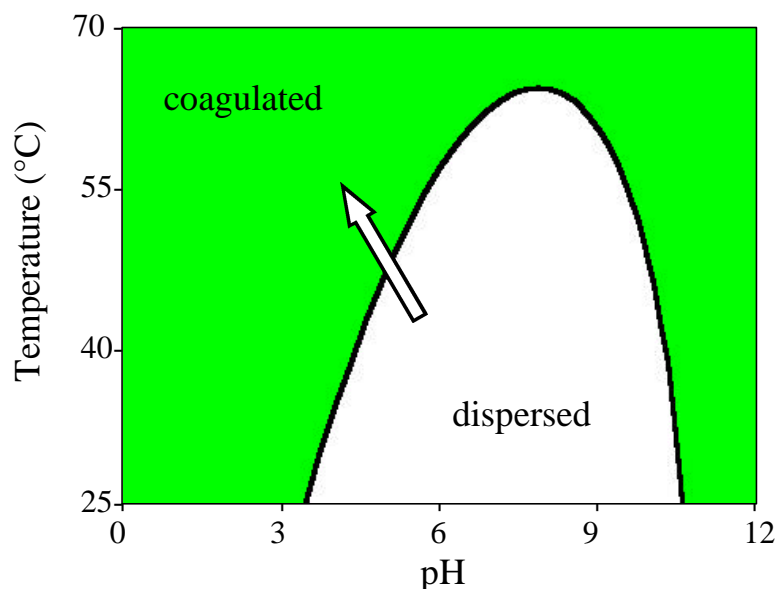


Figure 7.5 Coagulation diagram calculated using STABIL program

H^+ and OH^- are calculated according to dissociation of water at certain pH value (equation 6.1). Ion concentration from SiO_2 dissolving in water is cited from Figure 7.3. Balance charge is also used to calculate stability of SiC suspension. At room temperature, above pH 10.5 ionic strength of solution is increased because of the dissolution of SiO_2 . Here the electric double layer is compressed and the interparticle repulsive force is smaller than the long-range van der Waals attractive force (equation 3.3 and 4.4, Figure 4.11), thus the suspension coagulates. Below pH 4, SiC suspension is also coagulated because of a low zeta potential. The solvency of SiO_2 increases with increasing temperature, thus increasing the ion strength, which leads to a closure of the dispersing window with increasing temperature.

The viscosity of the SiC suspension was measured considering the change of temperature (Figure 7.6). At constant shear rate, the viscosity of a 20 vol% SiC suspension increases with increasing temperature, causing a coagulation of the SiC suspension. According to DLVO theory, when the zeta potential of a SiC suspension decreases with increasing temperature as Figure 7.2 shows, interparticle repulsive force will also be decreased (equation 3.3 and 3.4) and leads to agglomeration and high viscosity. According to

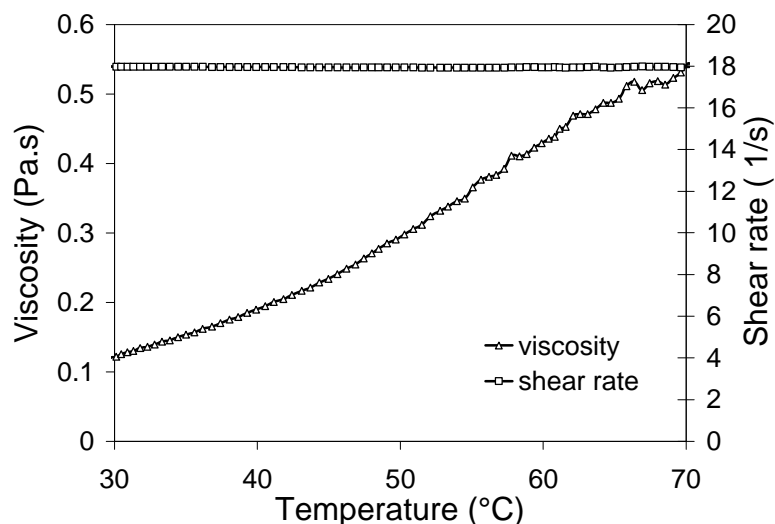


Figure 7.6: Viscosity change of SiC suspension with temperature at constant shear rate

Figure 7.1 and Figure 4.11, the pH value of the suspension decreases from pH 6.8 at room temperature to pH 5.2 at 85°C, which leads to a decrease of the zeta potential of the SiC suspension from 20 mV to 15 mV. Additionally, because a thin layer SiO₂ is covering the surface of SiC powder and the surface charge of SiO₂ decreases from -30 to -10 μC/cm² with pH value of the SiC suspension decreasing from 6.8 to 5.2 (Figure 7.4 curve a) [113], interparticle repulsive force decreases (equation 3.3 and 3.4), which also reflects high viscosity in the SiC suspension.

7.1.4 Hypothesis for temperature - induced direct casting

7.1.4.1 Reprecipitation of Y₂O₃ on to SiC surfaces

Y₂O₃ and AlN are added to SiC powder as additives for liquid phase sintering. SiC powder is dispersed at pH 10 by two hours ball milling and is negatively charged under those conditions (Figure 4.11). AlN powder display similar surface properties after being protected with Si-Al-O-N layer (Figure 4.12). In contrast, Y₂O₃ is positively charged at this pH (Figure 4.13) thus an electrostatic adsorption on the SiC and AlN surface is expected.

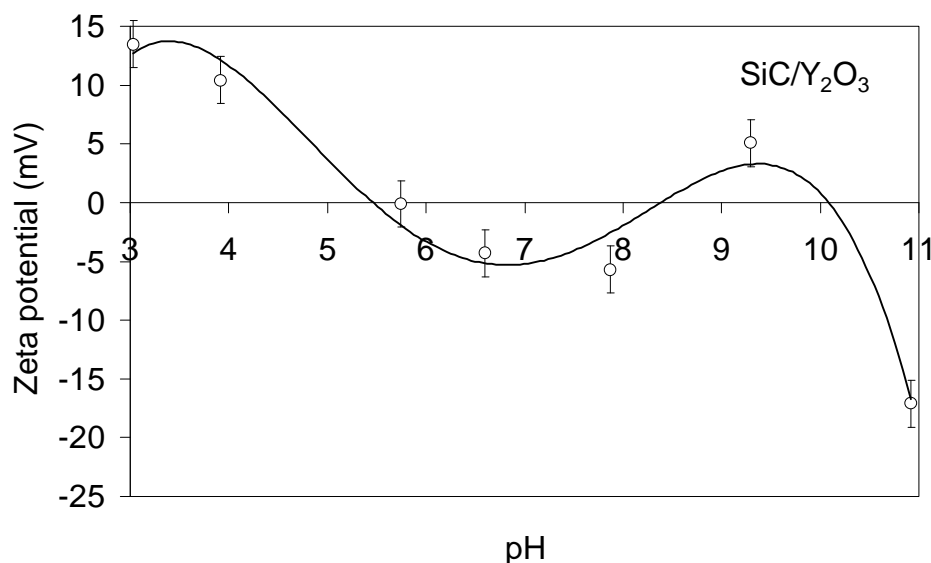


Figure 7.7: Zeta potential of SiC with 14vol% Y_2O_3 (0.01 M KNO_3)

A SiC suspension was prepared with 14 vol% Y_2O_3 and used for determining zeta potential of SiC/ Y_2O_3 . The result is shown in Figure 7.7. The curve is divided into four sections. Below pH 5.5, both powders are positively charged. Between pH 5.5 and pH 8.3, positively charged Y_2O_3 begins to be adsorbed on negatively charged SiC surface. However, the surface displays negative properties. Between pH 8.3 to pH 10.2 the surface is positively charged and above pH 10.2 negatively. Heterocoagulation should occur possibly yielding the smaller amount of Y_2O_3 powder adsorbed on the SiC surface.

Considering the zeta potential curve of Y_2O_3 (Figure 4.13) and SiC (Figure 4.11) and the solubility curve of Y_2O_3 (Figure 4.14), the following behavior can be concluded:

- In the low pH area Y_2O_3 is soluble in water and present as $Y(OH)_x^{(3-x)+}$. If the pH value is less than 3.4, the surface of SiC is positively charged and $Y(OH)_x^{(3-x)+}$ does not adsorb at the SiC surface. In the pH range above pH 3.4, SiC surface would be negative. However, because of the adsorption of $Y(OH)_x^{(3-x)+}$, it remains positive, thus the zeta potential remains also positive.

- Above pH 5.5, the solvency of Y_2O_3 decreases rapidly with increasing pH (Figure 4.14). Therefore, the content of $Y(OH)_x^{(3-x)+}$ decreases and by that the amount of those

adsorbed at the SiC surface. Consequently the strong negative charges of the SiC surface can not be balanced completely and dominate against the positive charges of Y_2O_3 particles. Therefore, the overall zeta potential value is slightly negative.

- Above pH 8.3, the zeta potential of SiC suspension becomes less negative and the solvency of Y_2O_3 increases again (Figure 4.14), thus $Y(OH)_x^{(3-x)+}$ reduces. Additionally the negative charges of the SiC surface, thus they do not balance the positive charges of Y_2O_3 . As a consequence, the overall zeta potential is positive between pH 8.3 and pH 10.2. Above pH 10.2 the Y_2O_3 dissolves as $Y(OH)_4^-$ and becomes negative as the SiC particles are. Therefore, the zeta potential turns into negative values. In conclusion, there are three pH_{IEP} for slurries of mixture of SiC and Y_2O_3 . The surface charges of SiC and Y_2O_3 particles as a function of pH are shown schematically in Figure 7.8.

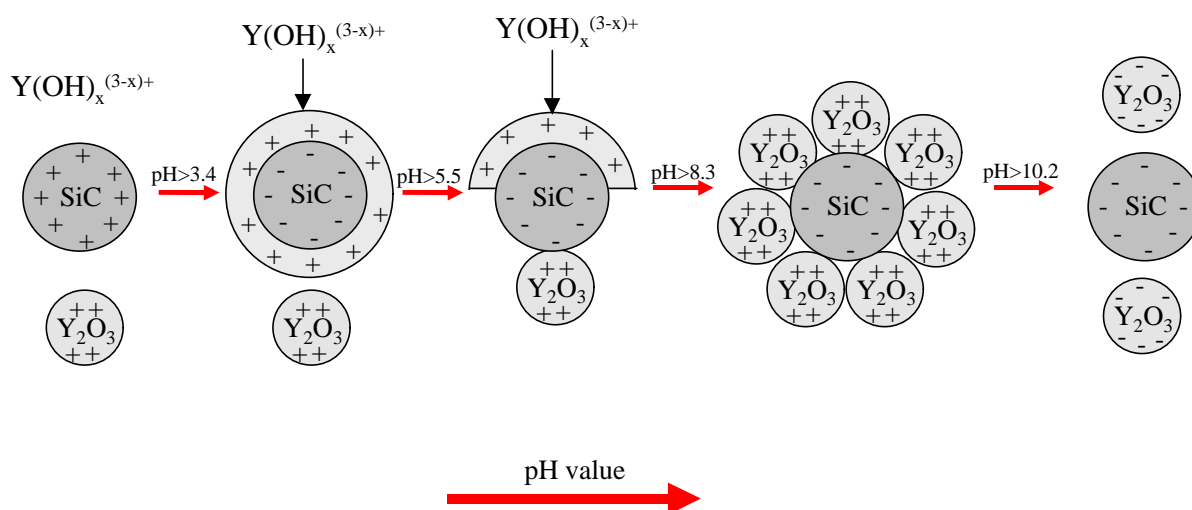


Figure 7.8: Schematic representation of adsorption of Y_2O_3 on SiC surface

7.1.4.2 Near net shape forming by modification of Y_2O_3

As the zeta potential curve of SiC/ Y_2O_3 shows (Figure 7.7), the conditions are neither suitable to get stable suspension of SiC and Y_2O_3 nor a perfect coagulation occurs. Therefore, Y_2O_3 was dispersed by Tri-ammonium citrate (TAC), which shifts the isoelectric point of Y_2O_3 to pH 2.6 (Figure 7.9). As a consequence its colloidal behavior in water is rather similar to that of SiC (Figure 4.11) and AlN powders (Figure 4.12).

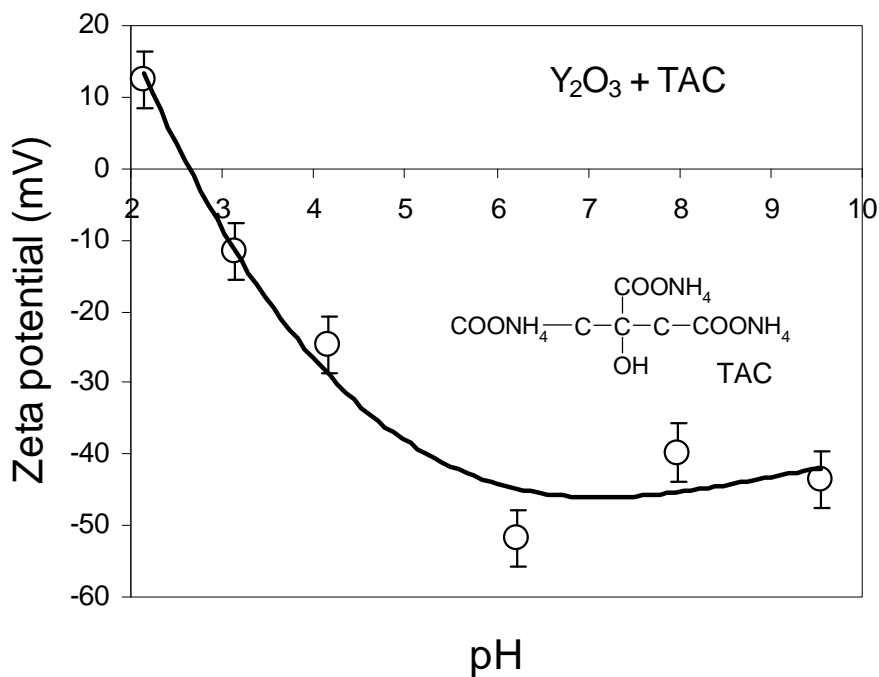


Figure 7.9: Zeta potential curve of Y_2O_3/TAC

The results of viscosity measurements carried out at pH 10 are shown in Figure 7.10.

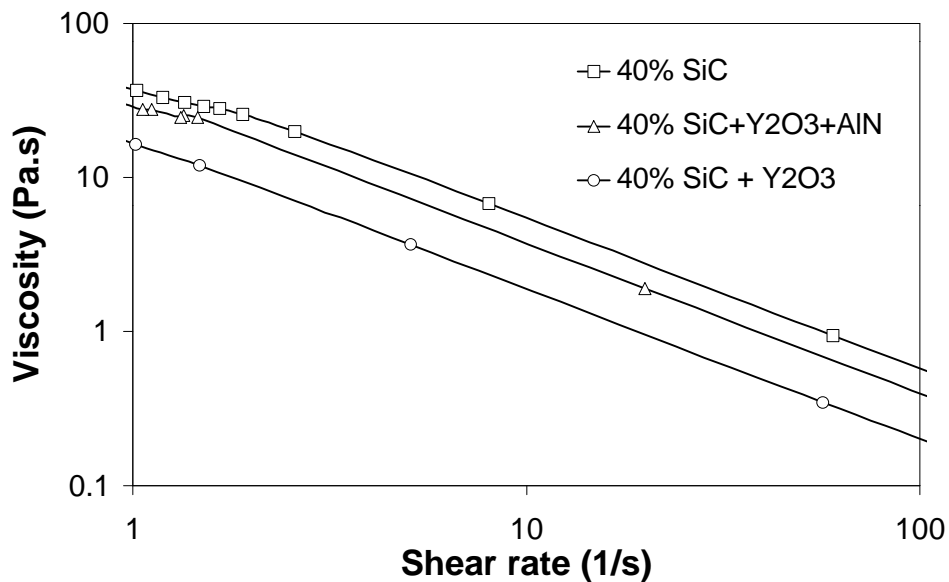


Figure 7.10: Viscosity change of SiC suspension with sinter additives (pH 10)

Suspensions of SiC, of a mixture of SiC and Y_2O_3 and of a mixture of SiC, Y_2O_3 and AlN were prepared by mixing known amounts of dry powder (90vol% SiC and 10vol%

additives, which consists of 60mol% AlN and 40mol% Y₂O₃) with water and pH adjusting to obtain the desired volume fraction. A 40 vol% SiC suspension was prepared through two hour planetary ball milling. Meanwhile, a 20 vol% Y₂O₃ suspension was milled for half hour and added to SiC suspension and milled for a further half an hour. Finally, a 20 vol% AlN suspension was prepared and added to the mixed SiC/Y₂O₃ suspension and milled for another half an hour. Results of viscosity measurements are shown in Figure 7.10. The viscosities of the mixtures are lower than that of the SiC suspension because of a lower solid content of the additive slurries and similar surface properties of the powders. The viscosity of the SiC/Y₂O₃/AlN mixture increases by the addition of the AlN slurry to the SiC/Y₂O₃ mixture, but it is still lower than that of the SiC suspension.

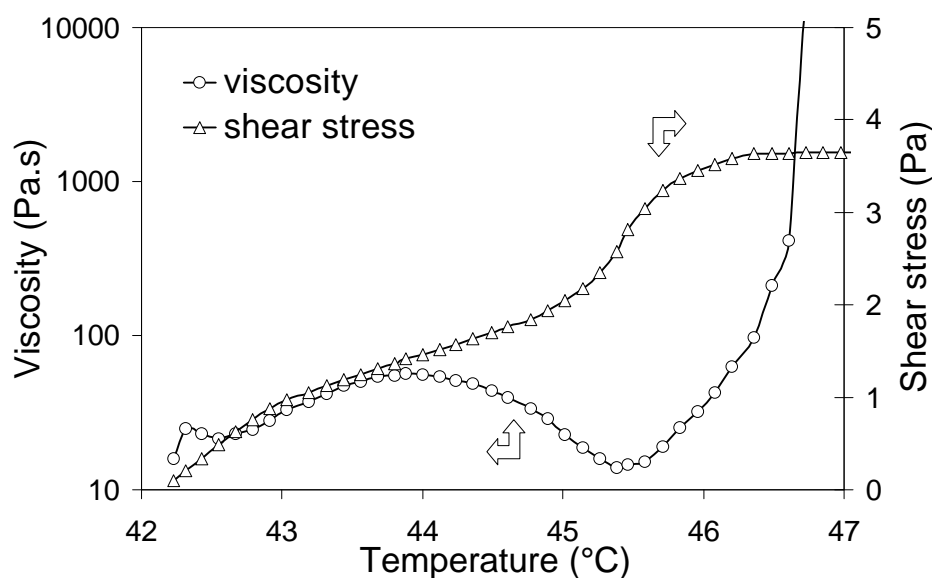


Figure 7.11: Viscosity change of 40 vol% SiC/Y₂O₃/AlN mixture with temperature (pH 10)

The viscosity of mixed 40 vol% SiC/Y₂O₃/AlN suspension increases with increasing temperature (Figure 7.11). The minimum around 45.5 °C is because of inconstant shear stress, which is caused by unstable suspension or high viscosity. Above 46°C the viscosity is too high to get clear results.

7.1.4.2.1 Rheological behavior of a mixed 20 vol% SiC/Y₂O₃/AlN suspension

In order to understand the properties of mixed suspensions at elevated temperatures more clearly, suspensions with reduced solid content (20 vol% and 30 vol%) were investigated.

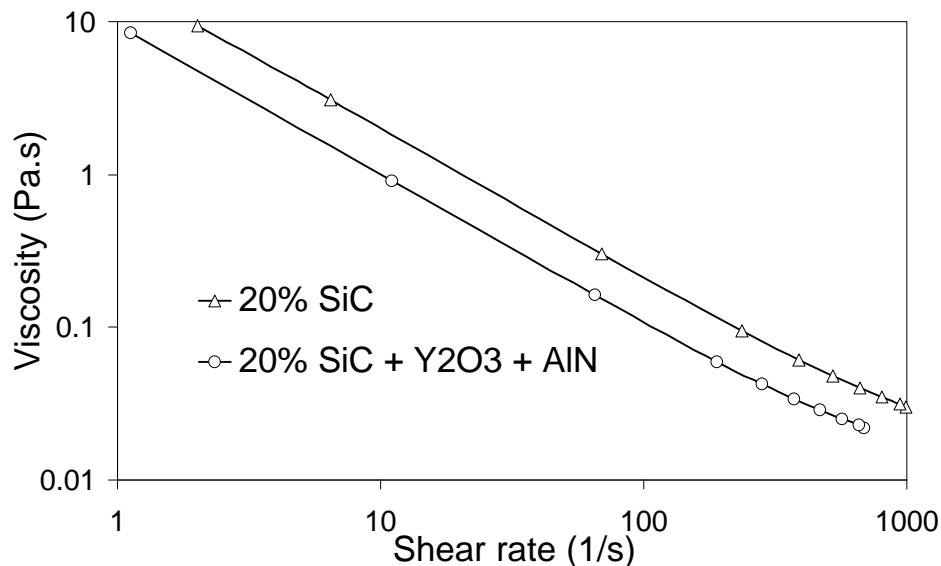


Figure 7.12: Viscosity changes of a 20 vol% SiC suspension through the addition of sintering additives (pH 10)

A 20 vol% SiC suspension was prepared and milled for 2 hours. AlN and Y₂O₃/TAC were milled for half an hour. Subsequently both suspensions were mixed and milled for another half an hour. The viscosity measurements are shown in Figure 7.12. The viscosity of the mixture is lower than that of the SiC suspension, because of the lower viscosity of the Y₂O₃/TAC suspension and similar surface properties of the powders. After the viscosity was measured at room temperature, it was heated and thereafter cooled for measuring the influence of temperature on viscosity.

As Figure 7.13 shows, the viscosity decreases slightly with raising temperature and increases by cooling. According to DLVO theory (equation 3.4), interparticle energy (V_R) depends on temperature and ion strength. V_R and ion strength increase with increasing temperature. But increasing ion strength lowers V_R . The viscosity decreases as a result of a combined effect.

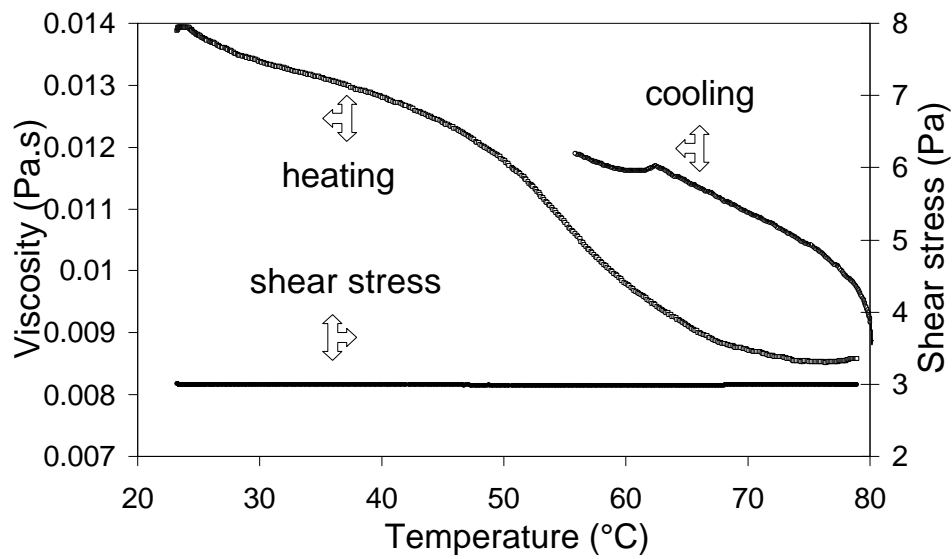


Figure 7.13: Temperature effects on viscosity of SiC/AlN/Y₂O₃ mixture (pH 10)

7.1.4.2.2 Rheological behavior of a mixed 30 vol% SiC/Y₂O₃/AlN suspension

SiC suspensions with 30 vol% solid loading were prepared by the same procedure as those with 20 vol% (of chapter 7.1.4.2.1). The results of viscosity measurements are shown in Figure 7.14 and of the influence of temperature on heating in Figure 7.15.

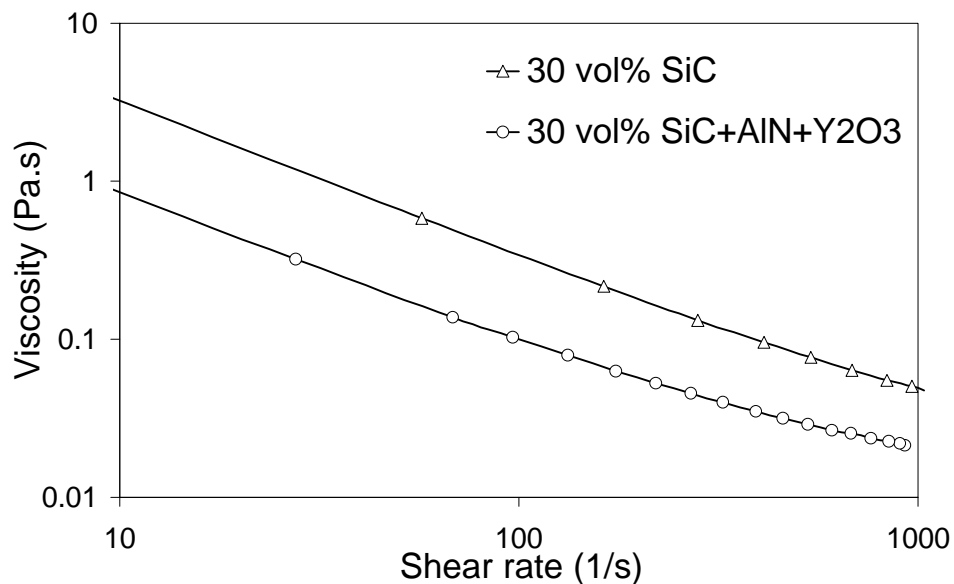


Figure 7.14: Effect of sintering additives on the viscosity of 30 vol% SiC suspension (pH 10)

The viscosity of the SiC suspension decreases by the addition of sintering additives (Figure 7.14). The viscosity of the SiC/AlN/Y₂O₃ suspension increases with elevated temperature (Figure 7.15), which suggests a temperature - induced direct casting above 30 vol% solid content. From the decrease of viscosity by cooling (Figure 7.16), a reversible coagulation mechanisms is expected.

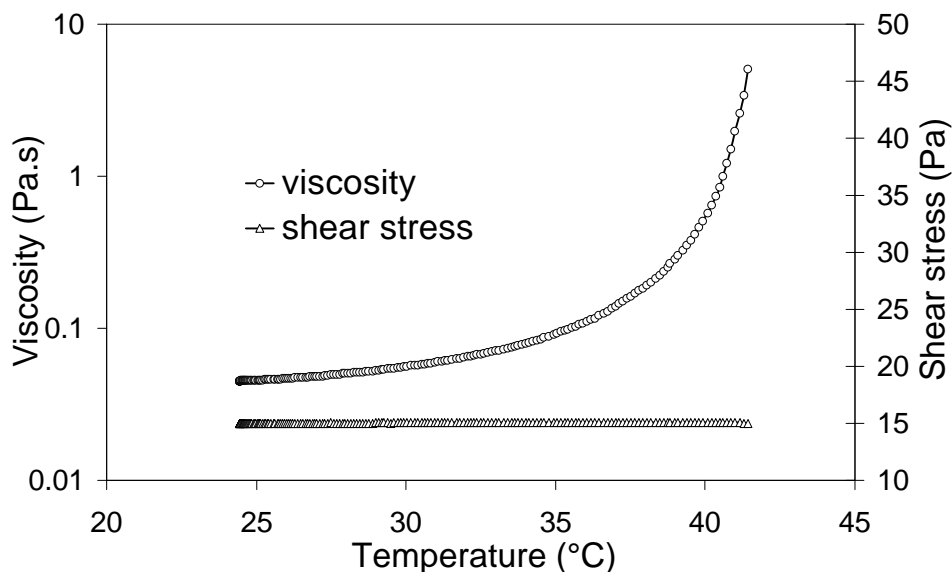


Figure 7.15: Temperature effect on viscosity of suspension with 30 vol% SiC/AlN/Y₂O₃ (pH 10)

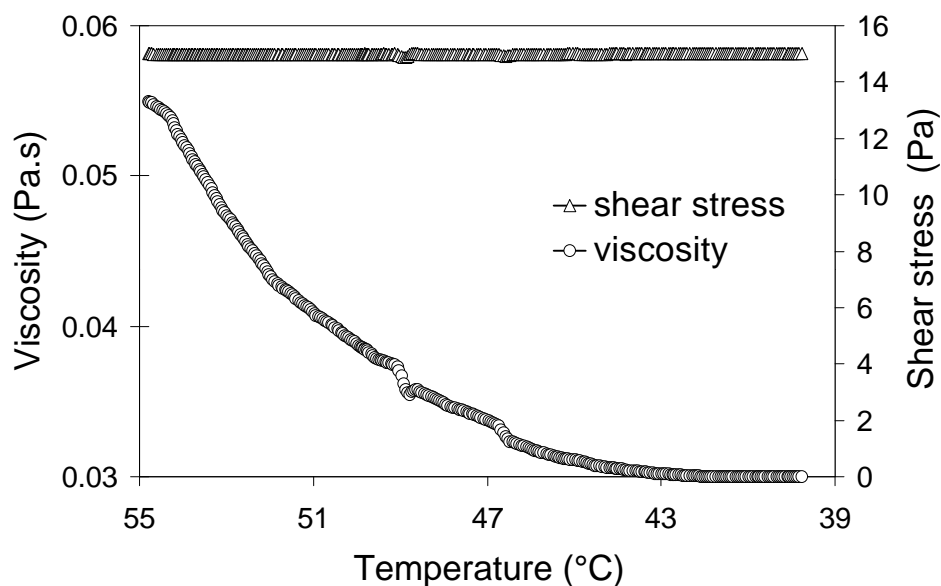


Figure 7.16: Viscosity change of a mixed 30 vol% SiC/AlN/Y₂O₃ suspension by cooling (pH 10)

7.2 Temperature effects on SiC suspensions with dispersant

Different SiC/Y₂O₃/AlN suspensions are obtained by pH adjusting. However they are only at a minimum solid content of 40 vol% SiC/Y₂O₃/AlN. Polyethylenimine (PEI) is used as dispersant to raise solid loading.

7.2.1 High solid content SiC suspension and steric stability

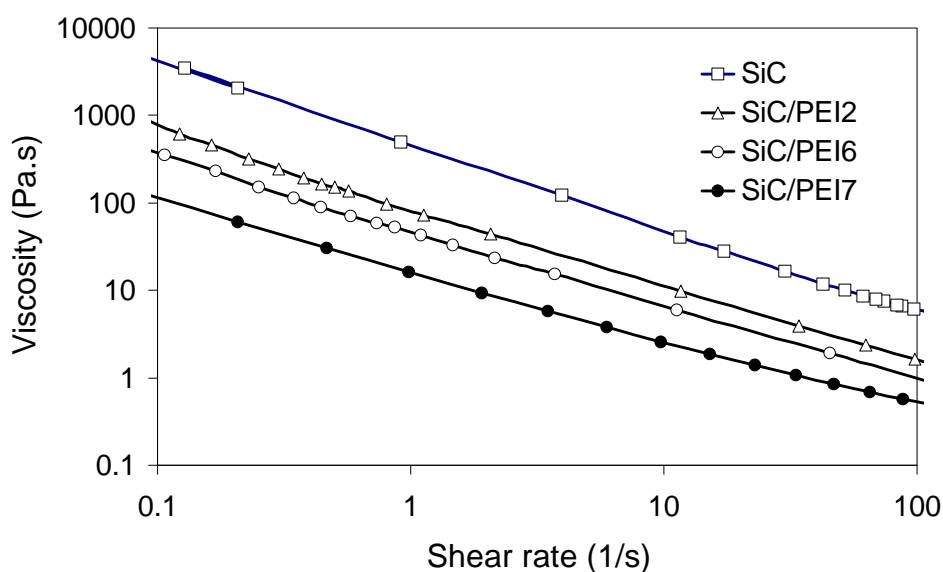


Figure 7.17: Viscosity changes caused by addition of PEI with different average molecular weight (at pH 10 with 1 wt% polymer)

In Figure 7.17, the viscosity result of 50 vol% SiC suspensions dispersed by 1 wt% PEI with different molecular weights are shown. PEI2, PEI6 and PEI7 are Polyethylenimine with average molecular weight of 2000, 25000 and 70000, respectively. The SiC suspension with PEI7 displays the lowest viscosity.

Zeta potential of SiC powder with 1 wt% PEI7 is measured in 0.01 M KNO₃ electrolyte (Figure 7.18).

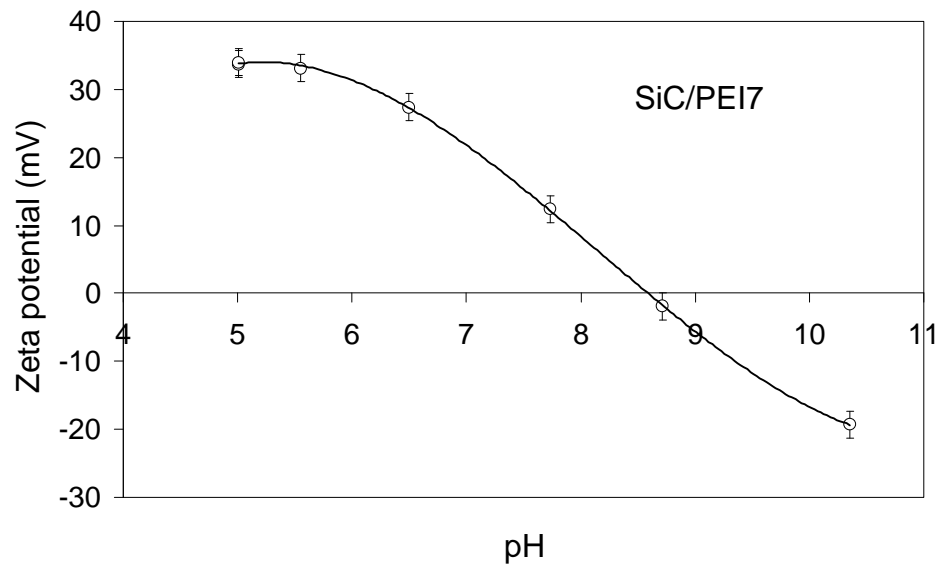


Figure 7.18: Zeta potential of SiC powder with 1 wt% PEI7

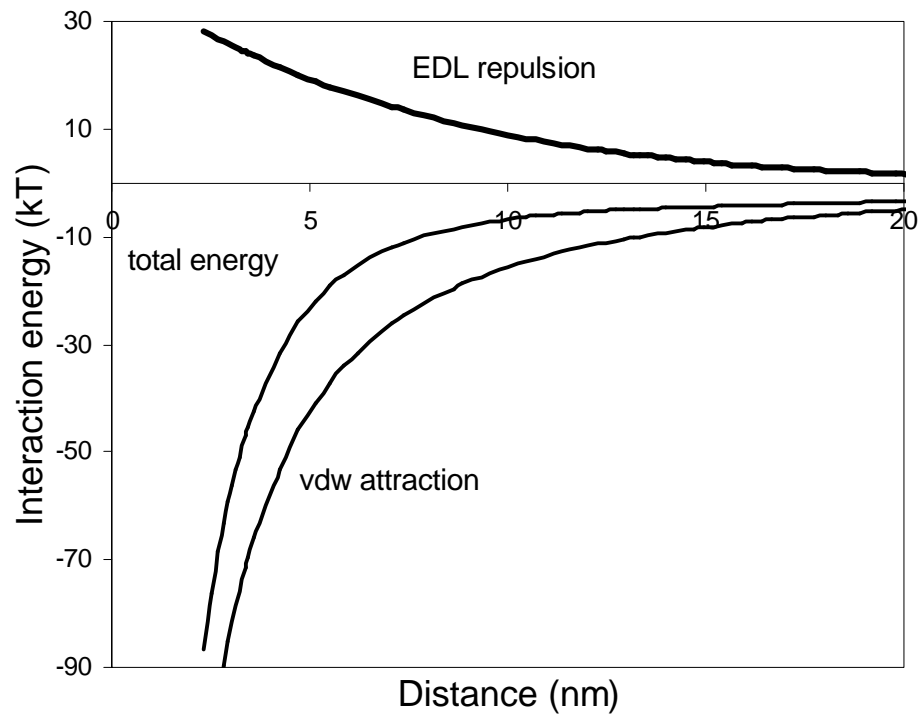


Figure 7.19: Interaction energy of SiC powder dispersed with 1 nm PEI7 at the surface (calculated using STABIL with 1 nm polymer thickness at pH 10)

The interaction energy of SiC particles dispersed with PEI7 were calculated using STABIL program. The PEI7 layer is supposed to have a 1 nm thickness at the surface for the calculation. The results are shown in Figure 7.19.

It can be supposed that steric repulsion plays an important role as stabilization mechanism. Although SiC/PEI7 suspension was prepared without pH adjusting, its pH value is pH 10 after two hours of planetary ball milling due to the ammonic function groups of PEI7. Subsequently, it was diluted and directly used for zeta potential measurements (Figure 7.18). The result shows that the absolute value of zeta potential is below 20 mV at pH 10. That means the repulsive EDL force is not sufficient for dispersion. Additionally, the interaction energy was also calculated (Figure 7.19) and it shows, there is no energy barrier at all for a electrostatic stabilization. Therefore, under such a condition the dispersion of SiC/PEI7 as indicated in Figure 7.17 takes place by steric repulsion.

7.2.2 pH change with temperature

The pH value of a 40 vol% SiC suspension was measured as a function of temperature starting from pH 6.6 (Figure 7.20). It decreases by heating and increases again by cooling. The change of the pH is caused by the dissolution and reprecipitation of SiO₂ at the SiC surface due to equation 7.4 in a similar way as was shown in Figure 7.1. Therefore, the

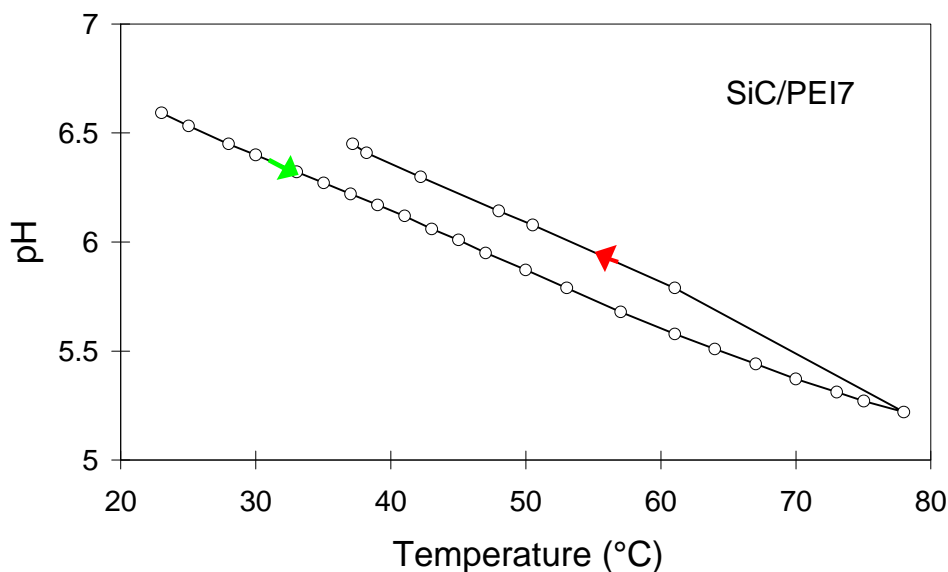


Figure 7.20: pH change of 40 vol% SiC/PEI suspension with temperature

adsorption of PEI7 on to the SiC surface obviously does not affect the dissolving reaction of SiO_2 deposited at the SiC surface.

7.2.3 SiC/PEI7 flocculation

Suspensions with 40 vol% and 50 vol% were prepared using 1 wt% percent PEI7 as dispersant. The viscosity is determined at pH 9 by using Rheometer and is shown in Figure 7.21.

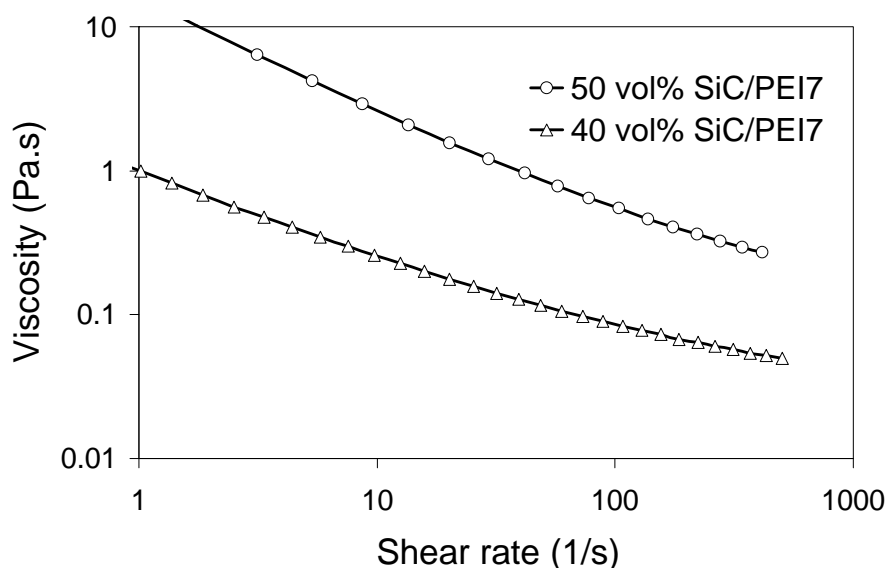


Figure 7.21: Viscosity of SiC suspensions with 1 wt% PEI7 (pH 9)

Such high solid content SiC suspensions show increased shear thinning because the magnitude of the interparticle attraction increases, i.e. they have no Newtonian behavior at high shear rate. To insure full coverage of the SiC surface and to provide some free PEI in the suspension, an amount of 1 wt% of PEI7 was used. The free PEI is suggested to provide a depletion function (s. Chapter 3.2.3.2) [99]. Additionally, some free PEI is needed for mixing with suspension of AlN.

The two SiC/PEI7 suspensions were prepared by planetary ball milling for two hours at pH 9. The effect of temperature on to viscosity are shown in Figure 7.22. The viscosity of both suspensions increase significantly with increasing temperature. However, they display a

dissimilar behavior. The viscosity of the 40 vol% SiC suspension does not increase until 75°C, whereas the one with 50 vol% starts to increase already at approximately 30°C.

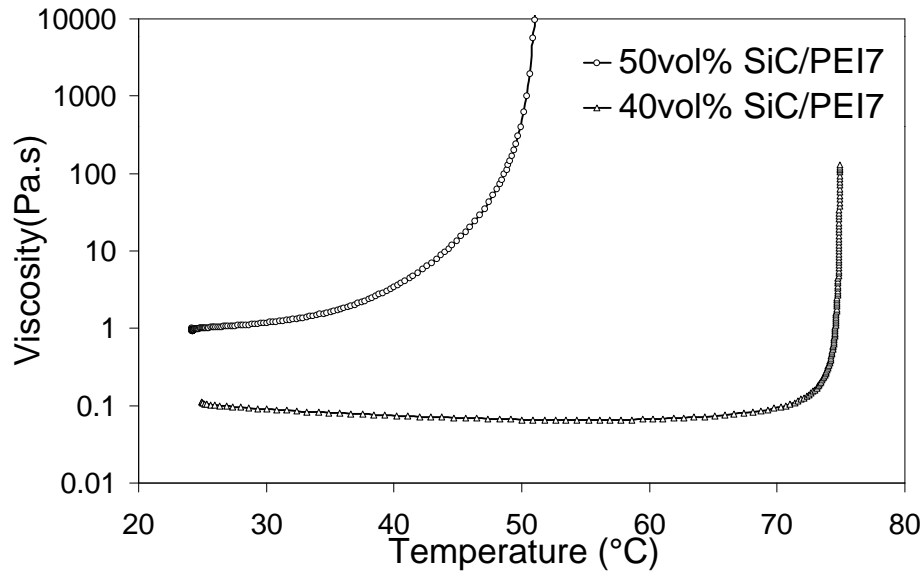


Figure 7.22: Temperature effect on to viscosity of different SiC/PEI7 suspensions (pH 10)

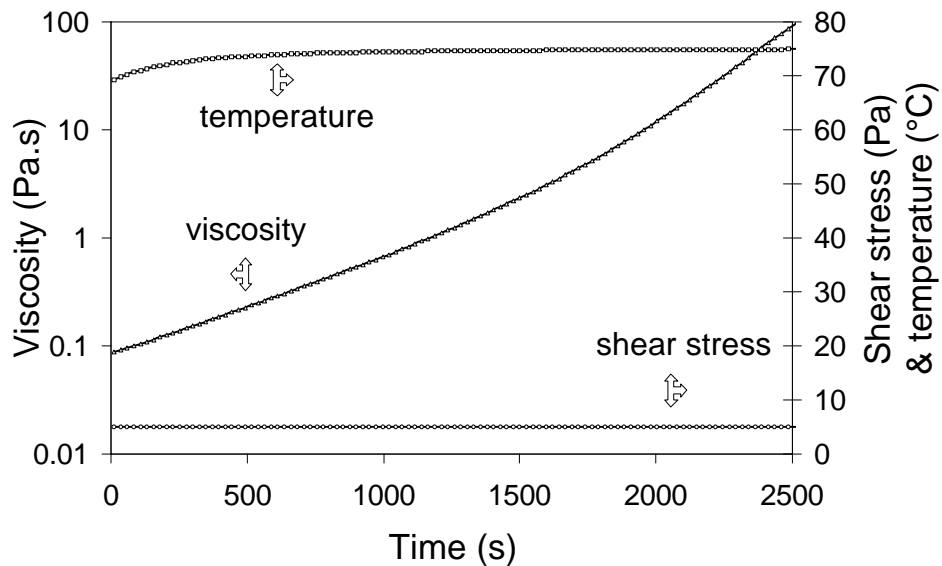


Figure 7.23: Viscosity change of 40 vol% SiC suspension versus time at 75°C (pH 9)

The viscosity of the 40 vol% SiC suspension was studied versus time at 75°C. As can be seen from Figure 7.23, the viscosity increases not dramatically but slowly with time at this temperature. It is supposed that the conformation of the polymer molecules changes with temperature. Bergström studied the conformation change of an amphiphilic polymer, Hypermer KD3, and supposed that the decrease in the magnitude of the polymer-induced repulsion with solvency can be estimated from the temperature scaling of ΔG_m [53]:

$$\Delta G_m \propto \left(1 - \frac{q}{T}\right) = \frac{\Delta T}{T}, \quad (7.5)$$

where q denotes the temperature where ΔG_m becomes zero. It is supposed that thermodynamically limited flocculation is expected close to the q -temperature where ΔG_m becomes very small and eventually changes its sign. A schematic of the conformation change of the polymer is presented in Figure 7.24. Changing temperature has a drastic influence on the layer thickness of the adsorbed polymer. Therefore, when the solvency of the polymer reaches a critical level, sterically stabilized dispersion flocculates commonly (incipient flocculation).

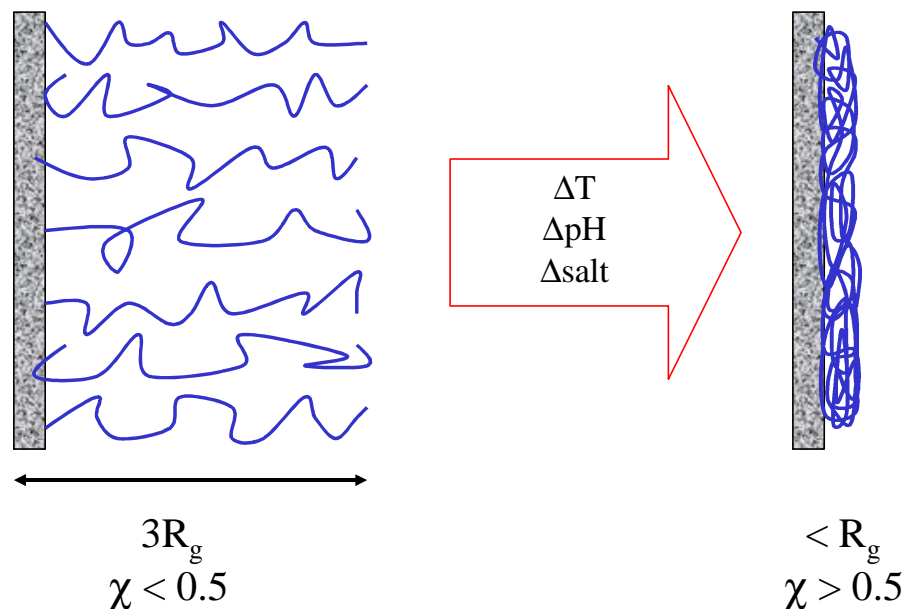


Figure 7.24 Schematic diagram showing the effect of external stimuli on to the conformation of reactive polymers [1]

To investigate the detail of the incipient flocculation process, a 40 vol% SiC suspension was prepared and cast in an closed mold and heated to 70 °C in a drying oven. The slurry is flocculated after two hours and divided into two phases, a stiff SiC/PEI7 phase and clear water/PEI phase, respectively. A scheme of the process on heating is represented in Figure 7.25.

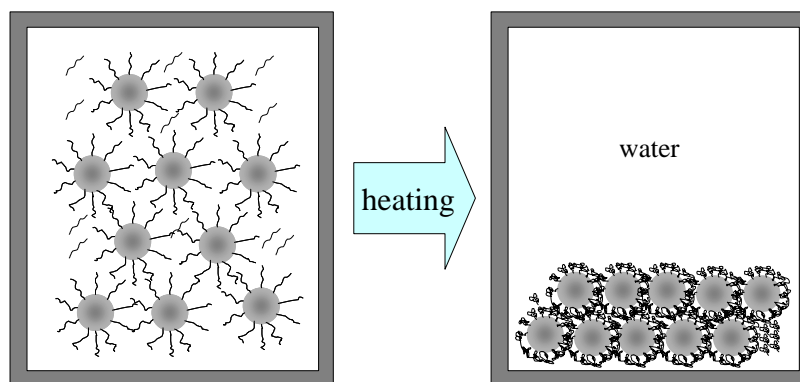


Figure 7.25: Scheme of the behavior of a SiC/PEI7 suspension during heating

Beside temperature, other parameters as, for example, solid content and ion strength, also have an influence on the polymer induced flocculation. At high solid contents, the flocculation temperature is lower such as 50 °C. Possibly stronger interparticle reaction and high ion strength at 50 vol% solid content compresses the conformation of polymer like a “pan cake” (Figure 7.24) at lower temperature, which leads to coagulation. For lower solid contents it needs high temperature to raise the ion strength through dissolving SiO₂ and to strengthen interparticle reaction for flocculation. The role of “pan cake”-formed polymer is supposed as a binder after flocculation and to strengthen the green body (Figure 7.25).

7.2.4 Suspension with sintering additives

As was shown earlier SiC is charged negatively in water and Y₂O₃ is partly dissolved in water and remains in suspension below pH 9.8 as Y(OH)_x^{(3-x)+}. Mixed SiC/Y₂O₃ powder is dispersed by ball milling and heating respectively. The zeta potential has been determined after ball milling and heating at different pH range. It is lower than that of a SiC suspension. It is not appropriate to make stable suspensions of mixed SiC/Y₂O₃ powder (Figure 7.7). The pH of the mixed suspension decreases with increasing temperature. The solubility of Y₂O₃

does not change significantly by heating, thus no significant change of the ion strength can be obtained for flocculation.

According to DLVO theory and Y_2O_3 zeta potential measuring results, Y_2O_3 suspensions can be made up at $pH < 9$ with positive surface charges. The zeta potential curve of Y_2O_3 is shown in Figure 4.11. After adsorption of PEI7, SiC surface is changed into positive values at $pH < 8.6$ (Figure 7.18). The zeta potential of AlN protected with a surface layer of Si-Al-O-N is changed also into positive by PEI7 at $pH < 7.8$ in water because the isoelectric point of AlN is shifted from $pH 2$ to $pH 7.8$ (Figure 7.26).

According to measurements of zeta potential there is an appropriate pH range from $pH 4$ to $pH 8$, in which all three materials display similar properties. In order to prepare a SiC suspension with sintering additives of Y_2O_3 and AlN (SiC/sintering additives: 90 vol%/10 vol%; AlN/ Y_2O_3 : 60 mol%/40 mol%), a SiC suspension was prepared through ball milling for 2 hours and mixed with a slurry of the sintering additives which was prepared also through ball milling for half an hour. The mixture then was stirred for half an hour and put into a drying oven at $60-80^\circ C$ for 1-2 hours for flocculation. The same procedure was used to prepare a mixed SiC/ Y_2O_3 suspension. The viscosity changes due to the added sintering additives are shown in Figure 7.27.

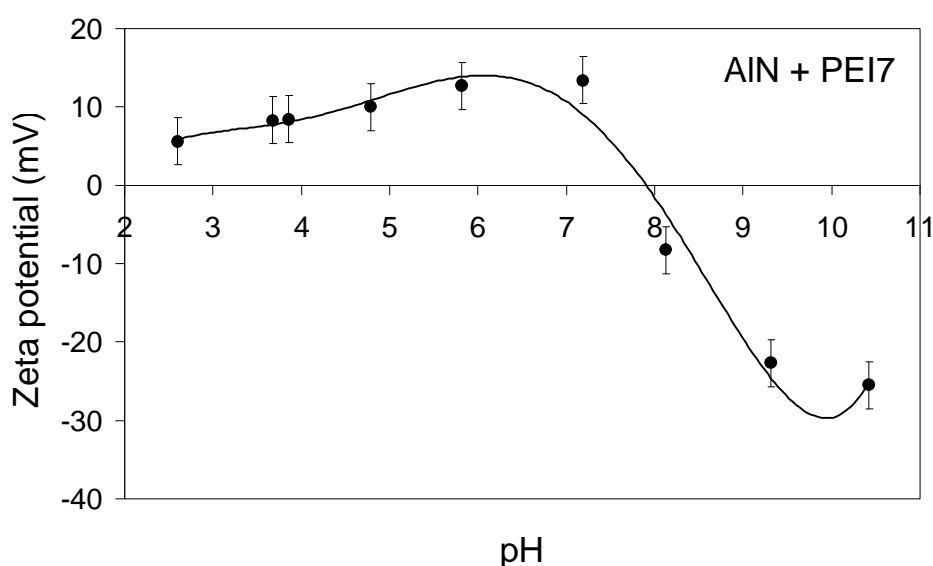


Figure 7.26: Zeta potential of surface-modified AlN/PEI7 suspension

As Figure 7.27 shows, the viscosity of the SiC suspension decreases through the addition of Y_2O_3 suspension due to a lower viscosity of the Y_2O_3 suspension as compared to that of the SiC suspension. After the addition of AlN the viscosity increases and is similar like that of the pure SiC suspension. However the degree of shear thinning decreases significantly, which corresponds to a stable suspension.

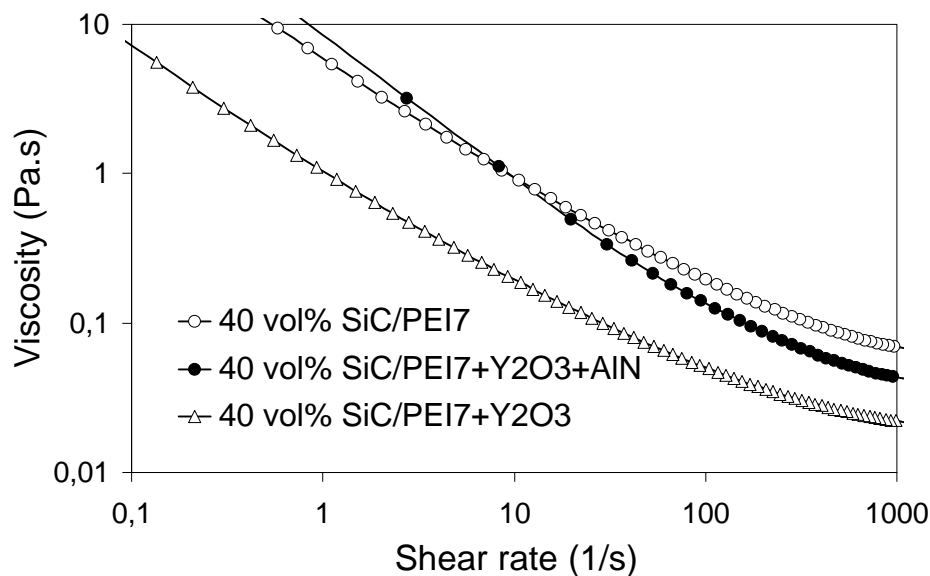


Figure 7.27: Viscosity change of SiC/PEI7 suspension by addition of sintering additives (pH 7)

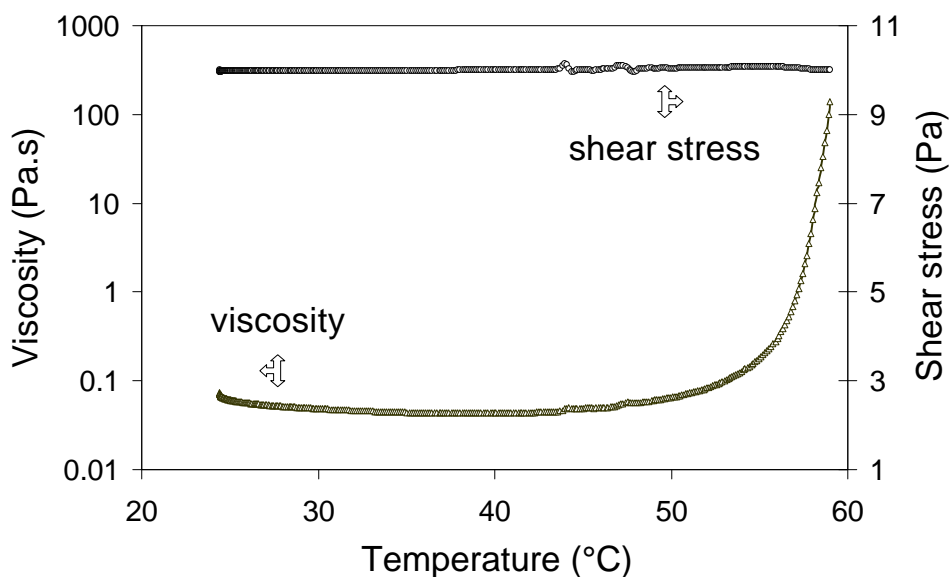


Figure 7.28: Viscosity change of 40 vol% SiC/AlN/ Y_2O_3 suspension by heating (pH 7)

Figure 7.28 shows the viscosity change of the mixed 40 vol% SiC/AlN/Y₂O₃ suspension versus temperature at a constant shear stress. A dramatic increase of viscosity is obtained on heating starting at a temperature around 50 °C. Obviously, the colloidal stability of sterically stabilised SiC/AlN/Y₂O₃ suspension can be controlled by temperature. On the basis of that a ceramic forming processing was developed. A flow sheet of this process is shown in Figure 7.29.

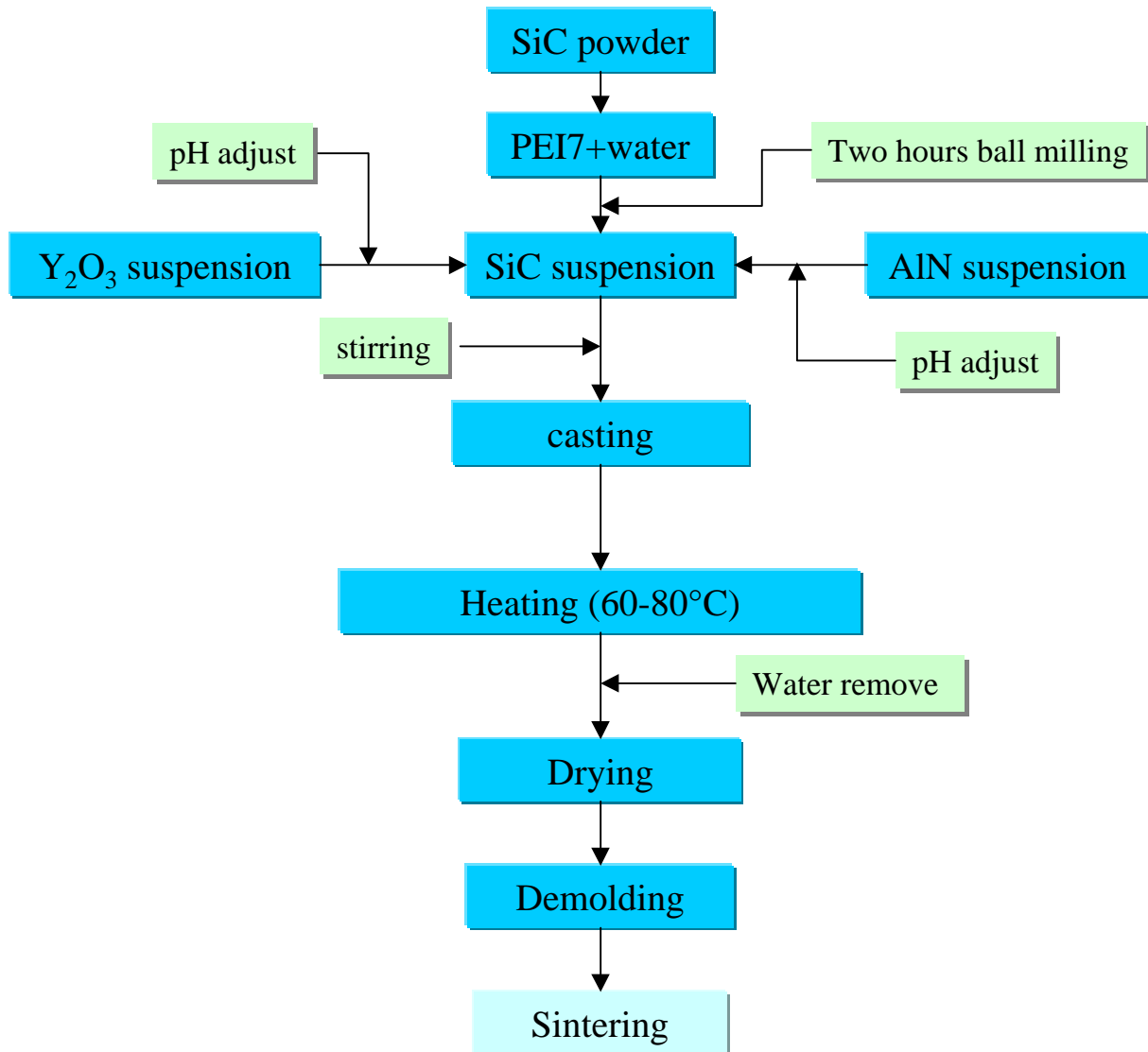


Figure 7.29: Temperature induced forming of SiC with addition of Y₂O₃ and AlN

8 Outlook

The current researching work provide a fundamental frame to apply temperature-induced direct casting to liquid phase sintering of SiC. AlN powder has similar surface properties as SiC powder after it is protected by oxide layer Si-Al-O-N. Therefore, it seems to be possible to apply temperature - induced direct casting also to AlN materials.

9 Zusammenfassung

1. Problemstellung und Literatur

Auf Grund von Fortschritten im grundlegenden Verständnis der Teilchenwechselwirkung in Suspensionen finden Direktgießverfahren zur Herstellung von Grünteilen in der Technik im Hinblick auf eine Erhöhung der Zuverlässigkeit keramischer Bauteile und eine Reduktion der Fertigungskosten zunehmendes Interesse. Durch Kontrolle von pH, Ionenstärke und adsorbierter Mengen organischer Hilfsstoffe (Dispergiermittel) können Schlicker kontrolliert flockuliert werden und damit eine „Erstarrung“ eines in eine Form gefüllten Schlickers bewirkt werden. Grundlegende Untersuchungen zeigen, dass dies auch allein durch eine Erhöhung der Temperatur möglich ist. Die Temperaturerhöhung erstreckt sich dabei lediglich von Raumtemperatur auf ca. 60 bis 70°C. Ein weiterer Vorteil dieses Verfahrens beruht auf minimalen Mengen (< 1 Gew.-%) benötigter organischer Hilfsstoffe. Die Herstellung von keramischen, sinterfertigen Grünteilen mit diesem neuen Verfahren war bisher nur mit Aluminiumoxid möglich. Es ist das Ziel dieser Arbeit die Vorgehensweise auf Siliziumkarbid (SiC) zu übertragen und dazu die Teilchenwechselwirkung in wässrigen SiC-Suspensionen detailliert zu studieren.

Beim Überblick über die aktuellen keramischen Gießverfahren wurde besonderer Wert auf die direkten Verfahren gelegt. Diese umfassen die Gießverfahren, die chemische Gele nutzen, wie FC (Freeze Casting), GC (Gel Casting), AIM (Aqueous Injection Molding) und HAS (Hydrolysis Assisted Solidification) sowie die, die physikalische Gele verwenden, wie DCC (Direct Coagulation Casting), TIF (Temperature Induced Forming) und CIP (Colloidal Isopressing). Mit diesen direkten Gießverfahren können komplexe keramische Teile gefertigt werden, ohne dass diese weiter bearbeitet werden müssen. So können mögliche Oberflächenfehler vermieden werden, die durch eine zudem teure Nachbearbeitung entstehen könnten. Die direkten Gießverfahren besitzen aber auch Nachteile. Die Grünkörper können zerbrechlich sein und die Schlicker sind manchmal empfindlich, d. h. sie haben nur eine begrenzte Zeit- und Temperaturstabilität. Weiterhin werden mitunter teure oder umweltschädliche organische Additive benötigt.

Die DLVO-Theorie (Derjaguin, Landau, Verwey und Overbeek) und die Kenntnisse über kolloidchemische Zusammenhänge erlauben Aussagen über die Oberfläche und kolloiden Eigenschaften von keramischen Pulvern. Keramische Pulver können elektrisch durch die Modifikation der EDL (Electric Double Layer) oder durch den Aufbau einer sterischen Schicht in der wässrigen Phase dispergiert werden.

2. Experimentelle Strategie

Zur Untersuchung der Teilchenwechselwirkung in wässrigen SiC-Suspensionen wurde zunächst die Oberfläche des verwendeten SiC-Pulvers analysiert, dann deren Dispergierung in einem wässrigen System studiert und schließlich das rheologische Verhalten von daraus abgeleiteten Schlickern in Abhängigkeit von der Art des Dispergierhilfsmittels, des pH-Werts und der Temperatur unter Berücksichtigung der dem System zugesetzten Sinteradditive (AlN und Y_2O_3) untersucht.

3. Experimenteller Teil

Im Hinblick auf das Flüssigphasensintern von SiC wurde bei dieser Arbeit ausgehend von vorherigen Untersuchungen [104] folgende Stoffzusammensetzung gewählt: 90 Vol.-% SiC und 10 Vol.-% Sinteradditive, die sich wiederum aus 60 mol.-% AlN und 40 mol.-% Y_2O_3 zusammensetzen. Die spezifische Oberfläche der Pulver wurde mittels der BET-Methode (Brunauer-Emmett-Teller) mit Stickstoff bestimmt. Die Teilchengrößenverteilung wurde mittels Laserbeugung (Mastersizer 2000) gemessen. Die Partikelgrößenmessung von SiC musste mit einem Dispergierhilfsmittel durchgeführt werden, da SiC in Wasser bei pH 10 (max. pH-Wert, für den das Messgerät ausgelegt ist) mit der beim Messgerät Mastersizer 2000 vorhandenen Rührvorrichtung nicht komplett zu dispergieren ist. Deshalb wurde das SiC-Pulver vor der Messung unter Verwendung von PEI in Wasser mittels einer Planetenkugelmühle dispergiert. AlN wurde mit verschiedenen Methoden beschichtet und mit Wasser vor der Messungen in der Planetenkugelmühle dispergiert. Y_2O_3 wurde unbehandelt, aber ebenfalls mit Wasser in der Planetenkugelmühle dispergiert. Die chemische Zusammensetzung der Pulver wurde durch ICP-OES (Inductively Coupled Plasma – Optical Emission Spectroscopy / Jobin Yvon, Grasbrunn,, Deutschland) in Argon analysiert. DRIFT (Diffuse Reflectance Infrared Fourier Transform Spectroscopy) wurde benutzt, um die funktionellen Gruppen an der Oberfläche von trockenen Pulvern qualitativ zu bestimmen. Für

die Charakterisierung der kolloiden Eigenschaften wurden sowohl das Zetapotential, als auch Sedimentations- und Viskositätsmessungen durchgeführt.

Für die Zetapotentialmessungen wurden die Pulver mit 0,01M KNO_3 (dem Elektrolyt) versetzt und mit der Planetenkugelmühle dispergiert. Danach wurden diese Schlicker ebenfalls mit 0,01M KNO_3 verdünnt. Zetapotentialmessungen wurden ebenfalls mit verschiedenen Dispergierhilfsmitteln, wie z.B. den Polymeren PEI, MELA, DMA, PEOP, BUMA, PMAA, OLAK, DEMA, SILO und STEA, durchgeführt.

Für die Sedimentationsmessungen wurde mit Hilfe von Ultraschall ein SiC-Schlicker mit 7 Vol.-% Feststoffgehalt hergestellt. Es wurden Messungen im pH-Bereich 2 - 14 durchgeführt. Beim Einsatz von verschiedenen Dispergierhilfsmitteln wurden die Sedimentationsmessungen im jeweils optimalen pH-Bereich durchgeführt.

Für die Viskositätsmessungen kam ein Rotationsviskosimeter (DSR 500 / Rheometrics Scientific, Bensheim) zum Einsatz, der mit einer koaxialen Bob-Zylinder-Geometrie-Paarung ausgerüstet ist. Die Schlicker wurden mit der Planetenkugelmühle dispergiert und vor den Messungen für 30 Sekunden bei einer Scherspannung vorgeschert, wodurch die im nicht ideal stabilisierten Schlicker absedimentierten Pulverteilchen wieder homogen im Suspensionsmedium verteilt wurden. Die Temperatur des Schlickers wurde durch ein Wärmebad bei 25°C konstant gehalten. Für die Messungen bei höherer Temperatur wurde die Meßzelle mit einer dünnen Ölschicht bedeckt um die Verdünnung der Suspension zu verhindern. Die Sinteradditive wurden zuerst jeweils separat als Schlicker mit der Planetenkugelmühle hergestellt und danach zu dem SiC-Schlicker hinzugefügt und nochmals dispergiert.

4. Ergebnisse

Auf der SiC-Oberfläche waren mittels DRIFT-Spektroskopie NH- und Si-O-Si-Banden zu erkennen. Die AlN- und Y_2O_3 -Oberflächen werden diesen Messungen zufolge von OH-Gruppen dominiert. Das SiC-Pulver wurde vor der Messung unter Verwendung von PEI in Wasser mittels einer Planetenkugelmühle dispergiert. Die Teilchengröße von SiC ergab sich danach als 0,18 μm bei d (0,5). AlN (wie weiter unten beschrieben beschichtet, mit Wasser in der Planetenkugelmühle dispergiert) zeigt eine mittlere Teilchengröße von 0,89 μm

bei $d(0,5)$. Bei Y_2O_3 (unbehandelt, ebenfalls mit Wasser in der Planetenkugelmühle dispergiert) ergibt sich eine Größe von $0,89 \mu m$ bei $d(0,5)$. Die spezifischen Oberflächen von SiC, AlN und Y_2O_3 betragen 11,4, 12,9 und $4,8 m^2/g$. Der pH_{IEP} Werte von SiC liegt bei $pH 3,41$. Die entsprechenden pH_{IEP} -Werte von Y_2O_3 und modifiziertem AlN betragen 2,0 und 10,3. Die Zetapotentialmessungen mit Dispergierhilfsmitteln zeigen, die Oberfläche von SiC wurde von PEI am stärksten von allen getesteten Dispergierhilfsmitteln verändert und führte im Bereich von $pH < 10$ zu einer positiven Oberflächenladung. Bei allen anderen Dispergierhilfsmitteln resultierte hier eine negative Oberflächenladung. STEA, SILO und DEMA schieben pH_{IEP} in den sauren Bereich.

Bei Sedimentationsmessungen im Bereich von $pH 10 - 12$ wurden 41 % der theoretischen Dichte erhalten. Beim Einsatz von verschiedenen Dispergierhilfsmitteln wurden im jeweils optimalen pH -Bereich lediglich 10 - 18 % der theoretischen Dichte erreicht.

10 Vol.-% und 20 Vol.-% SiC-Schlicker wurden stabilisiert, indem mit Salpetersäure und Ammoniak verschiedene pH -Werte eingestellt wurden. Bei verschiedenen pH -Werten wurden nun die Viskositäten als Maß für die Kolloidstabilität gemessen. Bei $pH 10$ ist die Viskosität bei beiden Feststoffgehalten minimal. SiC-Schlicker mit höheren Feststoffgehalten zeigen thixotrope Eigenschaften. Der Schlicker wird höherviskos beim höheren Temperatur. Der SiC/AlN/ Y_2O_3 -Schlicker geliert mit steigender Temperatur, wenn der Feststoffgehalt den Wert von 30 Vol.-% übersteigt. Allerdings ist die resultierende Viskosität bei Raumtemperatur bei Feststoffgehalten über 40 Vol.-% zu hoch um dieses Material noch gießen zu können. PEOP, DEMA, STEA und BUMA erhöhen die Viskosität der SiC-Schlicker. Die SiC-Schlicker mit SILO, OLAK und PEI2 haben eine relativ niedrige Viskosität. Ein jeweils mit PEI, SILO oder OLAK hergestellter SiC-Schlicker mit 20 Vol.-% Feststoffgehalt zeigt Newtonsche Eigenschaften. Mit PEI (Polyethylenimin, MW 70,000) werden SiC-Schlicker bis zu 50 Vol.-% Feststoffgehalt stabilisiert. Mit steigender Temperatur sinkt der pH -Wert. Am wichtigsten ist es jedoch, dass hier die Viskosität mit steigender Temperatur höher wird. Die Ergebnisse zeigen, dass bei 40 Vol.-% Feststoffgehalt der Schlicker ab $60 \text{ }^\circ C$ zu gelieren beginnt und bei 40 Vol.-% bereits ab $30 \text{ }^\circ C$.

PEI wurde als Dispergierhilfsmittel zur sterischen Kolloidstabilisierung eingesetzt. Damit wurde ein gießbarer SiC/AlN/ Y_2O_3 -Schlicker mit 50 Vol.-% Feststoffgehalt

hergestellt. Die Stabilität dieser sterisch stabilisierten Schlicker ist in geeigneter Weise temperaturabhängig. Der Schlicker beginnt bei 60 °C zu gelieren. Nach zwei Stunden kann der Grünkörper entformt werden.

5. Diskussion

Das Ergebnis von Zetapotentialmessungen mit Dispergierhilfsmitteln ist von der Adsorption von Polymeren abhängig. Die Adsorption auf der SiC-Oberfläche wird bestimmt von Wasserstoffbrückenbindungen, der Wechselwirkung zwischen der Kohlenwasserstoffkette der Polymers und den Kohlenstoffatomen von SiC sowie elektrostatischen Kräften.

Bei Sedimentationsmessungen im Bereich von pH 10 - 12 wurden 41 % der theoretischen Dichte erhalten. Dabei spielt die elektrische Doppelschicht eine dominierende Rolle. SiC ist bei pH-Werten über 3,41 negativ geladen und die Oberflächenladung erreicht bei pH-Werten über 8 ca. -25 mV. Eine erreichte Abstoßungskraft zwischen beiden Partikeln wird erhalten, wenn die Partikel einen absoluten Zetapotential-Wert über 25 mV haben. Deshalb sind die SiC-Pulver im pH-Bereich 10-12 dispergiert und haben eine hohe theoretische Dichte. Beim Einsatz von verschiedenen Dispergierhilfsmitteln wurden im jeweils optimalen pH-Bereich lediglich 10 - 18 % der theoretischen Dichte erreicht. Der Grund liegt darin, dass diese Dispergierhilfsmittel nicht hinreichend gut auf der SiC-Oberfläche adsorbieren, weil durch Ultraschall nur ein geringer Teil der Oberfläche von SiO₂ befreit wird.

Bei der Verwendung der Sinteradditive AlN und Y₂O₃ muss man folgende Dinge beachten. AlN reagiert mit Wasser unter Bildung von Gibbsit, so dass das Pulver vor Hydrolyse geschützt werden muss. Die begrenzte Löslichkeit von SiO₂ (von der SiC-Oberfläche) in Wasser ergibt nach dessen Abscheidung auf AlN eine dünne, aber effektive SiO₂-Schicht, die zu der bereits existierenden Al₂O₃-Schicht auf der AlN-Oberfläche dazukommt. Damit kann eine Hydrolyse bei Raumtemperatur weitestgehend vermieden werden. Da das Gießverfahren aber bei erhöhten Temperaturen durchgeführt werden soll, wurde AlN mit TEOS beschichtet und dann eine Stunde in bewegter Luft bei 600°C kalziniert, bei der diese Schicht nicht stabil ist. Durch diese zusätzliche Behandlung wird eine Si-Al-O-N-Schutzschicht gebildet. Damit wird AlN gegen Hydrolyse bis 80°C geschützt. Das

Y_2O_3 -Pulver wurde mit Triammoniumcitrat (TAC) stabilisiert. TAC erzeugt durch seine Adsorption auf der Y_2O_3 -Oberfläche eine negativ geladene Oberfläche. Somit weisen alle anorganischen Bestandteile des Schlickers ähnliche Oberflächeneigenschaften auf und bei allen Bestandteilen ist eine Salzbildung mit PEI (Polyethylenimin) möglich, das zur besseren Dispergierung des SiC in Wasser verwendet wurde.

Es wurden elektrostatische und sterische Stabilisierungsarten von SiC-Schlickern untersucht.

5.1 Elektrostatisch stabilisierte SiC-Schlicker

10 Vol.-% und 20 Vol.-% SiC-Schlicker wurden stabilisiert, indem mit Salpetersäure und Ammoniak verschiedene pH-Werte eingestellt wurden und die Viskosität als Maß für die Kolloidstabilität gemessen wurde. Bei pH 10 ist die Viskosität bei beiden Feststoffgehalten minimal und damit der optimale pH-Wert für die Stabilisierung eines SiC-Schlickers. Auf dieser Basis wurde ein rheologisches Modell für einen reinen SiC-Schlicker erstellt. Hierfür wurde das SiC-Pulver mit einer Planetenkugelmühle dispergiert und der pH-Wert des Schlickers auf 10 eingestellt. Das rheologische Modell gestattet die Viskosität der SiC-Schlicker mit verschiedenen Feststoffgehalten vorauszusagen. Die berechneten Daten stimmen gut mit den experimentellen Daten überein.

Ein Fest-Flüssig-Phasendiagramm in Abhängigkeit von pH und Temperatur konnte mit Hilfe des STABIL-Computerprogramms von J. Adair und unter Verwendung der DLVO-Theorie erhalten werden. Damit kann man die Phase des Schlickers in Abhängigkeit von pH und Temperatur theoretisch bestimmen.

SiC-Schlicker mit höheren Feststoffgehalten zeigen thixotrope Eigenschaften. Die Viskosität ist von pH, Ionenstärke, Feststoffgehalt und der Temperatur abhängig. Mit steigender Temperatur löst sich das an SiC-Oberflächen vorhandene SiO_2 auf. Dadurch steigt die Salzkonzentration des Schlickers an und der pH-Wert sinkt (s. Zetapotentialmessung in Figure 7.2). Dadurch wird die elektrische Doppelschicht komprimiert. Der Schlicker wird höherviskos. Die Sinteradditive wurden zuerst jeweils separat als Schlicker mit der Planetenkugelmühle hergestellt und danach mit dem SiC-Schlicker gemischt und nochmals gemahlen. Der SiC/AlN/ Y_2O_3 -Schlicker geliert mit steigender Temperatur, wenn der

Feststoffgehalt den Wert von 30 Vol.-% übersteigt. Allerdings ist die resultierende Viskosität bei Raumtemperatur bei Feststoffgehalten über 40 Vol.-% zu hoch um dieses Material noch gießen zu können. Somit wäre für eine mögliche Verarbeitung solcher SiC-Schlicker der Bereich zwischen 30 - 40 Vol.-% Feststoffgehalt optimal. Allerdings wäre infolge des hohen pH-Wertes der Geräteverschleiß zu groß.

5. 2 sterisch stabilisierte SiC-Schlicker

Im Hinblick auf einen stabilen Schlicker für mittlere pH-Bereiche und eine geeignete Temperaturabhängigkeit des Schlickers wurden mehrere Konzepte verfolgt. Die Dispergiermittel PEOP, DEMA, STEA und BUMA erhöhen die Viskosität der SiC-Schlicker aufgrund einer schlechten Adsorption auf der SiC-Oberfläche. Die SiC-Schlicker mit SILO, OLAK und PEI2 haben hingegen eine relativ niedrige Viskosität. Mit diesen Dispergiermitteln zeigen SiC-Schlicker mit 20 Vol.-% Feststoffgehalt Newtonsche Eigenschaften. Sie werden aufgrund von H-Brücken zwischen den Kohlenwasserstoffketten der Polymere und den Kohlenstoffatomen des SiC sowie aufgrund elektrostatischer Kräfte auf der SiC-Oberfläche besser adsorbiert. Am erfolgreichsten erwies sich Polyethylenimin (PEI). Dieses Polymer reagiert basisch und ist unterhalb von pH 8,60 protoniert und somit positiv geladen. Eine Adsorption auf der SiC-Oberfläche ist über Salzbildung (Brönsted-Säure-Base-Reaktion) und elektrostatische Kräfte möglich. Aufgrund der starken Anbindung des Moleküls sowie eines hohen Molekulargewichts ist eine sterische Stabilisierung des Schlickers möglich. Bei einem Molekulargewicht von 70,000 werden SiC-Schlicker bis zu einem Feststoffgehalt von 50 Vol.-% stabilisiert. Am wichtigsten ist jedoch, dass damit die Viskosität mit steigender Temperatur höher wird.

Die kolloidalen Eigenschaften von PEI-dispergierten Schlickern wurden mittels pH- und Viskositätsmessungen untersucht. Mit steigender Temperatur löst sich das gebildete SiO₂ wieder auf. Dadurch steigt die Salzkonzentration des Schlickers an und der pH-Wert sinkt. Die Konformation der Polymerschicht ist wie die elektrische Doppelschicht von der Salzkonzentration, dem pH und der Temperatur abhängig. Die büstenartige Polymerschicht wird komprimiert, indem sich die Polymermoleküle zusammenknäueln. Wenn die Polymerschichten auf den Pulverteilchen komprimiert sind, reicht der Abstand zwischen den Teilchen nicht mehr aus, die van-der-Waalschen Kräfte zu überwinden, so dass der Schlicker

koaguliert, wozu nur 1 Gew.-% Polymer benötigt wird. Der Feststoffgehalt kann dabei bis zu 50 Vol.-% sein. Die Ergebnisse zeigen, dass unter 40 Vol.-% Feststoffgehalt der Schlicker ab 60 °C zu gelieren beginnt und über 40 Vol.-% bereits ab 30 °C.

6. Gießverfahren

SiC-Schlicker und modifiziertes AlN-Pulver jeweils mit 40 Vol.-% Feststoffgehalt wurden mittels Ammoniak bzw. Salpetersäure auf pH 10 eingestellt. Ferner wurde ein Y₂O₃-Schlicker mit 40 Vol.-% Feststoffgehalt mit Hilfe von TAC hergestellt (Kapitel 7.1.4.2). Alle drei Schlicker wurden mit einer Planetenkugelmühle bei niedriger Drehrate gemischt, in eine Form gegossen und der Grünkörper nach zwei Stunden im Trockenschrank bei 70 °C entformt. Ein Schlicker mit mehr als 40 Vol.-% Feststoffgehalt ist auf diese Weise nicht gießbar.

Zur sterischen Kolloidstabilisierung wurde PEI als Dispergierhilfsmittel eingesetzt. Auf diese Weise wurden gießbare SiC- und AlN-Schlicker mit 50 Vol.-% Feststoffgehalt hergestellt. Außerdem wurde ein Y₂O₃-Schlicker mit 40 Vol.-% Feststoffgehalt ohne TAC hergestellt, der die gleichen Kolloideigenschaften wie die SiC- und AlN-Schlicker hat. Alle drei Schlicker wurden eine halbe Stunde in der Planetenkugelmühle gemischt. Die Stabilität dieses sterisch stabilisierten SiC/AlN/Y₂O₃-Schlickers ist in geeigneter Weise temperaturabhängig. Der Schlicker beginnt bei 50 °C zu gelieren. Nach 2 Stunden kann der Grünkörper entformt werden.

Durch eine Optimierung der Schlickerformulierung wurde also ein Direktgießverfahren gefunden, das auf einer erfolgreichen temperaturabhängigen Koagulation von SiC-Schlicker beruht. Bei diesem Verfahren werden lediglich 1 Gew.-% organischer Additive benötigt.

10 Figures

Figure 1.1 Current powder processing	12
Figure 2.2: Change in viscosity and gelation of an aqueous solution of 2wt.% methylcellulose (Methocel A100, Dow Chemical Co., Midland, MI) on heating at 0.25°C/min [2]	14
Figure 2.3: Colloidal stability diagram for HAS process of alumina suspensions [2].....	16
Figure 2.4: Stability limits for an aqueous alumina suspension (a) without a specific adsorbing deflocculant and (b) with 0.35 wt% citric acid as deflocculant [17].....	18
Figure 2.5: Gelation diagram of alumina suspension in water [1]	19
Figure 2.6: Mechanism for TIF process [21]	20
Figure 3.1: Two spheres model	30
Figure 3.2: Schematic representation of electrical double layer	31
Figure 3.3: DLVO theory	32
Figure 3.4: Schematic representation of (a) steric and (b) depletion stabilization.....	34
Figure 3.5: Schematic representation of electrosteric stabilization: (a) charged particles in combination with nonionic polymers and (b) polyelectrolytes attached to uncharged particles.	36
Figure 3.6 Effect of ion concentration on interparticle potential in colloidal suspension (calculated using STABIL [69]).....	37
Figure 4.1: Particle size distribution of SiC: 1) SiC-KOH-0-U is SiC powder dispersed with two hours ball milling at pH 10 and without ultrasonic treatment; 2) SiC-PEI-0-U is	

SiC powder dispersed with dispersant and without ultrasonic treatment; 3) SiC-PEI-1-U with dispersant and one minute ultrasonic treatment and 4) SiC-PEI-D-0-U with degas after ball milling and without ultrasonic treatment 40

Figure 4.2: Particle size distribution of Y_2O_3 1) Y_2O_3 powder dispersed in water by physical stirring (0-U); 2) dispersed at pH 3 using 0.1M HNO_3 (HNO_3 -0-U); 3) dispersed by TAC (TAC-0-U); and 4) dispersed by TAC and one minute ultrasonic treatment (TAC-1-U)..... 41

Figure 4.3: Particle distribution of AlN 1) AlN powder is dispersed by physical stirring (curve AlN-0-U); and 2) by half a minute ultrasonic treatment additionally (curve AlN-05-U) 42

Figure 4.4: DRIFT spectrum of as received SiC powder 44

Figure 4.5: pH change of suspension with milling time 45

Figure 4.6: DRIFT spectrum of as received Y_2O_3 powder..... 45

Figure 4.7: DRIFT spectrum of modified Si-Al-O-N AlN powder 46

Figure 4.8: Sediment volume of SiC suspension versus pH after 175 days..... 47

Figure 4.9: Salt effect on zeta potential measurement of SiC powder (SiC suspension with 0.01M KNO_3 and KCl salt concentration) 49

Figure 4.10: SiC powder zeta potential at different time of ball milling (SiC suspension with 0.01M KNO_3 salt concentration)..... 50

Figure 4.11: Zeta potential of SiC suspension (0.01M KNO_3 solution) 51

Figure 4.12: Zeta potential of modified AlN powder(0.01M KNO_3 solution) 51

Figure 4.13: Zeta potential of Y_2O_3 powder (0.01M KNO_3 solution) 52

Figure 4.14: Calculated solubility of Y_2O_3 in water	53
Figure 5.1: Coagulation probability of a SiC suspension.....	55
Figure 5.2: Relationship of viscosity and pH value of SiC suspension	56
Figure 5.3: Theoretical fit curves and measured points of SiC slurry viscosity.....	58
Figure 5.4: Dispersants for sedimentation experiments	60
Figure 5.5: Structures of dispersant.....	61
Figure 5.6: Zeta potential of SiC powder with various dispersants (1wt%)	62
Figure 5.7: Viscosity of SiC suspension with dispersants ($\phi=20\text{vol}\%$)	64
Figure 5.8: Hydrolysis of carboxyl [103].....	66
Figure 5.9: Temperature effect on viscosity of SiC suspensions ($\phi=20\text{vol}\%$, 1 wt% dispersant) at pH 6 using PEOP and BUMA and at pH 9 using SILO and PEI7....	66
Figure 5.10: pH_{IEP} shift by adsorption of PEI2	67
Figure 5.11: Influence of sintering additives on the viscosity of SiC suspensions with a solid loading of 10 vol% at pH 8	68
Figure 6.1: X-ray diffraction of a) as-received AlN powder, b) AlN powder after 2 hours ball milling in water, and c) aqueous AlN powder + SiC suspension after two hours of ball milling (0.89 mol AlN in 27.14 mol SiC)	70
Figure 6.2: Reprecipitation scheme for silicic acid onto AlN powder [111]	71
Figure 6.3: X-ray diffraction of AlN powder a), and AlN powder after heating at 350 °C in flowing O_2 for two hours b)	72

Figure 6.4: X-ray diffraction of AlN powder after heating a), and after heating in water for 24 hours b)..... 73

Figure 6.5: pH change of different AlN suspensions on heating 74

Figure 6.6: Schematic representation of AlN protection processing..... 75

Figure 7.1: pH change of SiC suspensions with temperature ($\emptyset=10$ vol% SiC, in 0.01 M KNO_3 solution) 76

Figure 7.2: Zeta potential change with temperature (0.01M KNO_3)..... 78

Figure 7.3: Calculated solubility of SiO_2 in water at different temperature (using Debye-Hückel model) 78

Figure 7.4: Variation of surface charge of oxides with pH in 0.1 mol/L (---) and 1 mol/L KCl (—) solutions at 20 °C a)Precipitated silica ; b) TiO_2 ; c)Hematite [113]..... 79

Figure 7.5 Coagulation diagram calculated using STABIL program 80

Figure 7.6: Viscosity change of SiC suspension with temperature at constant shear rate 81

Figure 7.7: Zeta potential of SiC with 14vol% Y_2O_3 (0.01 M KNO_3)..... 82

Figure 7.8: Schematic representation of adsorption of Y_2O_3 on SiC surface..... 83

Figure 7.9: Zeta potential curve of $\text{Y}_2\text{O}_3/\text{TAC}$ 84

Figure 7.10: Viscosity change of SiC suspension with sinter additives (pH 10)..... 84

Figure 7.11: Viscosity change of 40 vol% SiC/ Y_2O_3 /AlN mixture with temperature (pH 10) 85

Figure 7.12: Viscosity changes of a 20 vol% SiC suspension through the addition of sintering additives (pH 10) 86

Figure 7.13: Temperature effects on viscosity of SiC/AlN/Y₂O₃ mixture (pH 10) 87

Figure 7.14: Effect of sintering additives on the viscosity of 30 vol% SiC suspension (pH 10)
..... 87

Figure 7.15: Temperature effect on viscosity of suspension with 30 vol% SiC/AlN/Y₂O₃
(pH 10) 88

Figure 7.16: Viscosity change of a mixed 30 vol% SiC/AlN/Y₂O₃ suspension by cooling
(pH 10) 88

Figure 7.17: Viscosity changes caused by addition of PEI with different average molecular
weight (at pH 10 with 1 wt% polymer)..... 89

Figure 7.18: Zeta potential of SiC powder with 1 wt% PEI7..... 90

Figure 7.19: Interaction energy of SiC powder dispersed with 1 nm PEI7 at the surface 90

Figure 7.20: pH change of 40 vol% SiC/PEI suspension with temperature..... 91

Figure 7.21: Viscosity of SiC suspensions with 1 wt% PEI7 (pH 9)..... 92

Figure 7.22: Temperature effect on to viscosity of different SiC/PEI7 suspensions (pH 10).. 93

Figure 7.23: Viscosity change of 40 vol% SiC suspension versus time at 75°C (pH 9)..... 93

Figure 7.24 Schematic diagram showing the effect of external stimuli on to the conformation
of reactive polymers [1] 94

Figure 7.25: Scheme of the behavior of a SiC/PEI7 suspension during heating..... 95

Figure 7.26: Zeta potential of surface-modified AlN/PEI7 suspension 96

Figure 7.27: Viscosity change of SiC/PEI7 suspension by addition of sintering additives
(pH 7) 97

Figure 7.28: Viscosity change of 40 vol% SiC/AlN/Y₂O₃ suspension by heating (pH 7)..... 97

Figure 7.29: Temperature induced forming of SiC with addition of Y₂O₃ and AlN 98

11 References

- 1 W. M. Sigmund, N. S. Bell, L. Bergström, "New Powder-Processing Methods for Advanced Ceramics", *J. Am. Ceram. Soc.*, 83 (7), 1557-74, 2000.
- 2 T. Kosmoc, "Near-Net-Shape of Engineering Ceramics: Potentials and Properties of Aqueous Injection Molding (AIM)", pp. 13-22 in *Proceedings of NATO ARW on Engineering Ceramics'96*. Edited by G. N. Batini, M. Havier, and P. Sejgalik. Kluwer Academic Publishers, New York, 1997.
- 3 R. M. German, "Powder Injection Molding", Metal Powder Industries Federation, Princeton, New Jersey, 1990.
- 4 B. E. Novich, C. A. Sunback and R. W. Adams, "Quickset Injection Molding of High Performance Ceramics", *Ceram. Trans.*, 26, 157-64, 1992.
- 5 H. Bollman, "Unique New Forming Technique", *Cera. Age*, 791, 36-38, 1957.
- 6 R. D. Rivers, U.S. Pat. No. 4113480, 1978.
- 7 A. J. Fanelli, R. D. Silvers, W. S. Frei, J. V. Burlew, and G. B. Marsh, "New Aqueous Injection Molding Process for Ceramic Powders", *J. Am. Ceram. Soc.*, 72 (10), 1833-36, 1989.
- 8 S. Arnolt et al., *J. Mol. Biol.* 90, 269, 1974.
- 9 E. W. Golibersuch, "Method of Making Cemented Carbide Articles and Articles Produced Thereby", *Can. Pat. No. 642 217*, 1962.

- 10 O. O. Omatete, M. A. Janeey, and R. A. Strehlow, "Gelcasting – A New Ceramic Forming Process for Ceramic Powders", *Am. Ceram. Soc. Bull.*, 70 (10), 1641-49, 1991.
- 11 M. A. Janney, O.O. Omatete, C.A. Walls, S. D. Nunn, R. J. Ogle and G. Westmoreland, "Development of Low-Toxicity Gelcasting Systems", *J. Am. Ceram. Soc.*, 81(3), 581-91, 1998.
- 12 P. R. Chu, and J. K. Cochran, "UV Polymerization of Aqueous Slurries for Application in Ceramic Processing", Paper No. XVIIb-81-94, Presented at 96th Annual Meeting of Am. Ceram. Soc., Indianapolis, IN, 1994.
- 13 S. L. Morissette and J. A. Lewis, "Chemorheology of Aqueous Alumina-Poly(Vinyl Alcohol) Gelcasting Suspension", *J. Am. Ceram. Soc.*, 82 (3), 521-528, 1999.
- 14 T. Kosmac, S. Novak and M. Sajko, "Hydrolysis-Assisted Solidification (HAS): A New Setting Concept for Ceramic Net-Shaping", *J. Europ. Ceram. Soc.*, 17, 427-32, 1997.
- 15 A. Abid, R. Bensalem and J. Sealy, "The Thermal Stability of AlN", *J. Mater. Sci.*, 21, 1301-304, 1986.
- 16 G. A. Slack and T. F. McNelly, "Growth of High Purity AlN Crystals", *J. Cryst. Growth*, 34, 263-79, 1976.
- 17 T. J. Graule, F. H. Baader and L. J. Gauckler, "Shaping of Ceramic Green Compacts Direct from Suspension by Enzyme Catalyzed Reactions", *cfi/Ber. DKG*, 71(6), 317-323, 1994.

- 18 L. J. Gauckler, Th. Graule and F. Baader, "Ceramic Forming Using Enzyme Catalyzed Reactions", *Mat. Chem. and Phy.* 2509, 1-25, 1999.
- 19 B. Balzer, M. K. M Hruschka and L. J. Gauckler, "Coagulation Kinetics and Mechanical Behavior of Wet Alumina Green Bodies Produced via DCC", *J. Col. and Inter. Sci.*, 216, 379-386, 1999.
- 20 W. Sigmund, J. Yanez and F. Aldinger, European Patent Application, PCT/EP98/03555, 1998.
- 21 N. S. Bell, L. Wang, W. M. Sigmund and F. Aldinger, "Temperature Induced Forming: Application of Bridging Flocculation to Near-Net Shape Production of Ceramic Parts", *Zeitschrift für Metallkunde*, vol.90, no.6, June 1999, pp.388-92. Publisher: Carl Hanser Verlag, Germany.
- 22 F. Aldinger, W. Sigmund and J. Yanez, "Formgebungsmethode für Keramiken und Metalle in wässrigen Systemen mittels Temperaturänderung Aktenzeichen", German patent 197 51 696.3, 1998.
- 23 Y. Zhang, K. Uematsu, "A Novel Consolidation Approach for Ceramic Colloidal Forming," *Proceedings of CICC-1*, Beijing China, 1999, pp 128-9.
- 24 B. Yu, Sonderseminar, "Colloidal Isopressing: A New Forming Technique", Universität Stuttgart, Max-Planck-Institut für Metallforschung, PML, 1999.
- 25 S. K. Lee, Y. C. Kim, and C. H. Kim, "Microstructural Development and Mechanical Properties of Pressureless-Sintered SiC with Plate-like Grains Using Al₂O₃ + Y₂O₃ Additives", *J. Mater. Sci.*, 29 (20), 5321-5326, 1994.

- 26 L. Zhou, Y. Huang and Zh. Xie, "Gelcasting of Concentrated Aqueous Silicon Carbide Suspension", *J. Euro. Ceram. Soc.*, 20, 85-90, 2000.
- 27 I. Patzak, K. Wohlleben and K. Konopicky, *Glas Email Keramo Tech.* 22, 2–9, 1971.
- 28 R. Kiefer, E. Gugel, P. Ettmayer and A. Schmidt, *Ber. Dtsch. Keram. Ges.* 43, 621–623, 1966.
- 29 Ullmanns Encyklopädie der technischen Chemie (Ullmann's Encyclopedia of Industrial Chemistry), hrsg. von Ernst Bartholomé - 4., neubearb. u. erw. Aufl.. - Weinheim (Bergstr.) : Verl. Chemie; (dt.), Germany, 21, 431–438, 1972-1984.
- 30 P. T. B. Shaffer, *J. Am. Chem. Soc.*, 47, 466, 1964.
- 31 E. Gugel, P. Schuster and G. Senftleben, *Stahl Eisen* 92, 144–149, 1972.
- 32 JANAF Thermochemical Tables, 2nd ed., NSRDS-NBS37, Washington D.C., June 1971.
- 33 P. Wecht, "Feuerfest-Siliciumcarbid", *Applied Mineralogy*, vol. 11, Springer Verlag, Wien, New York 1977.
- 34 "Gmelin handbook of inorganic and organometallic chemistry (Gmelin-Handbuch der anorganischen Chemie)", prep. and iss. by Gmelin-Institut für Anorganische Chemie der Max-Planck-Gesellschaft zur Förderung der Wissenschaften. Director: Ekkehard Fluck. Founded by Leopold Gmelin - 8. ed., - Berlin; Heidelberg: Springer, 15 Silicium, part B, 1998.

- 35 K. Zückler in W. Schottky (ed.), Halbleiterprobleme III, pp. 207–229, 1956.
- 36 D. Henschler (ed.), Gesundheitsschädliche Arbeitsstoffe. Toxikologisch-arbeitsmedizinische Begründung von MAK-Werten, VCH Verlagsgesellschaft, Weinheim 1987.
- 37 A. L. Lea, Trans. Br. Ceram. Soc. 40, 93-118, 1941; E. G. Acheson, Pat. No. DE 76 629, 1892; E. G. Acheson, Pat. No. DE 85 197, 1894.
- 38 G. Wiebke, L. Korndörfer and E. Korndörfer, Elektroschmelzwerk Kempten GmbH, Pat. No. DE 2 364 106, 1976; A. Korsten et al., Elektroschmelzwerk Kempten GmbH, Pat. No. DE 2 364 107. 1976; G. Wiebke, A. Korsten, T. Benecke and F. Petersen, Elektroschmelzwerk Kempten GmbH, Pat. No. DE 2 364 108, 1976; G. Wiebke, A. Korsten, T. Benecke and F. Petersen, Elektroschmelzwerk Kempten GmbH, Pat. No. DE 2 364 109, 1975; G. Wiebke, A. Korsten, T. Benecke and F. Petersen, Elektroschmelzwerk Kempten GmbH, Pat. No. DE 2 421 818, 1977; F. Petersen and A. Korsten, Elektroschmelzwerk Kempten GmbH, Pat. No. DE 2 630 198, 1978.
- 39 S. Prochazka, General Electric Co, Pat. No. DE 2 518 950, 1975.
- 40 F. Aldinger, University lecture, “Werkstoffwissenschaft VI Pulvermetallurgie und Sintern”, University Stuttgart, 1999-2000.
- 41 G. Petzow, W. A. Kaysser, “Basic Mechanism of Liquid Phase Sintering, sintering key paper”, London and New York, 1990; D. Foster, “Densification of silicon carbide with mixed oxide additives”, PhD Thesis, University of Newcastle upon Tyne, Materials Division, 1996.

- 42 K. Suzuki and M. Sasaki, "Pressureless Sintering of Silicon Carbide," *Fundamental Structural Ceramics*, Reynier Banham, Tokyo, Japan, 1987.
- 43 K. Suzuki, "Pressureless-Sintered Silicon Carbide with Addition of Aluminium Oxide", in *Silicon Carbide Ceramics-2, Ceramic Research and Development in Japan Series*, Eds. S. Somiya and Y. Inomata, London, Elsevier Applied Science, 163-182, 1991.
- 44 M. Omori M and H. Takei, "Pressureless Sintering of SiC", *J. of Am. Ceram. Soc.*, 65 (6), C92, 1982.
- 45 M. A. Mulla and V. D. Krstic, "Low Temperature Pressureless Sintering of α -SiC with Aluminium Oxide and Yttrium Oxide Additions", *J. Mat. Sci. Lett.*, 29, 934-938, 1991.
- 46 K. Y. Chia, W. D. G. Boecker and R. S. Storm, "Silicon Carbide Bodies Having High Toughness and Fracture Resistance and Method of Making Same", United States Patent, 5.298.470, USA, 1994.
- 47 L. Coes, Jr. : "Abrasives", *Applied Mineralogy*, vol. 1, Springer Verlag, Wien 1971.
- 48 Th. Benecke, Elektroschmelzwerk Kempten GmbH, Der Einsatz von metallurgischem Siliziumkarbid, company brochure, München 1978.
- 49 Elektroschmelzwerk Kempten GmbH, Siliziumkarbid für spannungsabhängige Widerstände, company brochure, München 1990.
- 50 W. von Münch, W. Kürzinger and I. Pfaffeneder in "Solid State Electronics", vol. 19, Pergamon Press, Oxford, pp. 871–874, 1976; M. M. Rahman and S. Furukawa, *Jpn. J. Appl. Phys.* 23, 524–525, 1984; Matsushita Electric Industrial Co, Pat. No.

- JP 80 127080, 1980;Chem. Abstr. 94, 56964, 1981; Matsushita Electric Industrial Co, JP 81 14241, 1981;Chem. Abstr. 95, 52673, 1981; H. Kukimoto, *Semicond. Semimetals D* 21, 239–48, 1984;Chem. Abstr. 102, 175100, 1985.
- 51 H. Knoch and J. Kracker, *Ber. Dtsch. Keram. Ges.*, 64, 159 – 163, 1987.
- 52 K. Uematsu, L. Guo, Y. Zhang and N. Uchida, “Role of Temperature on the Interfacial Chemistry of Ceramic Slurries”, *Key Engineering Materials*, Vols 111-112, pp. 405-416, 1995.
- 53 L. Bergström and E. Sjöström, "Temperature Induced Gelation of Concentrated Ceramic Suspensions: Rheological Properties", *J. Euro. Ceram. Soc.* 19, 2117-2123, 1999.
- 54 G. J. Fleer, M. A. Cohen Stuart, J. M. H. M. Scheutjens, T. Cosgrove and B. Vincent, “Polymers at Interfaces”, Chapman and Hall, London, U.K., 1993.
- 55 CF. Jr. Baes and R. E. Mesmer, “Review of the Hydrolysis of Ions in Aqueous Solution”, *Mat. Res. Soc. Symp. Proc.*, 180, 85-96, 1990.
- 56 CF. Jr. Baes and R. E. Mesmer, “ The Thermodynamics of Cation Hydrolysis”, *Am. J. Sci.*, 281, 935-62, 1981.
- 57 W. Stumm and J. J. Morgan, "Aquatic Chemistry: Introduction Emphasizing Chemical Equalibria in Natural Waters", John Wiley & Sons, New York, 1996.
- 58 D. H. Napper, "Polymeric Stabilization of Colloidal Dispersions", Academic Press, London, U.K., 1983
- 59 V. K. La Mer, *J. Colloidal Sci.* 19, 291, 1964.

- 60 H. C. Hamaker, "The London-van der Waals Attraction between Spherical Particles", *Physica*(Amsterdam), 4, 1058-1072, 1937.
- 61 R. G. Horn, "Surface Forces and Their Action in Ceramic Materials," *J. Am. Ceram. Soc.*, 73 (5), 1117-1135, 1990.
- 62 F. F. Lange and E. P. Luther, "Colloidal Processing of Structurally Reliable Si_3N_4 ", *Tailoring of Technical Properties of Si_3N_4 Ceramics*, edited by M. J. Hoffmann & G. Petzow, Stuttgart: Borntraeger, 3-18, 1994.
- 63 D. J. Shanefield, "Organic Additives and Ceramic Processing, with applications in Powder Metallurgy, Ink, and Paint", Kluwer Academic Publications, 1995.
- 64 D. Myers, "Surfaces, Interfaces, and Colloids: Principles and Applications", hrsg. von Wilhelm Albrecht - Neue, aktualis. u. erw. Aufl.. - Weinheim: Wiley-VCH, 1990.
- 65 W. B. Russel, D. A. Saville and W. R. Schowalter, "Colloidal Dispersions", Cambridge University Press, Cambridge, U.K. 1989.
- 66 P. G. De Gennes, "Conformations of Polymers Attached to an Interface", *Macromolecules*, 13, 1069-75, 1980.
- 67 P. G. De Gennes, "Polymers at an Interface; a simplified View", *Adv. Colloid Interface Sci.*, 27, 189-209, 1987.
- 68 F. Aldinger, University lecture, "Keramische Werkstoffe I: Strukturkeramik", University Stuttgart, 1999-2000.
- 69 R. V. Linhart and J. H. Adair, *STABIL Vision 1.45*, Philadelphia, 1985.

- 70 J. A. Horn and B. R. Patterson, "Thermally Induced Reversible Coagulation in Ceramic Powder-Polymer Liquid Systems", *J. Am. Ceram. Soc.*, 80, 1789-1797, 1997.
- 71 A. W. M. de Laat, and H. F. M. Schoo, "Reversible Thermal Flocculation of Aqueous α -Fe₂O₃ Dispersions Stabilized with Novel Poly(vinyl ether) Block Copolymers", *J. Coll. Inter. Sci.*, 200, 228-234, 1998.
- 72 L. Bergström, "Hamaker Constants of Inorganic Materials", *Adv. Coll. Inter. Sci.*, 70, 125-69, 1997.
- 73 R. G. J. Miller and H. A Willis, "IRSCOT: Infrared Structural Correlation Tables and Data Cards", London, Hyden, Losebl Aug. Quer., 1969
- 74 R.J.H Clark and R.E Hester, "Spectroscopy of Inorganic-Based Materials", Chichester: Wiley, 1987. - xix, 472 S. : Ill.; (Advances in spectroscopy; 14).
- 75 Y. Hirata, S. Yamada and Y. Fukushige, "Colloidal Processing of Silicon Carbide", *Mat. Lett.*, 16, 295-299, 1993.
- 76 Y. Kim, M. Mitomo and J. Lee, "Influence of Silica Content on Liquid Phase Sintering of Silicon Carbide with Yttrium-Aluminum Garnet," *J. Cera. Soc. Japan*, 104 (9), 816-818, 1996.
- 77 L. S. Cerovic et al., "Intrinsic Equilibrium Constants of β -Silicon Carbide Obtained from Surface Charge Data", *J. Am. Ceram. Soc.*, 78 (11), 3093-96, 1995.
- 78 L. Bergström and M. Ernstsson et al., "The Effect of Wet and Dry Milling on the Surface Properties of Silicon Nitride Powders", *Ceramic Today - Tomorrow's*

- Ceramics, by P. Vincenzini, Elsevier Science Publishers B. V., N.Y., 1991, pp 1005-1014.
- 79 "Vibrational spectra and structure": a series of advances VBSSB. - New York, NY: Dekker; Amsterdam : Elsevier, 1972.
- 80 R. F. Willis, "Vibrational Spectroscopy of Adsorbates", with contrib. by B. K. Agrawal - Berlin: Springer, 1980. - XII, 184 S. : Ill.; (engl.) (Springer series in chemical physics; 15).
- 81 T. M. Riddick, "Control of Colloidal Stability through Zeta Potential", Zeta Meter Corp., New York, 1968.
- 82 P. Tuorilla, *Kolloid-Beihefte*, 27, 44, 1928.
- 83 L. Wang, "Colloidal Processing and Rapid Prototyping of Si_3N_4 ", dissertation, Max-Planck-Institut für Metallforschung/University of Stuttgart, Germany, 1998.
- 84 P. K. Whitman and D. L. Feke, *Adv. Ceram. Mat.*, 1, 366-70, 1986.
- 85 M. Persson, L. Hermansson and R. Carlsson, "Ceramic Powders", Ed. By P. Vincenzini, Elsevier Scientific Pub., N. Y., pp. 735-42, 1983.
- 86 R. V. Linhart and J. H. Adair, *OPAL Vision 1.93*, Philadelphia, 1997.
- 87 R. J. Hunter, "Zeta Potential in Colloid Science", Academic Press, London, 1981.
- 88 M. P. Albano and L. B. Garrido, "Dispersion of Concentrated Aqueous Si_3N_4 - Y_2O_3 - Al_2O_3 Slips with Tetramethylammonium Hydroxide", *Ceramic International.*, 25, 13-18, 1999.

- 89 R. Lenk and A. Krivoshepov, "Effect of Surface-Active Substances on the Rheological Properties of Silicon Carbide Suspensions in Paraffin", *J. Am. Ceram. Soc.*, 83 (2), 273-76, 2000.
- 90 F. M. Fowkes, "Role of Acid-Base Interactions in Inorganic Powder Dispersions and Composites", In "Interfacial Phenomena in Biotechnology and Material Processing", Aug. 3-7, 1987, Boston Mass., ed. by Yosry A. Attia. - Amsterdam : Elsevier, 1988, 171-186.
- 91 E. Liden, L. Bergström, M. Persson and R. Carlsson, "Surface modification and dispersion of silicon nitride and silicon carbide powders", *J. Euro. Cera. Soc.*, 7 (6), 361-8, 1991.
- 92 Zh. Huang, D. Jiang and Sh. Tan, *J. Am. Ceram. Soc.*, 78 (8), 2240-42, 1995.
- 93 P. Lin and D. Tsai, "Preparation and Analysis of a Silicon Carbide Composite Membrane", *J. Am. Ceram. Soc.*, 80 (2), 365-72, 1997.
- 94 Zh. Chen and L. Zeng, "Pressurelessly Sintering Silicon Carbide with Additives of Holmium Oxide and Alumina", *Materials Research. Bulletin*, 30 (3), 265-270, 1995.
- 95 J. K. Lee, H. Tanaka and H. Kim, "Movement of Liquid Phase and the Formation of Surface Reaction Layer on the Sintering of β -SiC with an Additive of Yttrium Aluminium Garnet", *Journal of Materials Science Letters*, 15, 409-411, 1996.
- 96 J. Iskra, "Flotation Properties of Silicon Carbide I. Flotation of Silicon Carbide with Anionic and Cationic Collector", *Ceramics International*, 23, 337-342, 1997.

- 97 S. Assmann, U. Eisele and H. Böder, "Processing of Al₂O₃/SiC Composites in Aqueous Media", *J. Euro. Ceram. Soc.*, 17, 309-317, 1997.
- 98 F. Valdivieso, P. Goeuriot and F. Thevenot, "Dispersion of Three Ceramic Powders in a Slurry: The Al₂O₃-AlN-SiC Mixture", *J. Euro. Ceram. Soc.*, 17, 377-382, 1997.
- 99 L. Wang and W. Wei, "Colloidal Processing and Liquid-Phase Sintering of SiC", *J. Ceram. Soc. Japan*, 103 (5), 434-443, 1995.
- 100 S. Sano, T. Banno, et al., "Slip Casting and Sintering of Silicon Carbide (Part 1): Slip Preparation of Silicon Carbide Powder Produced by Acheson Method", *J. Ceram. Soc. Japan*, 104 (10), 984-988, 1996.
- 101 B. Baron et al., "SiC Particle Reinforced Oxynitride Glass: Processing and Mechanical Properties", *J. Euro. Soc.*, 17, 773-780, 1997.
- 102 E. Liden et al., "Homogeneous Distribution of Sintering Additives in Liquid-Phase Sintered Silicon Carbide", *J. Am. Ceram. Soc.*, 78 (7), 1761-68, 1995.
- 103 J. Sindel, "Direkte Bestimmung von zwischenpartikulären Kräften in wäßrigen Bariumtitanatsuspensionen", Dissertation, Max-Planck-Institut für Metallforschung/University of Stuttgart, Germany, 1999.
- 104 I. Wiedmann, "Herstellung und mechanische Eigenschaften von flüssigphasengesintertem Siliziumkarbid", Dissertation, Max-Planck-Institut für Metallforschung/University of Stuttgart, Germany, 1998.
- 105 P. Bowen, J.G. Highfield, A. Mocellin and T. A. Ring, "Degradation of Aluminum Nitride Powder in an Aqueous Environment", *J. Am. Ceram. Soc.*, 73 (3), 724-728, 1990.

- 106 M. Egashira, Y. Shimizu, Y. Takao, R. Yamaguchi and Y. Ishikawa, "Effect of Carboxylic Acid Adsorption on the Hydrolysis and Sintered Properties of Aluminum Nitride Powder", *J. Am. Ceram. Soc.*, 77 (7), 1793-1298, 1994.
- 107 D. Hotza, O. Sahling and P. Greil, "Hydrophobing of Aluminium Nitride Powders", *J. Mat. Sci.*, 30, 127-132, 1995.
- 108 M. Uenishi, Y. Hashizume and T. Yokote, "Aluminium Nitride Powder Having Improved Water-Resistance", U.S. Pat. 4,923,689, May 8, 1990.
- 109 K. Krnel and T. Kosmac, "Modification of AlN powder surface to prevent its reactivity with water", 33rd International Conference on Microelectronics, Devices and Materials. MIDEM conference '97. Proceedings. MIDEM Soc. Microeletron., Electron. Components & Mater., pp-99-104. Ljubljana, Slovenia, 1997.
- 110 K.E.Howard, "Method of making Moisture Resistant Aluminum Nitride Powder and Powder Produced thereby", U.S. Pat. 5,234,712, 1993.
- 111 K. Krnel and T. Kosmac, "Reactivity of Aluminum Nitride Powder in Dilute Inorganic Acids", *J. Am. Ceram. Soc.*, 83 (6), 1375-78, 2000.
- 112 K. S. Pitzer, " Thermodynamics of Electrolytes. I. Theoretical Basis and general Equations", *J. Phy. Chem.*, 77 (2), 268-77, 1973.
- 113 Ullmanns Encyklopädie der technischen Chemie (Ullmann's Encyclopedia of Industrial Chemistry), hrsg. von Ernst Bartholomé - 5., neubearb. u. erw. Aufl.. - Weinheim (Bergstr.) : Verl. Chemie; (dt.), Germany, 1985-1996.

LEBENS LAUF

Name	Ruishuo Li
Geboren	10.09.1968 in Shanxi / V. R. China
Familienstand	verheiratet
Schulbildung	
Feb. 1976 – Jul. 1980	Grundschule, Heshun, Shanxi, VR China
Sep. 1980 – Jul. 1983	Mittelschule, Heshun, Shanxi, VR China
Sep. 1983 – Jul. 1986	Oberschule, Yuci, Shanxi, VR China
Studium:	
Sep. 1986 – Jul. 1990	Diplomstudium im Fach Chemie an der Nankai-Universität, Tianjing, VR China. Studienfach: Physikalische Chemie. Thema der Diplomarbeit: "Study on The Deactivation of Basic Oxide Catalyst for Cyclohexnone Dimerization".
Sep. 1990 – Jun. 1993	Masterstudium am Institut für Kohlechemie der Chinesischen Akademie der Wissenschaften, Taiyuan, Shanxi, VR China. Studienfach: Physikalische Chemie. Thema der Arbeit: "The Preparation of Fine Particles by NCP and its Application in Catalysis "; Qualifikation: Master of Science.
Promotionsstudium:	
Apr. 1996 – Jun.2001	Am Max-Planck-Institut für Metallforschung, Abteilung Prof. Dr. F. Aldinger (PML, Pulvermetallurgisches Laboratorium) und Institut für Nichtmetallische Anorganische Materialien der Universität Stuttgart.
Berufstätigkeit	
Jun. 1993 – Sep. 1995	Wissenschaftlicher Mitarbeiter am Institut für Kohle-Chemie der Chinesischen Akademie der Wissenschaften, Taiyuan, Shanxi, VR China.